# FUNCTIONAL ANALYSIS OF THE HUMAN SMC5/6 COMPLEX IN HOMOLOGOUS RECOMBINATION AND TELOMERE MAINTENANCE

APPROVED BY SUPERVISORY COMMITTEE

Hongtao Yu, Ph.D. (Mentor)

Matthew Porteus, M.D. Ph.D. (Chair)

David Chen, Ph.D.

Zhijian Chen, Ph.D.

# DEDICATION

I would like to dedicate my thesis to my parents, Robert and Brenda Potts. Over the past twenty-eight years they have supported and encouraged me in every aspect of my life. Their unceasing love and comfort have gotten me through the many challenges and hard times. They have taught me the importantance of hard work, determination, and focus that have certainly been keys to my success. Perhaps even more notably, they have always taught the significance of family values, generosity, sincerity, and caring for others. Undoubtedly they have been absolutely essential in my success. I love and thank them dearly for everything that they have done and sacrificed for me.

In addition to my parents, I would also like to acknowledge several others family members for their support. First and foremost, I would like to thank my wife, Malia Potts. She has provided me with more support and love than I ever thought possible. Furthermore, she has contributed immensely to the work by giving intellectual advice that was instrumental in my success. I would like to also thank my brothers, Brandon and Britt Potts, for their advice and help over the years.

I would also like to acknowledge several others who were instrumental in getting me interested in scientific research. First, Dr. Louis Underwood and the rest of the UNC Pediatric-Endocrinology department that not only provided me

with the very best patient care, but also gave me my first opportunity to experience life in a research lab while I was an undergraduate at UNC. Second, I would like to thank Mohanish Deshmukh for his patience while teaching me essential experimental techniques, basic scientific reasoning, and how to read scientific literature.

Finally, I would like to thank those people at UT Southwestern that have helped me during my graduate work. First and most importantly, I would like to thank my mentor Hongtao Yu. Hongtao has allowed me to work independently in the lab to pursue my own interests without financial limitations. In addition, I am extremely grateful for him giving me many opportunities that not every graduate student is given, such as going to meetings to present my research, writing my own papers, reviews, and grants, reviewing manuscripts, hiring a technician, and managing rotation students. Also, I would like to thank Hongtao for his insightful scientific and technical advice, as well as promoting my career. Lastly, I would like to thank the past and present members of the lab that have provided me with an extremely productive and fun environment for doing research.

FUNCTIONAL ANALYSIS OF THE HUMAN SMC5/6 COMPLEX IN
HOMOLOGOUS RECOMBINATION AND TELOMERE MAINTENANCE


by


PATRICK RYAN POTTS


Dissertation


Presented to the Faculty of the Graduate School of Biomedical Sciences

The University of Texas Southwestern Medical Center at Dallas

In Partial Fulfillment of the Requirements

For the Degree of


DOCTOR OF PHILOSOPHY

The University of Texas Southwestern Medical Center at Dallas

Dallas, Texas

December, 2007

FUNCTIONAL ANALYSIS OF THE HUMAN SMC5/6 COMPLEX IN
HOMOLOGOUS RECOMBINATION AND TELOMERE MAINTENANCE

PATRICK RYAN POTTS, Ph.D.

The University of Texas Southwestern Medical Center at Dallas, 2007

HONGTAO YU, Ph.D.

DNA repair is required for the genomic stability and well-being of an
organism.  The structural maintenance of chromosomes (SMC) family of proteins
has been implicated in the repair of DNA double-strand breaks (DSBs) by
homologous recombination (HR).  The SMC1/3 cohesin complex promotes HR
by localizing to DSBs where it holds sister chromatids in close proximity to allow
HR-induced strand invasion and exchange.  The SMC5/6 complex is also required
for DNA repair, but the mechanism by which it accomplishes this has been
unclear.  We have characterized the role of the human SMC5/6 complex in HR-
mediated DNA damage repair.  The yeast SMC5/6 complex has been shown to be
composed of the SMC5-SMC6 heterodimer and six non-SMC element (NSE)
proteins.  We show that the human homolog of one of these NSE proteins,
MMS21/NSE2, is a ligase for small ubiquitin-like modifier (SUMO).  Depletion

vi

of MMS21 by RNA interference (RNAi) sensitizes cells toward DNA damage-induced apoptosis. This hypersensitization of MMS21-RNAi cells is not due to a defect in DNA damage-induced cell cycle checkpoint, but rather in the kinetics of DNA damage repair. Since the yeast SMC5/6 complex has been implicated in HR-mediated DSB repair, we investigated the role of the human SMC5/6 complex in HR-mediated DSB repair. RNAi-mediated knockdown of the SMC5/6 complex components specifically decreases sister chromatid HR, but not non-homologous end-joining (NHEJ) or intra-chromatid, homologue, or extrachromosomal HR. We show that one potential mechanism by which the SMC5/6 complex specifically promotes sister chromatid HR is by facilitating the recruitment of the SMC1/3 cohesin complex to DSBs.

We next examined whether the SMC5/6 complex is also required for sister chromatid HR of telomeres. Specific types of cancer cells, known as alternative lengthening of telomeres (ALT) cells, rely on telomere recombination for telomere lengthening and unlimited replicative potential. We show that the SMC5/6 complex promotes telomere recombination and lengthening in ALT cells by MMS21-dependent sumoylation of telomere-binding proteins. Sumoylation of these telomere-binding proteins relocalizes telomeres to nuclear PML bodies where HR proteins facilitate telomere recombination. These studies identify the human SMC5/6 complex and SUMO modification as critical mediators of sister chromatid HR.

# TABLE OF CONTENTS

# PRIOR PUBLICATIONS

Potts, P.R., Yu H. (2007). The SMC5/6 Complex Maintains Telomere Length in ALT Cancer Cells through Sumoylation of Telomere-Binding Proteins.  Nat. Struct. Mol. Biol. *14*, 581-590.

Potts, P.R., Porteus, M.H., and Yu, H. (2006). Human SMC5/6 complex promotes sister chromatid homologous recombination by recruiting the SMC1/3 cohesin complex to double-strand breaks. EMBO J. *25*, 3377-3388.

Potts, P.R., and Yu, H. (2005). Human MMS21/NSE2 is a SUMO ligase required for DNA repair. Mol. Cell. Biol. *25*, 7021-7032.

Wright, K.M., Linhoff, M.W., Potts, P.R., and Deshmukh, M. (2004). Decreased apoptosome activity with neuronal differentiation sets the threshold for strict IAP regulation of apoptosis. J. Cell Biol. *167*, 303-313.

Olteanu, A., Patel, C.N., Dedmon, M.M., Kennedy, S., Linhoff, M.W., Minder, C.M., Potts, P.R., Deshmukh, M., and Pielak, G.J. (2003). Stability and apoptotic activity of recombinant human cytochrome c. Biochem. Biophys. Res. Commun. *312*, 733-740.

Potts, P.R., Singh, S., Knezek, M., Thompson, C.B., and Deshmukh, M. (2003). Critical function of endogenous XIAP in regulating caspase activation during sympathetic neuronal apoptosis. J. Cell Biol. *163*, 789-799.

# LIST OF FIGURES

# LIST OF TABLES

# LIST OF DEFINITIONS

ABC – ATP-binding cassette
ALT – alternative lengthening of telomeres
APB – ALT-associated PML body
BrdU – 5-bromo-2-deoxyuridine
ChIP – chromatin immunoprecipitation
CO-FISH – chromosome orientation fluorescent *in situ* hybridization
DAPI – 4'-6-diamidino-2-phenylindole
DR-GFP – direct repeat green fluorescent protein
DSB – double-strand break
GFP – green fluorescent protein
HEAT – Huntington, elongation A subunit, TOR
HR – homologous recombination
IR – ionizing irradiation
IRES – internal ribosome entry site
IVEC – *in vitro* expression cloning
IVT – *in vitro* transcription/translation
kb – kilobase pair
LM-PCR – ligation-mediated PCR
LTGC/SCR – long tract gene conversion sister chromatid recombination
MAGE – melanoma-associated antigen gene
MEF – mouse embryonic fibroblast
MMC – mitomyocin C
MMS – methylmethane sulfonate
MRN – MRE11/RAD50/NBS1
NHEJ – non-homologous end-joining
NSE – non-SMC element
PML – promyelocytic leukemia
QFISH – quantitative fluorescent *in situ* hybridization
QPCR – quantitative PCR
rDNA – ribosomal DNA
RING – really interesting new gene
RNAi – RNA interference
SA-β-GAL – senescence-associated β-galactasidase activity
SCE – sister chromatid exchange
shRNA – short hairpin RNA
siRNA – small interfering RNA
SMC – structural maintenance of chromosomes
SSB – single-strand break

SUMO – small ubiquitin-like modifier
TEV – tobacco etch virus
TRAX – translin-associated factor-X protein
T-SCE – telomere sister chromatid exchange
UV – ultraviolet irradiation

# CHAPTER I:  INTRODUCTION

## DNA DAMAGE REPAIR

The accurate replication and segregation of a cell's genome to its daughter cells is essential for the survival of the organism. At the same time, a cell must be competent to cope with damaged DNA that occurs both intentionally and unintentionally.  Mutations that prevent a cell's ability to repair damaged DNA cause many human diseases, including cancer and immune deficiencies.

### DNA Damage Response

Damage to DNA occurs through multiple mechanisms, including free radicals, chemical carcinogens, ultraviolet (UV) radiation, ionizing radiation (IR), stalled replication forks, and replication errors.  These damages result in multiple types of lesions, including single-stand breaks (SSB), double-strand breaks (DSB), base alkylation, thymidine dimers, and intrastrand crosslinks.  To prevent such damages from causing mutations that can be hazardous, cells have evolved surveillance mechanisms to sense damaged DNA.

The cellular DNA damage surveillance machinery elicits multiple responses upon encountering damaged DNA.  These responses include recruiting

DNA repair proteins to the site of damage, blocking cell cycle progression to allow time for repair, and if the damage is too great, triggering apoptosis. A signaling network composed of multiple proteins at distinct levels carry out these responses. Three PI(3)-kinase-like proteins, ATM, ATR, and DNA-PK, are key proximal components of the DNA damage response (Abraham, 2004). They phosphorylate many downstream substrates involved in the DNA damage response, including P53, BRCA1, CHK1, CHK2, and NBS1 (Abraham, 2004). Mutations in each of these DNA damage response proteins results in increased cancer susceptibility in humans (Achatz et al., 2007; Bartek and Lukas, 2003; Digweed and Sperling, 2004; Ford et al., 1994). Two downstream substrates of ATM and ATR that promote G2/M-phase cell cycle arrest after DNA damage are the CHK1 and CHK2 protein kinases (Liu et al., 2000; Matsuoka et al., 1998). CHK1 and CHK2 prevent cell cycle progression by phosphorylating and inhibiting the CDK1 phosphatase CDC25C (Matsuoka et al., 1998; Sanchez et al., 1997). Phosphorylation of CDC25C by CHK1 and CHK2 prevents dephosphorylation of inactivating phosphates on CDK1 by sequestering CDC25C in the cytoplasm (Peng et al., 1997).

**Double-Strand Break Repair**

One particularly dangerous type of DNA damage is DNA double-strand breaks (DSBs). Although DSBs are the most hazardous form of DNA damage, they occur frequently during immune system development, DNA replication, and meiosis (Wyman and Kanaar, 2006). Therefore, several cellular mechanisms mediate efficient repair of DSBs to prevent genomic instability that can result in tumorigenesis. The two major DSB repair mechanisms are non-homologous end-joining (NHEJ) and homologous recombination (HR; Sonoda et al., 2006).

*Non-homologous End-Joining*

NHEJ is the error-prone DSB repair process by which two ends of a DSB are religated together based on microhomology between the two broken ends (Lieber et al., 2004). Several proteins, such as KU70, KU80, DNA-PKcs, XRCC4, and LIGASE IV, are essential for the repair of DSBs by NHEJ (Burma et al., 2006). KU70 and KU80 form a heterodimeric, doughnut-shaped structure that binds the ends of DSBs (Walker et al., 2001). KU70/80 then recruits and stabilizes DNA-PKcs at DSBs promoting its kinase activity towards itself and other DNA damage response proteins (Chan et al., 2002; Yaneva et al., 1997). The assembly of KU70/80 and DNA-PKcs at DSBs facilitates recruitment of the XRCC4-LIGASE IV complex and the subsequent ligation of the two free DNA ends of a DSB (Calsou et al., 2003).

*Homologous Recombination*

Unlike the error-prone NHEJ, HR-mediated DSB repair does not introduce genomic mutations.  HR repairs DSBs by using an intact sister chromatid as a template for DNA synthesis across the DSB (Wyman et al., 2004).  Three sequential steps facilitate HR:  DSB end processing and recruitment of proteins, strand invasion and DNA synthesis, and resolution of the Holliday junction intermediates (Figure 1-1).  Similar to NHEJ, a number of proteins are recruited to DSBs that facilitate the various steps of HR.  One of the earliest proteins recruited to DSBs is the ATM protein kinase (Lisby et al., 2004).  In addition to activating many downstream events such as cell cycle arrest, ATM also phosphorylates the histone variant H2AX at DSBs (Burma et al., 2001).  This phosphorylated histone, known as γH2AX, establishes a chromatin domain around DSBs that facilitates recruitment of other proteins, such as MDC1 (Stewart et al., 2003).  The MRE11/RAD50/NBS1 (MRN) protein complex also rapidly localizes to DSBs (Mirzoeva and Petrini, 2001).  The MRN complex is composed of a homodimer of the SMC-like ATPase RAD50 (Hopfner et al., 2002).  RAD50 dimerizes through its zinc-hook region and forms a V-shaped structure upon binding DNA (Moreno-Herrero et al., 2005).  This structure binds and tethers free DNA ends and presumably immobilizes broken DNA ends of a DSB to facilitate HR (de Jager et al., 2001).  The MRN complex also contains MRE11, an endonuclease that may mediate end resection at DSBs, resulting in

single-stranded 3' overhangs (Paull and Gellert, 1998). These single-stranded 3' overhangs are rapidly bound and stabilized by RPA (Gasior et al., 1998).

Once the DSB has been completely processed, RAD51 forms a nucleofilament on the 3' overhang single-strand DNA, displacing RPA (Sugiyama and Kowalczykowski, 2002). Formation of the RAD51 nucleofilament is dependent on the HR mediators, such as RAD52, RAD51 paralogs, and BRCA2 (Sung et al., 2003). The RAD51 nucleofilament promotes strand invasion of the broken sister chromatid into the intact sister chromatid (Sugawara et al., 1995). This strand invasion event presumably requires the loading of cohesin at DSBs to hold sister chromatids in close proximity (Strom and Sjogren, 2007). The joint molecule after strand invasion and homology pairing acts as a template for DNA polymerase to travel across the DSB and incorporate any missing nucleotides. After DNA synthesis is complete, the joint molecule, known as a Holliday junction, is resolved. Unlike the bacterial RuvC resolvase, there has been no single eukaryotic resolvase identified (West, 2003b). However, the RAD51C-XRCC3 complex, topoisomerase III, RecQ helicases, and unknown resolvases are thought to promote Holliday junction resolution in eukaryotes (Heyer et al., 2003; Liu et al., 2007).

## STRUCTURAL MAINTENANCE OF CHROMOSOMES PROTEINS

Chromosomal rearrangement is an active process that allows gene expression, sister chromatid cohesion and condensation, and DNA repair. The structural maintenance of chromosomes (SMC) family of proteins are involved in such rearrangements of chromosomes to allow these processes to occur.

## Architecture of SMC Protein Complexes

SMC proteins contain a Walker A motif at their N-termini and a Walker B motif at their C-termini (Figure 1-2). These motifs are brought together by an intramolecular coiled-coil domain to form a functional ATPase domain, which is similar to other ATP-binding cassette (ABC) ATPases, such as RAD50 (Melby et al., 1998). SMC proteins heterodimerize with one another through their hinge domains to form three unique complexes: cohesin (SMC1-SMC3), condensin (SMC2-SMC4), and SMC5-SMC6 (Hirano, 2002; Nasmyth and Haering, 2005b). The head domains of the heterodimeric pairs of SMC proteins are linked by proteins known as kleisins (Nasmyth and Haering, 2005b). In addition to kleisins, SMC complexes contain additional non-SMC proteins.

## The SMC1/3 Cohesin Complex

The propagation of genetic information during cell division is a complex and highly regulated process that involves extensive changes to the interphase chromatin.  The somatic cell cycle is divided into four phases: G1, S, G2, and M.  During S phase, DNA is replicated to form sister chromatids (Blow and Tanaka, 2005).  Each sister chromatid contains the same genetic information.  Therefore, it is imperative to ensure equal segregation of sister chromatids to daughter cells during mitosis (M-phase).  Unequal segregation of chromosomes results in daughter cells with wrong chromosome numbers, a condition known as aneuploidy.  One important mechanism that ensures proper segregation of chromosomes to daughter cells is sister chromatid cohesion.

*Architecture of the Cohesin Complex*

Sister chromatid cohesion is primarily established by the cohesin complex. (Nasmyth and Haering, 2005b).  The cohesin complex is a multi-subunit complex that consists of the heterodimeric SMC1-SMC3 core, SCC1/MCD1/RAD21, and SA2/SCC3 (Figure 1-3; Hirano, 2006b; Nasmyth and Haering, 2005b).  The function of SA2 is unknown.  SCC1 is the kleisin subunit of the cohesin complex. SCC1 contains a winged helix domain at its C-terminus that mediates binding to the head domain of SMC1 (Haering et al., 2004).  The binding of SCC1 to SMC1 facilitates the binding of SCC1's N-terminal domain to the SMC3 head domain (Haering et al., 2004).  In so doing, SCC1 links the two head domains of the

SMC1-SMC3 heterodimer to form a ring-shaped structure.  Cryo-electron microscopy has confirmed the ability of the cohesin complex to form a ring-shaped structure with an internal diameter of 30-40 nm (Gruber et al., 2003).

*Sister Chromatid Cohesion*

The cohesin complex is loaded onto chromatin during late G1 phase of the cell cycle (Michaelis et al., 1997).  The ATPase activity of SMC1-SMC3 is required for cohesin loading onto chromatin (Arumugam et al., 2003).  The mechanism by which the ATPase activity promotes cohesin loading is unclear. In addition to the ATPase activity of SMC1-SMC3, cohesin loading is dependent on the SCC2-SCC4 complex (Ciosk et al., 2000).  Both SCC2 and SCC4 contain Huntington, elongation A subunit, TOR (HEAT) repeats.  The exact mechanism by which SCC2-SCC4 promotes cohesion loading is unclear.  It has been proposed that SCC2-SCC4 stimulates the ATPase activity of SMC1-SMC3 (Arumugam et al., 2003; Nasmyth and Haering, 2005a).  In budding yeast, the cohesin complex is concentrated around centromeres and at intergenic regions (Tanaka et al., 1999).  Interestingly, the chromosomal localization of SCC2-SCC4 does not overlap with that of cohesin, suggesting that cohesin redistributes to intergenic regions after SCC2-SCC4 facilitates its loading onto chromatin (Lengronne et al., 2004).  The enrichment of cohesin at intergenic regions is thought to be a result of convergent transcription, possibly because of the physical

pushing of cohesin by the transcriptional machinery as it moves along chromatin (Lengronne et al., 2004). It is currently unclear whether cohesin is enriched at intergenic regions in organisms other than yeast.

Loading of cohesin onto chromatin is itself insufficient to establish functional cohesion between sister chromatids. Establishment of sister chromatid cohesion occurs subsequently to cohesin loading and is tightly coupled to DNA replication in S phase. Several factors are required for the establishment of functional sister chromatid cohesion after the loading of cohesin onto chromatin. These factors include the acetyl transferase ECO1/CTF7, the replication factor C (RFC) complex (CTF18/DCC1/CTF8), and the chromatin structure remodeling (RSC) complex (Baetz et al., 2004; Hanna et al., 2001; Kenna and Skibbens, 2003). The precise mechanism by which chromatin-bound cohesin establishes sister chromatid cohesion is unresolved. Elegant studies have shown that cohesin binds chromatin by entrapping DNA within its ring-shaped structure. These studies inserted an artificial tobacco etch virus (TEV) protease cleavage site into one cohesin subunit to allow inducible cleavage. Upon expression of TEV, the cohesin complex was rapidly removed from chromatin and sister chromatid cohesion was destroyed (Gruber et al., 2003). In addition, using circular minichromosomes in which cohesin is loaded, cleavage of the circular DNA results in the removal of cohesin from these chromosomes (Ivanov and Nasmyth, 2005). These studies show that DNA is entrapped within the cohesin ring. How

DNA is encircled by the cohesin ring is unclear. Several possible mechanisms have been proposed, most of which involve the transient dissociation of proteins within the cohesin complex to open the ring structure. These include dissociation of the SMC1 and SMC3 hinge domains, SMC1 head domain and SCC1 C-terminus, or SMC3 head domain and SCC1 N-terminus. Another outstanding question is how cohesin actually mediates sister chromatid cohesion. Two equally viable models have been proposed (Figure 1-4). The embrace model proposes that a single cohesin complex encircles both sister chromatids within its ring-shaped structure as the DNA replication fork progresses (Figure 1-4, left). With a diameter of 30-40 nm, the cohesin ring is large enough to accommodate both sister chromatids (10 nm each; Haering et al., 2002b). However, it is unclear how the cohesin ring copes with the massive DNA replication machinery that would presumably need to move through the cohesin ring. Alternatively, a cohesin dimerization model proposes that each sister chromatid is trapped by separate cohesin complexes. In this model, the individually trapped sister chromatids are held together by the dimerization of the two cohesin complexes (Figure 1-4, right). However, intermolecular interaction between cohesin complexes has not been detected.

*Cohesin and DNA Repair*

In addition to the role of cohesin in mediating faithful segregation of sister chromatids to daughter cells during mitosis, the cohesin complex is also involved in the repair of DNA damage.  The SCC1/RAD21 cohesin complex component was originally identified in a screen for radiation-sensitive mutants in yeast (Phipps et al., 1985).  Later studies confirmed that SCC1 mutants are hypersensitive to IR, UV, and hydroxyurea (HU; Tatebayashi et al., 1998).  Consistent with the role of cohesin in establishing sister chromatid cohesion, yeast hypomorphic mutants of the cohesin complex and the cohesin regulatory protein ECO1/CTF7 are hypersensitive to IR-induced DSBs only in S- and G2-phases of the cell cycle when sister chromatids are present (Skibbens et al., 1999; Tatebayashi et al., 1998; Toth et al., 1999).  In chicken DT40 cells, conditional deletion of SCC1 results in defective sister chromatid cohesion, increased IR-induced chromosomal aberrations, and decreased 4-nitroquinoline-1-oxide-induced sister chromatid HR (Sonoda et al., 2006).  Similar to other DNA repair proteins, the human cohesin complex is recruited to laser-induced DNA damage foci in S- and G2-phases of the cell cycle in an ATM-independent and MRE11-dependent manner (Bekker-Jensen et al., 2006; Kim et al., 2002a).  The yeast cohesin complex also localizes to HO-induced DSBs in S- and G2-phases of the cell cycle (Strom et al., 2004; Unal et al., 2004).  This localization is dependent on the cohesin chromatin loader SCC2 and the DNA damage response protein MRE11 (Strom et al., 2004; Unal et al., 2004).  In yeast, cohesin is required for

repair of DSBs in S- and G2-phases of the cell cycle (Sjogren and Nasmyth,

2001).  At HO-induced DSBs in yeast, the cohesin complex facilitates sister

chromatid cohesion (Strom et al., 2004).  It is currently thought that this cohesin-

induced sister chromatid cohesion at DSBs facilitates strand invasion and

exchange during HR-mediated DNA damage repair (Figure 1-1).  Interestingly,

cohesion between sister chromatids after DNA damage is not only induced at

DSBs, but throughout the genome even on undamaged chromosomes (Strom et

al., 2007; Strom et al., 2004; Unal et al., 2007).  These results suggest that cohesin

functions not only at the DSB but throughout the genome to protect chromosome

integrity.

In addition to establishing cohesion between sister chromatids during a

DSB response, the cohesin complex also facilitates the DNA damage-induced

intra-S-phase checkpoint response that delays S-phase progression until DNA

repair is complete to prevent aberrant mitosis from occurring.  Human SMC1 is

phosphorylated after IR on serine 947 and serine 966 in an ATM and NBS1-

dependent manner (Kim et al., 2002b; Yazdi et al., 2002).  Overexpression of a

non-phosphorylatable SMC1 mutant blocks initiation of the intra-S-phase

checkpoint.  Consistently, knock-in mouse embryonic fibroblasts (MEF) in which

the wild-type copy of SMC1 has been replaced with a non-phosphorylatable

SMC1 mutant are hypersensitive to IR and MMS, fail to initiate an intra-S-phase

checkpoint, and display increased chromosomal aberrations (Kitagawa et al.,

2004). Therefore, phosphorylation of SMC1 by ATM is required for initiation of an intra-S-phase checkpoint and genome stability.

**The SMC2/4 Condensin Complex**

In addition to cohesion between sister chromatids established during the S phase of the cell cycle, chromosomes are further condensed to allow for the movement and segregation of sister chromatids to daughter cells during mitosis. The formation of stable, rod-like chromosomes during prometaphase of mitosis is mediated by the condensin complex (Gassmann et al., 2004).

*Architecture of the Condensin Complex*

Chromosome condensation during mitosis is mediated by the condensin complex. Condensin has two subtypes: condensin I and condensin II (Figure 1-5; Hirano, 2006a; Nasmyth and Haering, 2005a). Both condensin I and condensin II contain the core SMC2-SMC4 heterodimer (Ono et al., 2003). Similar to SMC1 and SMC3, SMC2 and SMC4 dimerize through their hinge domains. An intramolecular coiled-coil domain brings together the Walker A and Walker B motifs at the N- and C-termini of SMC2 and SMC4. These functional ATPase heads are linked by kleisin proteins, CAP-H for condensin I and CAP-H2 for condensin II (Hirano, 2006a). The condensin complexes also contain additional

non-SMC proteins. Condensin I contains CAP-D2 and CAP-G, while condensin II contains CAP-D3 and CAP-G2 (Ono et al., 2003). The functions of these non-SMC proteins are unclear. Electron microscopy studies showed that the condensin complex can adopt a ring-shaped structure similar to cohesin. Condensin can also adopt a lollipop-like structure, with the coiled-coil and hinge domains of SMC2-SMC4 projecting away from a protein mass that includes the head domains of SMC2-SMC4 and the non-SMC proteins (Stray et al., 2005). How or whether condensin I and condensin II vary in function is unknown. Both condensin I and condensin II are excluded from the nucleus during interphase. Condensin I associates on chromatin after nuclear envelope breakdown during mitosis, whereas condensin II associates with chromatin before nuclear envelope breakdown (Ono et al., 2004). By cytological examination, chromosome-bound condensin I and condensin II do not overlap (Ono et al., 2004). Depletion of condensin I or condensin II causes distinct abnormalities in chromosome morphology (Ono et al., 2003), suggesting that the two complexes may not be functionally redundant.

*Chromosome Condensation*

The mechanism by which the condensin complex organizes chromosomes during mitosis into their fully compacted and stable structure is currently unresolved. Several studies in multiple organisms have established that

inactivation of condensin does not result in completely uncondensed chromosomes, but rather compacted chromosomes that are not properly structured into rigid rods (Hudson et al., 2003). The identity of those factors that mediate chromosome compaction in the absence of condensin is unknown. These studies suggest that condensin mediates the organization of compacted chromosomes into higher order structures that give rise to familiar metaphase chromosomes. Clues into how condensin organizes chromosomes come from its activities *in vitro*. Addition of DNA to purified Xenopus condensin stimulates its ATPase activity (Kimura and Hirano, 1997). Condensin promotes the positive supercoiling of closed circular DNA when in the presence of topoisomerase I and ATP, but not the nonhydrolyzable ATP analog, AMP-PNP (Kimura and Hirano, 1997). Furthermore, condensin purified from mitotic extracts was much more active in promoting DNA supercoiling than condensing from interphase extracts, suggesting that this activity of condensin might be cell-cycle regulated (Kimura and Hirano, 1997). The supercoiling of DNA by condensin could promote mitotic chromosome formation, but whether this activity of condensin occurs *in vivo* is unclear. Further evidence suggests that condensin functions with topoisomerase II. *In vitro* studies have shown that condensin can promote knotting of nicked circular DNA in the presence of topoisomerase II (Kimura et al., 1999). Electron microscopy revealed that most of these knots had a trefoil structure (Kimura et al., 1999). Based on this knot architecture, it has been proposed that topoisomerase II

intertwines condensin-induced positive supercoils to form the knot (Hirano, 2006a). By looping DNA in this manner, condensin would promote DNA compaction (Figure 1-6).

**The SMC5/6 Complex**

Cohesion and condensation of chromosomes during mitosis prevents aneuploidy by facilitating faithful segregation of sister chromatids to daughter cells during mitosis. In addition to these processes, DNA damage repair mechanisms safeguard a cell's genome from a wide variety of potentially mutagenic DNA damages. The SMC5/6 complex of proteins is intimately involved in facilitating repair of DNA damage.

*Architecture of the SMC5/6 Complex*

Similar to the SMC1/3 cohesin and SMC2/4 condensin complexes, the SMC5/6 complex is composed of two SMC family proteins, SMC5 and SMC6, as well as several non-SMC elements (NSE; Figure 1-7; Fujioka et al., 2002; Hu et al., 2005; McDonald et al., 2003; Morikawa et al., 2004; Pebernard et al., 2004; Pebernard et al., 2006; Sergeant et al., 2005; Taylor et al., 2001; Zhao and Blobel, 2005). Although the primary sequence of both SMC5 and SMC6 are more divergent than SMC1-4, they are speculated to form functional ATPases by

intramolecular coiled-coiled domains bringing together Walker A and B motifs

(Figure 1-8). SMC5 and SMC6 bind in their hinge region to form the core of the

SMC5/6 complex (Figure 1-7; Sergeant et al., 2005). The head domains of SMC5

and SMC6 are brought together by NSE4 (Figure 1-7; Palecek et al., 2006).

Secondary structure analysis has predicted that NSE4 has helix-turn-helix and

winged-helix folds similar to other kleisin family proteins, such as SCC1, CAP-H,

and CAP-H2 (Figure 1-8; Palecek et al., 2006). Additional NSE proteins have

been shown to bind to the SMC5/6 complex. These include NSE1,

MMS21/NSE2 (herein referred to as MMS21 for simplicity), NSE3, NSE5, and

NSE6 (Figure 1-7; Fujioka et al., 2002; Hu et al., 2005; McDonald et al., 2003;

Morikawa et al., 2004; Pebernard et al., 2004; Pebernard et al., 2006; Sergeant et

al., 2005; Taylor et al., 2001; Zhao and Blobel, 2005). The yeast NSE1, NSE3,

NSE4, NSE5, and NSE6 have been shown to bind to the head domains of

SMC5/6 in *in vitro* biochemical assays (Figure 1-7; Palecek et al., 2006).

However, MMS21 does not bind to the head domains of SMC5/6, but rather binds

to the coiled-coil region of SMC5 (Figure 1-7; Sergeant et al., 2005). *In vitro*

NSE1 binds to NSE3 and both NSE1 and NSE3 bind NSE4 (Figure 1-7; Palecek

et al., 2006).

Interestingly, several of these NSE proteins have potentially intriguing

activities. MMS21 contains a modified RING (really interesting new gene)

domain known as a SP-RING (SIZ/PIAS-RING) domain that is associated with

E3 SUMO (small ubiquitin-like modifier) ligase activity (Figure 1-8; McDonald et al., 2003; Pebernard et al., 2004).  SUMO is a small protein that is covalent attached to lysine residues on protein substrates by a multi-step enzymatic cascade involving SUMO E1 (AOS1/UBA2), E2 (UBC9), and E3 enzymes (Figure 1-9; Johnson, 2004).  Although SUMO is conjugated to substrates in a similar manner as ubiquitination, it does not generally target proteins for proteasome-dependent degradation (Johnson, 2004).  Instead, it can have wide-ranging, protein specific effects, such as alteration of protein-protein interactions, protein subcellular localization, or protein stability (Gill, 2004).  Intriguingly, the SMC5/6 complex component NSE1 contains a RING domain that is often found in E3 ubiquitin ligases (Figure1-8; Fujioka et al., 2002; McDonald et al., 2003).

In addition to MMS21 and NSE1, several other components have interesting domains, but their function is unknown.  NSE3 contains a MAGE (melanoma-associated antigen gene) domain that has no known function (Figure 1-8; Pebernard et al., 2004).  NSE6 contains HEAT domain repeats, but the function of these in NSE6 is unknown (Figure 1-8; Palecek et al., 2006; Pebernard et al., 2006).  NSE5 contains no known domains (Palecek et al., 2006; Pebernard et al., 2006).  The yeast SMC5/6 complex has also been shown to associate with several other proteins that are not thought to be core components of the SMC5/6 complex.  These SMC5/6 complex associated proteins include RAD60/NIP45 and RAD62 (Morikawa et al., 2004; Morishita et al., 2002).  Interestingly,

RAD60/NIP45 contains two SUMO-like domains that are important for

RAD60/NIP45-mediated replication stress response (Novatchkova et al., 2005;

Raffa et al., 2006).

*The SMC5/6 Complex Promotes Homologous Recombination*

The SMC5/6 complex was originally identified in a 1970s genetic screen

for radiation sensitive mutations in yeast (Nasim and Smith, 1975). Hypomorphic

mutation of any component of the SMC5/6 complex results in hypersensitivity to

a broad spectrum of DNA damaging agents, such as IR, UV, methylmethane

sulfonate (MMS), mitomycin C (MMC), and HU (Fujioka et al., 2002; Lehmann

et al., 1995; McDonald et al., 2003; Morikawa et al., 2004; Onoda et al., 2004).

SMC5/6 complex mutants have a decreased capacity to repair IR-induced double-

strand breaks (Verkade et al., 1999). They are epistatic with RAD51 suggesting

that the SMC5/6 complex functions in HR-mediated DNA damage repair (Harvey

et al., 2004; Lehmann et al., 1995; McDonald et al., 2003; Pebernard et al., 2004).

Mutation of the SMC5/6 complex in yeast and plants results in sister chromatid

HR defects (De Piccoli et al., 2006; Mengiste et al., 1999). Additionally, SMC5/6

complex mutants display gross chromosomal rearrangements, suggesting that the

SMC5/6 complex is required for genome maintenance and stability (De Piccoli et

al., 2006; Fousteri and Lehmann, 2000).

Importantly, the requirement for SMC5/6 in the proper response to DNA damage is not due to a defect in the DNA damage-induced cell cycle checkpoint, since activation of the critical checkpoint kinase, CHK1, is normal in SMC5/6 mutant yeast (Harvey et al., 2004; Verkade et al., 1999). However, SMC5/6 mutants reenter the cell cycle after DNA damage with similar kinetics as wild-type cells even though DNA repair is not complete (Harvey et al., 2004; Verkade et al., 1999). Therefore, the SMC5/6 complex may be required for DNA damage-induced cell cycle checkpoint maintenance.

The role of the SMC5/6 complex in HR is further supported by studies in yeast using chromatin immunoprecipitation (ChIP) followed by microarray experiments (ChIP-on-Chip). In undamaged cells, the SMC5/6 complex localizes to centromeric DNA, along chromosome arms in intergenic regions, and ribosomal DNA (rDNA) repeats (Lindroos et al., 2006). This localization partially overlaps with the chromosomal localization of the cohesin complex. Interestingly, the localization of the SMC5/6 complex is altered in SCC1 yeast mutants, suggesting potential crosstalk between the SMC5/6 and cohesin complexes (Lindroos et al., 2006). More importantly, the SMC5/6 complex has been shown to be recruited to HO-induced DSBs in yeast (De Piccoli et al., 2006; Lindroos et al., 2006). Consistent with its function in HR, the SMC5/6 complex does not localize to HO-induced DSBs in yeast without sister chromatids (G1-phase of the cell cycle) that cannot utilize HR to repair DSBs (De Piccoli et al.,

2006; Lindroos et al., 2006). This localization is dependent on the MRN complex component, MRE11 (Lindroos et al., 2006). In addition to its recruitment and function at DSBs, the SMC5/6 complex is required for generation of global cohesion between sister chromatids after DNA damage (Strom et al., 2007).

*The SMC5/6 Complex Promotes the Restart of Collapsed Replication Forks*

In addition to its role in repairing IR-induced or endonuclease-induced DSBs, the SMC5/6 complex has been shown to be important for repair of collapsed replication forks. During DNA replication, replication forks stall at sites of DNA damage (Branzei and Foiani, 2005). If the replication fork cannot proceed, it will eventually collapse, potentially generating a DSB (Kogoma, 1996). Previous studies suggest that one mechanism by which collapsed replication forks can be restarted is by HR (Arnaudeau et al., 2001). In fission yeast, the SMC5/6 complex is required for restart of collapsed replication forks (Ampatzidou et al., 2006). In addition, yeast mutants defective in the SUMO ligase activity of the SMC5/6 complex component MMS21 show an increased number of collapsed replication forks after MMS treatment (Branzei et al., 2006). The target of MMS21-induced sumoylation required for restarting collapsed replication forks is unknown.

Replication fork collapse can also occur when DNA replication and transcriptional machinery collide (Liu and Alberts, 1995). Because these

collapsed DNA replication forks are restarted by HR, they are particularly

dangerous in repetitive DNA elements, such as rDNA, that can be expanded and

contracted by unequal sister chromatid HR (Hawley and Marcus, 1989).

Therefore it is imperative that repetitive elements prevent replication fork

collapse.  To decrease the frequency of replication fork collapse, rDNA is

replicated unidirectionally to decrease the chances of transcriptional and

replication machinery colliding (Brewer and Fangman, 1988).  Unidirectional

replication is achieved by the binding of the FOB1 protein to specific sites in the

rDNA known as replication fork barriers (Brewer and Fangman, 1988).

Interestingly, the SMC5/6 complex localizes to rDNA and mutation of the

SMC5/6 complex results in defective rDNA segregation during mitosis (Lindroos

et al., 2006; Torres-Rosell et al., 2005b).  In addition, the SMC5/6 complex

localizes to nucleoli, the nuclear structures containing rDNA, and this localization

is increased upon replication stress (Ampatzidou et al., 2006; Torres-Rosell et al.,

2005b).  Consistent with a role of the SMC5/6 complex in facilitating collapsed

replication fork restart in rDNA, SMC5/6 mutants display increased rDNA

instability and increased number of HR protein foci in nucleoli (Torres-Rosell et

al., 2005a; Torres-Rosell et al., 2007).


*The SMC5/6 Complex and Telomeres*

In addition to rDNA, telomeres are a major repetitive component of the genome. Telomeres are proteinaceous, repetitive DNA elements, TTAGGG in humans, which comprise 5-15 kilobases at the ends of chromosomes (Blackburn, 2001). They form loops, known as T-loops, which hide the ends of chromosomes from being recognized as DSBs. Telomeres are shortened after every division due to the end-replication problem of the lagging strand (Harley et al., 1990). Critically short telomeres result in cellular senescence (Bodnar et al., 1998). Therefore, telomeres have been suggested to be a counting mechanism for cellular proliferation (Bodnar et al., 1998). The majority of cancer cells overcome this limited proliferative potential by the transcriptional upregulation of telomerase, the reverse transcriptase that elongates telomeres (Shay and Bacchetti, 1997). However, some cancer cells are incapable upregulating telomerase and rely on an alternative mechanism to elongate telomeres known as ALT (alternative lengthening of telomeres; Muntoni and Reddel, 2005). ALT facilitates telomere elongation by promoting telomere recombination (Dunham et al., 2000). The mechanism by which ALT cells promote telomere HR is unknown; however one hallmark of ALT cells that is thought to be required for telomere elongation is the recruitment of telomeres into PML bodies (Yeager et al., 1999). The recruitment of telomeres to these specialized PML bodies, known as APBs (ALT-associated PML bodies), is thought to localize telomeres and HR proteins together to facilitate telomere HR.

The SMC5/6 complex has been shown to localize to telomeres in yeast (Zhao and Blobel, 2005; Lindross et al., 2006). In addition, mutation of MMS21 in yeast impairs clustering of telomeres into telomeric bouquets during meiosis (Zhao and Blobel, 2005). Therefore, the SMC5/6 complex may be important in telomere biology, but the mechanisms by which it does so is unknown.

In this thesis, we have characterized the function of the human SMC5/6 complex. We first address the biochemical and functional properties of one component of the SMC5/6 complex, MMS21, in DNA repair. We next investigated the role of the SMC5/6 complex in homologous recombination-mediated repair of DSBs. Finally, we examined whether the SMC5/6 complex is important for telomere recombination and maintenance.
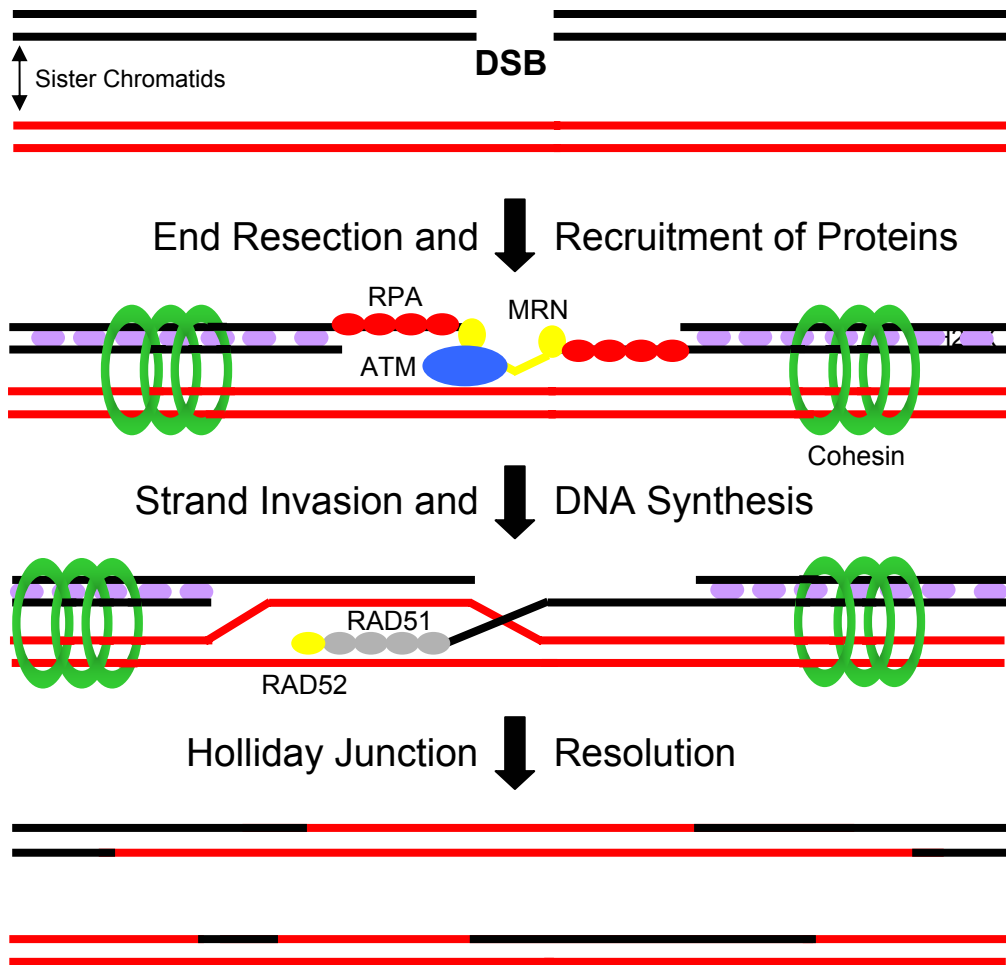
**Figure 1-1.  Homologous recombination-mediated DSB repair**
HR-mediated DSB repair uses the sister chromatid as a repair template.  First DSBs are recognized and a number of proteins are recruited.  The chromatin around a DSB is modified, such as phosphorylation of H2AX (γH2AX).  The MRE11/RAD50/NBS1 (MRN) protein complex binds and tethers the broken DNA ends.  DSBs are processed to generate 3' single strand DNA overhangs which are bound by RPA.  Protein kinases such as ATM localize to DSBs and mediate many downstream events.  After strand resection, RPA is displaced by RAD51 with the help of other HR mediators, such as RAD52.  The RAD51 nucleofilament promotes strand invasion and homology pairing to the sister chromatid.  DNA synthesis fills in the missing nucleotides across the DSB. Finally, the Holliday junction is resolved.
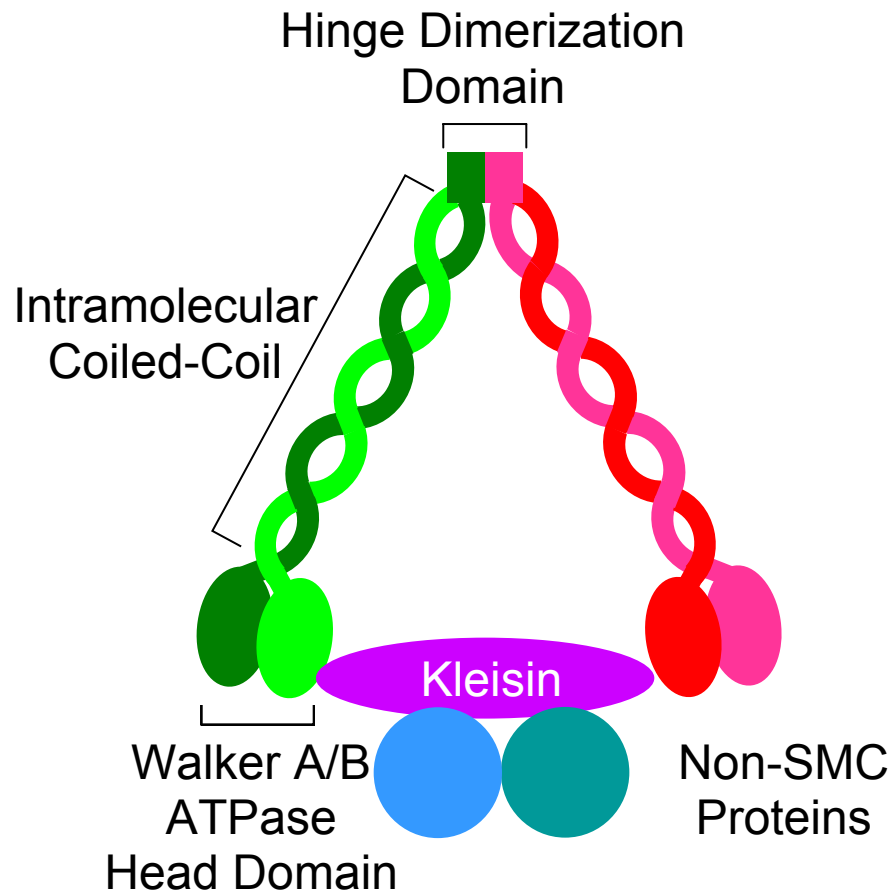
**Figure 1-2. General architecture of SMC protein complexes**
A functional ATPase head domain is formed by N-terminal Walker A and C-terminal Walker B motifs that are brought together by an intramolecular coiled-coil. Two SMC proteins heterodimerize through their hinge domains. Kleisin proteins link the two head domains of the SMC heterodimer. Other non-SMC proteins bind to the complex and perform additional functions.
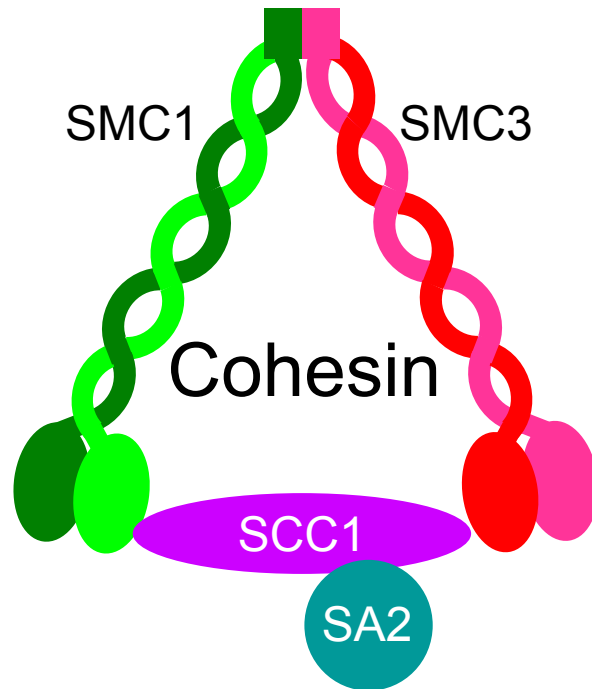
**Figure 1-3.  Architecture of the cohesin complex**
The cohesin complex is made up of the core heterodimer of SMC1-SMC3.  Both
SMC1 and SMC3 form a functional ATPase by intramolecular coiled-coil motif
that brings together Walker A/B motifs.  SMC1 and SMC3 dimerize in their hinge
region.  The head domains of the SMC1-SMC3 heterodimer are linked by the
SCC1/RAD21/MCD1 kleisin subunit to form a proposed ring-shaped structure.
The non-SMC component SA2/SCC3 also binds to the cohesin complex, but the
precise function of SA2 is still undetermined.
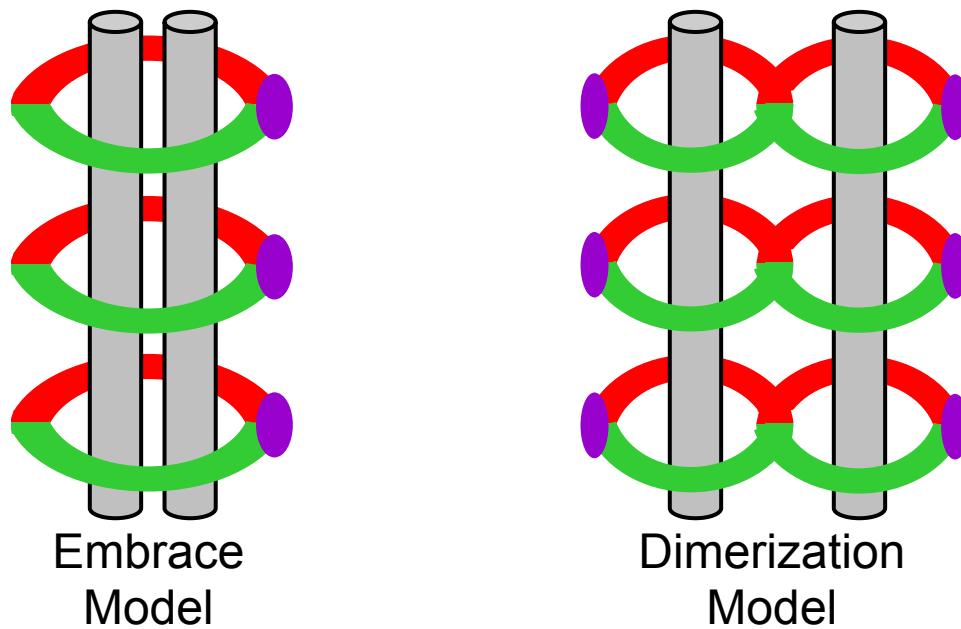
**Figure 1-4. Models for cohesin-induced sister chromatid cohesion**
The embrace model proposes that one cohesin ring molecule traps both sister chromatid DNA molecules (gray). The dimerization model proposes that each sister chromatid DNA molecule is trapped by a distinct cohesin complex and that these complexes somehow interact to form sister chromatid cohesion during mitosis.
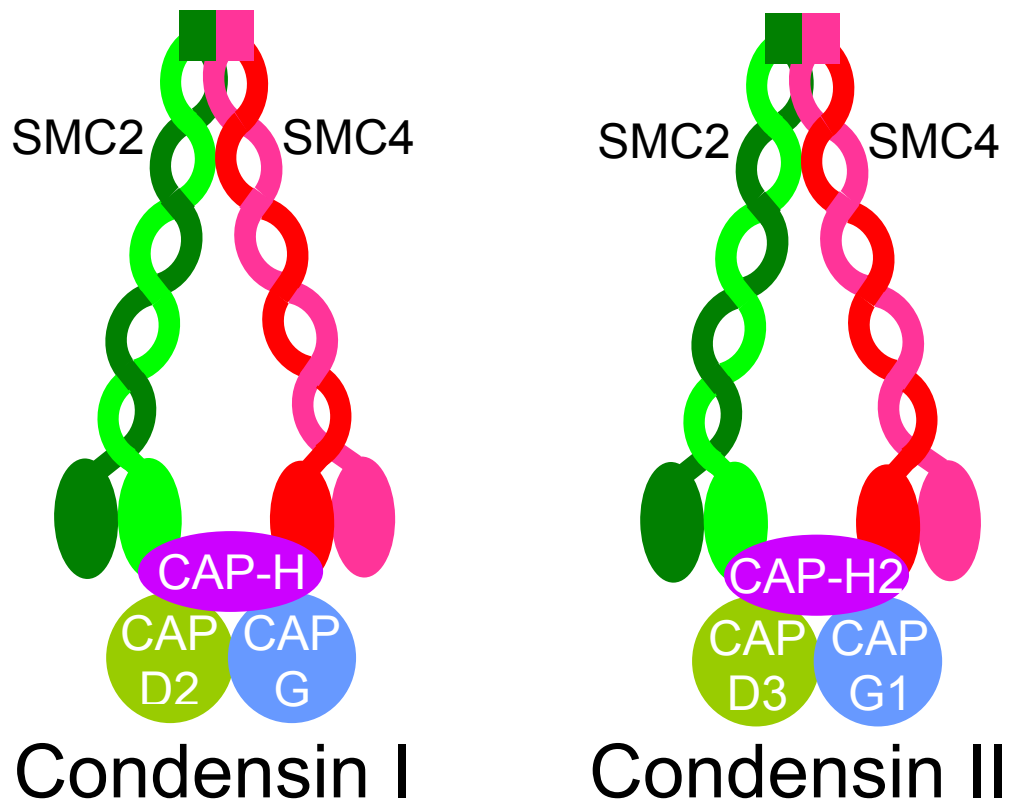
**Figure 1-5.  Architecture of the condensin I and II complexes**
Both condensin I and condensin II contain the SMC2-SMC4 heterodimer.  CAP-H and CAP-H2 are the kleisin subunits that link the head domains of SMC2-SMC4 in condensin I and condensin II, respectively.  Condensin I contains the non-SMC proteins, CAP-D2 and CAP-G, whereas condensin II contains CAP-D3 and CAP-G1.  Cryo-electron microscopy experiments have revealed a more condensed lollipop-shape of the condensin complex, as compared to the more ring-shape of the cohesin complex.
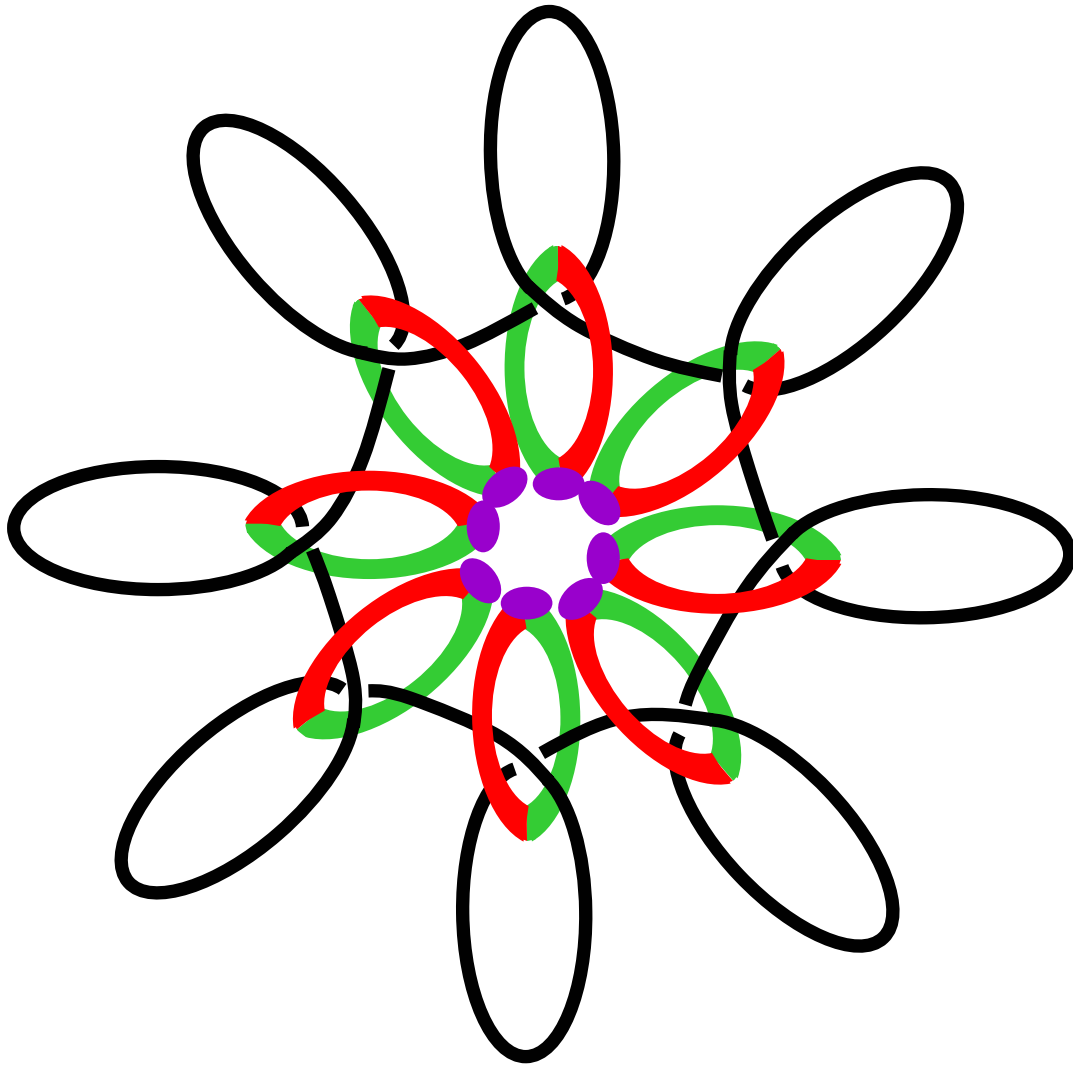
**Figure 1-6.  Model for condensin-mediated chromosome condensation**
Condensin complexes have been suggested to loop DNA (black lines) through the inside of the condensin ring structure.  Additionally, it has been proposed that further compaction of DNA during mitosis occurs by intermolecular interactions between numerous condensin molecules.
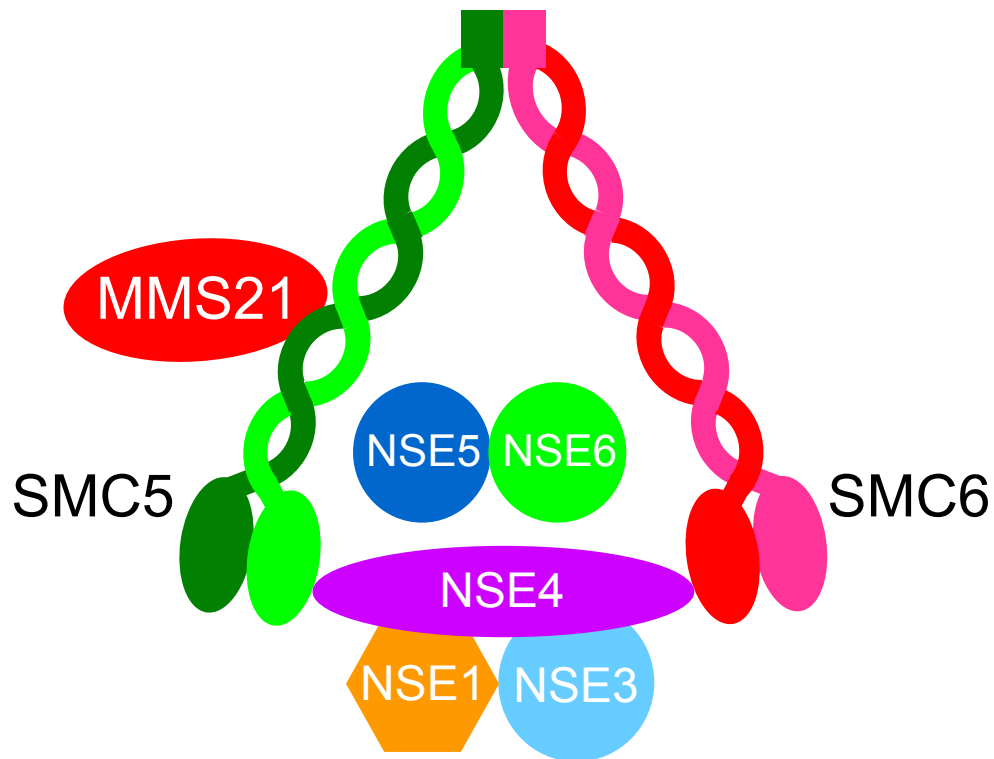
**Figure 1-7. Architecture of the SMC5/6 complex**
The SMC5/6 complex is composed of the SMC5-SMC6 heterodimer and six non-SMC element (NSE) proteins. The putative ATPase head domains of SMC5 and SMC6 are linked together by the kleisin-like protein NSE4. The putative E3 ubiquitin-ligase NSE1 binds the MAGE domain protein NSE3. The NSE1-NSE3 complex interacts with NSE4. NSE5 and NSE6 bind to the head domains of SMC5 and SMC6. The E3 SUMO ligase MMS21 binds to the coiled-coil region of SMC5.
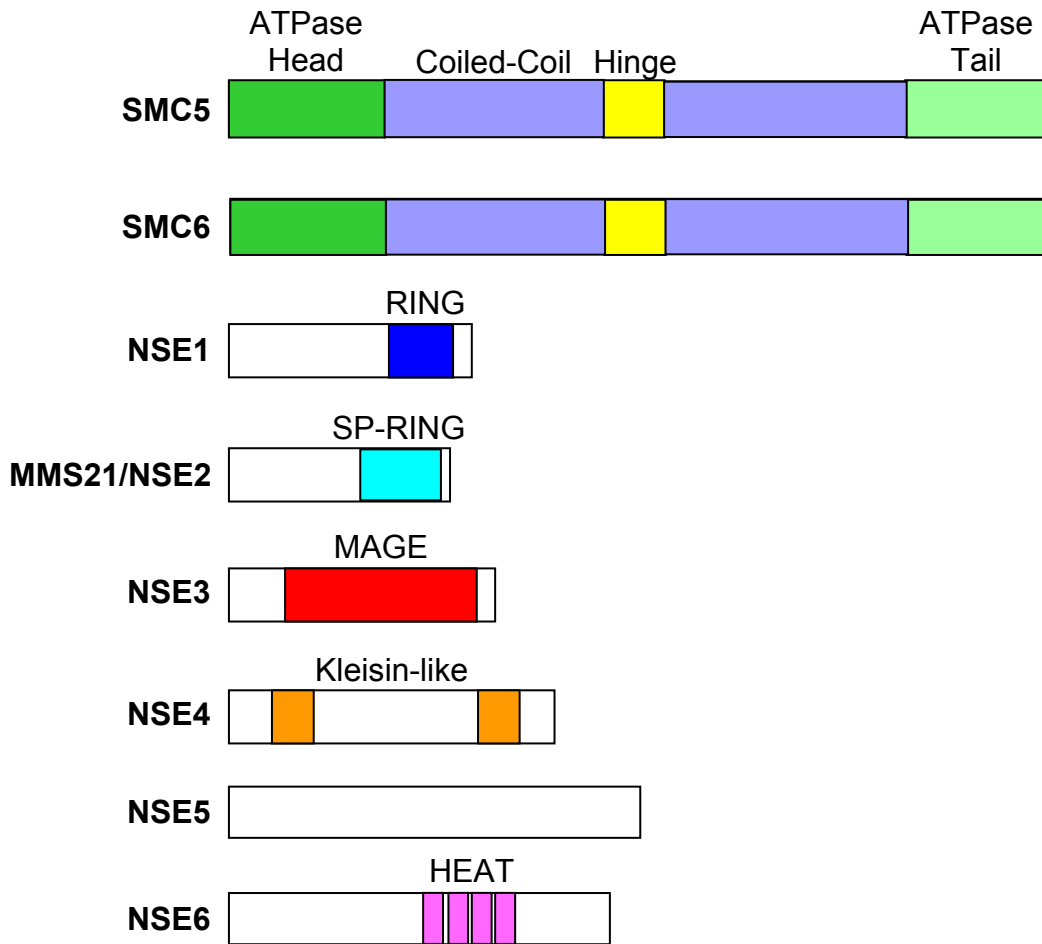
**Figure 1-8. Domain organization of SMC5/6 complex proteins**
SMC5 and SMC6 contain a N-terminal ATPase head domain with a Walker A motif and a C-terminal ATPase tail domain with a Walker B motif that are brought together by an intramolecular coiled-coil. The hinge domain mediates binding between SMC5 and SMC6. NSE1 contains a RING domain that is often associated with E3 ubiquitin ligase activity. MMS21/NSE2 contains a SP-RING domain that is often associated with E3 SUMO ligase activity. NSE3 contains a MAGE domain with unknown activity. Based on secondary structure prediction analysis, NSE4 contains helix-turn-helix and winged-helix motifs similar to other kleisins. NSE5 has no known domains. NSE6 contains several HEAT repeats.
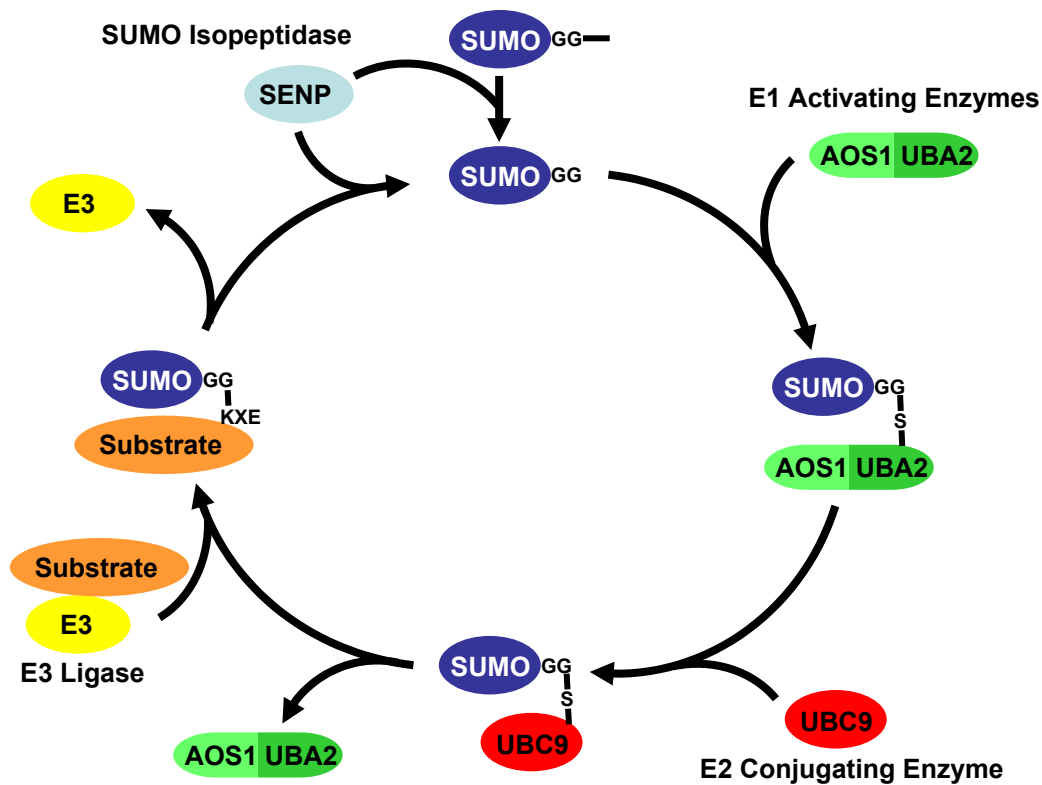
**Figure 1-9. The SUMO modification cycle**
SUMO is synthesized as a precursor and processed by SUMO isopeptidases to expose a diglycine motif. SUMO is activated by the E1 activating heterodimeric AOS1/UBA2 enzyme. The UBC9 E2 conjugating enzyme then promotes covalent attachment of SUMO to lysine residues on protein substrates. E3 SUMO ligases enhance sumoylation by facilitating interactions between E2 and substrates. SUMO modifications can be reversed by SUMO isopeptidases that remove SUMO conjugations from protein substrates.

# CHAPTER II: HUMAN MMS21 IS A SUMO LIGASE REQUIRED FOR DNA REPAIR

## INTRODUCTION

Accurate replication and segregation of a cell's genome to its daughter cells are essential for the survival of an organism (Bharadwaj and Yu, 2004; Nasmyth, 2002; Rajagopalan and Lengauer, 2004). To maintain genomic stability, cells must also be able to cope with DNA damage that occurs both intentionally and unintentionally, including double-strand breaks (DSBs), single-strand breaks, and other types of lesions (Kastan and Bartek, 2004; Zhou and Elledge, 2000). In addition to being caused by exogenous factors, certain types of DNA damage, such as DSBs, are also crucial intermediates during meiotic homologous recombination (HR), V(D)J recombination, and immunoglobulin class-switch recombination in immune cells (Khanna and Jackson, 2001; West, 2003a). To prevent DNA damage from compromising the genetic integrity of an organism, cells employ surveillance mechanisms to sense damaged DNA and to elicit coordinated cellular responses, such as DNA repair, cell cycle arrest, and apoptosis (Kastan and Bartek, 2004; Sancar et al., 2004; Zhou and Elledge, 2000). Mutations of genes involved in DNA damage response pathways can lead to cancer, immune deficiencies, and other human diseases (Kastan and Bartek, 2004; Khanna and Jackson, 2001; Zhou and Elledge, 2000).

Two related protein kinases, ATM and ATR, are key proximal signal transducers of the DNA damage response (Kastan and Bartek, 2004; Sancar et al., 2004; Zhou and Elledge, 2000). They phosphorylate distinct, yet overlapping, sets of downstream substrates, including CHK1, CHK2, p53, BRCA1, and NBS1 (Kastan and Bartek, 2004; Sancar et al., 2004; Zhou and Elledge, 2000). CHK1 and CHK2 are effector kinases, and in turn phosphorylate the CDC25 family of phosphatases and p53, leading to cell cycle arrest or apoptosis (Kastan and Bartek, 2004; Sancar et al., 2004; Zhou and Elledge, 2000). Upon DNA damage, many proteins involved in DNA damage sensing and repair are enriched in nuclear foci, which are thought to represent active cellular centers for DNA repair (Bartek et al., 2004; Lisby et al., 2004; Lisby and Rothstein, 2004; West, 2003a).

The structural maintenance of chromosomes (SMC) family of proteins is essential for chromosomal architecture and organization (Hagstrom and Meyer, 2003; Hirano, 2002; Petronczki et al., 2003). There are six known eukaryotic SMC proteins, SMC1-6, which form three types of heterodimers (Hirano, 2002). The SMC1/3 heterodimer is a part of the cohesin complex that maintains sister chromatid cohesion (Hagstrom and Meyer, 2003; Hirano, 2002; Koshland and Guacci, 2000; Petronczki et al., 2003). SMC2/4 are components of the condensin complex that mediates chromosome condensation during mitosis (Hirano, 2002; Swedlow and Hirano, 2003). A third SMC complex containing SMC5/6 is mainly involved in the cellular response to DNA damage (Fousteri and Lehmann, 2000;

Hagstrom and Meyer, 2003; Hirano, 2002; Lehmann et al., 1995; Onoda et al.,

2004).

Most studies on the SMC5/6 complex have been conducted in fission and

budding yeast. The yeast SMC5/6 complex contains several non-SMC elements

(NSE), including NSE1, MMS21/NSE2 (here after referred to MMS21 for

simplicity), NSE3, and NSE4 (Fujioka et al., 2002; Hu et al., 2005; McDonald et

al., 2003; Morikawa et al., 2004; Pebernard et al., 2004; Sergeant et al., 2005;

Zhao and Blobel, 2005). SMC5, SMC6, NSE1, and MMS21 are all essential

genes in yeast (Fousteri and Lehmann, 2000; Fujioka et al., 2002; Lehmann et al.,

1995; McDonald et al., 2003; Onoda et al., 2004; Pebernard et al., 2004; Prakash

and Prakash, 1977b). Cells harboring hypomorphic alleles of these genes show an

increased sensitivity to a broad spectrum of DNA damage agents, including

ionizing radiation (IR), UV, and methyl methanesulfonate (MMS; Fousteri and

Lehmann, 2000; Fujioka et al., 2002; Hu et al., 2005; Lehmann et al., 1995;

McDonald et al., 2003; Onoda et al., 2004; Pebernard et al., 2004; Prakash and

Prakash, 1977a; Prakash and Prakash, 1977b). Genetic analysis has shown that

SMC5/6, NSE1, and MMS21 function together with RAD51 in the repair of DNA

DSBs through HR in yeast (Harvey et al., 2004; McDonald et al., 2003;

Montelone and Koelliker, 1995; Onoda et al., 2004; Pebernard et al., 2004).

Recently, the SMC5/6 complex has also been shown to play a role in the

segregation of repetitive sequences during mitosis in budding yeast (Torres-Rosell

et al., 2005b).  A similar SMC5/6 complex exists in human cells, although the

non-SMC components of this complex have not been characterized (Taylor et al.,

2001).

Small ubiquitin-like modifier (SUMO) is an ubiquitin-like protein that can

be covalently conjugated to target proteins (Gill, 2004; Johnson, 2004).  Similar

to ubiquitination, sumoylation of substrates is catalyzed by a cascade of enzymes:

the E1 SUMO-activating enzyme (AOS1-UBA2), the E2 conjugating enzyme

(UBC9), and the E3 SUMO ligases (Gill, 2004; Johnson, 2004).  Several classes

of SUMO ligases have been identified (Gill, 2004; Johnson, 2004).  Among them,

the PIAS class of SUMO ligases contains an SP-RING domain that is similar to

the RING-finger domain found in many ubiquitin ligases (Gill, 2004; Johnson,

2004).  Unlike ubiquitination, sumoylation of substrates does not strictly require a

SUMO ligase.  UBC9 is sufficient to mediate sumoylation due to its ability to

directly recognize $\Psi$KXE ($\Psi$, hydrophobic residues; X any residue) motifs on

substrates.  SUMO ligases merely enhance the rate of sumoylation.  Furthermore,

sumoylation of substrate proteins does not generally lead to their degradation

(Gill, 2004; Johnson, 2004).  Instead, it appears to regulate the functions of target

proteins by multiple, context-dependent mechanisms, such as altering their

subcellular localization, increasing their stability, or mediating their binding to

other proteins (Gill, 2004; Johnson, 2004).

Interestingly, NSE1 contains a RING finger domain similar to ubiquitin ligases whereas MMS21 contains a SP-RING domain that is related to the PIAS family of SUMO ligases (McDonald et al., 2003). It has recently been reported that both budding and fission yeast MMS21 protein function as SUMO ligases (Andrews et al., 2005; Zhao and Blobel, 2005). Therefore, the SMC5/6 complex is a conserved chromatin-associated DNA repair complex that potentially has both ubiquitin ligase and SUMO ligase activities. Numerous studies have established multiple roles of sumoylation in regulating cellular responses for coping with DNA damage in both yeast and mammals (Hardeland et al., 2002; Ho et al., 2001; Hoege et al., 2002; Maeda et al., 2004; Mao et al., 2000; Stelter and Ulrich, 2003; Taylor et al., 2002). Recently, using an *in vitro* expression cloning (IVEC) strategy, we have identified a large panel of human SUMO substrates (Gocke et al., 2005). Several of these substrates are involved in DNA repair, including Ku80, XRCC1, and translin-associated factor-X protein (TRAX; Gocke et al., 2005).

Our interest in sister chromatid cohesion and ubiquitin-like protein ligases prompted us to investigate the function of the SMC5/6 complex in human cells. We show that, similar to the yeast MMS21, human MMS21 is a SUMO ligase that stimulates the sumoylation of SMC6 and TRAX. RNAi-mediated knockdown of MMS21 increases the propensity of HeLa cells to undergo apoptosis in response to various DNA damage agents. Importantly, ectopic

expression of the wild-type MMS21, but not a ligase-inactive mutant of MMS21, in MMS21-RNAi cells rescues their hypersensitivity to DNA damage. This indicates that the SUMO ligase activity of MMS21 is required for proper cellular response to DNA damage. Upon DNA damage, MMS21-RNAi cells contained higher ATM/ATR activity and an increased number of phospho-CHK2 nuclear foci. Consistently, we observed an increased amount of unrepaired DNA lesions in MMS21-RNAi cells as measured by the comet assay. These results suggest that MMS21 and the SMC5/6 complex play an important role in the repair of damaged cellular DNA.

## MATERIALS AND METHODS

### Plasmids and antibodies

The coding regions of human NSE1 and MMS21 were amplified by PCR from a human fetal thymus cDNA library (Clontech) and cloned into appropriate vectors. The coding region of human SMC6 was amplified by PCR from a human testes cDNA library (Clontech) and cloned into appropriate vectors. The amplified product from the testes library was an alternatively spliced form of SMC6 as was reported previously (Taylor et al., 2001). This form of SMC6 results in an N-terminal truncated protein of 95 kDa. The SMC5 plasmid was obtained from AR Lehmann (University of Sussex, United Kingdom). The ligase-inactive mutants of MMS21 were constructed with the QuikChange site-directed mutagenesis kit (Stratagene). The full-length and an N-terminal fragment of MMS21 (MMS21N; residues 1-165) and the N-terminal fragment of SMC5 (hSMC5N; residues 1-233) were expressed in bacteria and purified as GST-fusion proteins using glutathione-agarose beads (Amersham). GST-MMS21N and GST-hSMC5N were used for antibody production (Zymed Laboratories). Crude antibody sera were first pre-cleared with GST-coupled Affi-Gel beads (Bio-Rad) and subsequently affinity-purified using beads coupled to GST-MMS21N or GST-hSMC5N. An SMC5 antibody for western blotting was obtained from AR Lehmann (University of Sussex, United Kingdom). The

commercial antibodies used in this study are as follows: anti-myc and anti-HA

antibodies (Roche; 1 μg/ml), rabbit anti-ATM/ATR phospho-substrates antibody

(Cell Signaling Technology; 1:100), rabbit anti-phospho-CHK2 (T68) antibody

(Cell Signaling Technology; 1:100), mouse anti-Asp214 cleaved PARP antibody

(Cell Signaling Technology; 1:1000), and mouse anti-GMP1 (SUMO1) antibody

(Zymed Laboratories, 1:500).


**_In vitro_ sumoylation assay**

Proteins were _in vitro_ translated (IVT) from pCS2-myc plasmids in

reticulocyte lysate (Promega) in the presence of $^{35}$S-methionine.  IVT proteins

was then subjected to _in vitro_ sumoylation reactions that contained 2 μl of IVT

product, 2 μg of AOS1-UBA2, 0.5 μg of UBC9, 1 μg of SUMO1, and 1 μl of

energy mix (150 mM phosphocreatine, 20 mM ATP, 2 mM EGTA, 20 mM

$MgCl_2$, pH 7.7). Reactions were adjusted to 10 μl with XB buffer (10 mM HEPES

pH 7.7, 1 mM $MgCl_2$, 0.1 mM $CaCl_2$, 100 mM KCl, and 50 mM sucrose).  After 2

hrs at 30˚C, reactions were stopped with 10 μl of 2X SDS sample buffer, boiled,

and subjected to SDS-PAGE followed by autoradiography.  Reactions containing

GST-MMS21 were performed as described above except for 0.5 μg recombinant

GST-MMS21 purified from bacteria was used.  Detection of GST-MMS21

sumoylation was performed by incubating the SUMO reactions with glutathione-

agarose beads for 1 hr at 4˚C.  After washing, proteins bound to beads were eluted

with 2X SDS sample buffer, boiled, and subjected to SDS-PAGE followed by immunoblotting with anti-SUMO1.

Human AOS1-UBA2, UBC9, and SUMO1 proteins were expressed and purified in bacteria as described previously (Gocke et al., 2005). Briefly, pET28b-SUMO1 and pET28b-UBC9 were expressed as His$_6$-tagged proteins in BL21(DE3) and purified using Ni$^{2+}$-NTA beads per the manufacture's protocols (Qiagen). For the expression of AOS1-UBA2, pET11c-AOS1 and pET28b-UBA2 were co-transformed into BL21(DE3). The resulting AOS1-UBA2 complex was purified by Ni$^{2+}$-NTA beads followed by a Superdex 200 gel filtration column (Amersham Biosciences) to remove the excess amount of AOS1. MMS21 was expressed as a GST-tagged protein in BL21(DE3) and purified using glutathione-agarose beads (Amersham Biosciences).

**Cell Culture, transfections, and treatments**

HeLa cells were grown in DMEM (Invitrogen) supplemented with 10% fetal bovine serum (Invitrogen), and 100 μg/mL penicillin and streptomycin (Invitrogen). At 40-50% confluency, plasmid or siRNA transfection was performed using the Effectene reagent (Qiagen) and the Oligofectamine reagent (Invitrogen), respectively. The siRNA oligonucleotides against MMS21 (5'-CUCUGGUAUGGACACAGCUTT-3') and SMC5 (5'-GCAGUGGAUUCAGGGUUGATT-3') were chemically synthesized at an in-

house facility. The annealing and transfection of the siRNAs were performed as previously described (Elbashir et al., 2001). After 48 hrs, cells were treated with either 0.015% MMS or 40 μg/ml etoposide for the desired duration.

**Immunoblotting and immunoprecipitation**

At 24 hrs post-transfection of the desired plasmids, HeLa cells were lysed in SDS sample buffer, sonicated, boiled, separated by SDS-PAGE, and blotted with the indicated antibodies. Horseradish peroxidase-conjugated goat anti-rabbit or goat anti-mouse IgG (Amersham Biosciences) were used as secondary antibodies, and immunoblots were developed using the ECL reagent (Amersham Biosciences) per manufacturer's protocols. For immunoprecipitation of overexpressed proteins, whole cell lysate was made by lysing cells in NP-40 lysis buffer (50 mM Tris-HCl, pH 7.7, 150 mM NaCl, 0.5% NP-40, 1 mM DTT, and 1X protease inhibitor cocktail) on ice for 15 min, passed through a 25 gauge needle ten times, followed by centrifugation at 16,000 g for 15 min at 4˚C. Antibodies against myc and HA were covalently coupled to Affi-Prep Protein A beads (Bio-Rad) and incubated with the supernatants for 2 hrs at 4˚C. The beads were then washed three times with the NP-40 lysis buffer. The proteins bound to the beads were dissolved in SDS sample buffer, boiled, separated by SDS-PAGE, and blotted with the indicated antibodies.

For immunoprecipitation of endogenous proteins, whole cell lysate was made by lysing cells in buffer A (50 mM Tris-HCl, pH 7.5, 250 mM NaCl, 0.5% Triton X-100, 5 mM EDTA, 5 mM MgCl$_2$, 50 mM NaF, 80 mM ß-glycerophosphate, 1 mM DTT, and 1X protease inhibitor cocktail) on ice for 10 min and then sonicated for 30 sec. The lysate was then treated with 150 U/mL DNAse I at 25˚C for 1 hr to help solubilize chromatin bound proteins (Taylor et al., 2001). The lysate was cleared by centrifugation at 16,000 g for 15 min at 4˚C. Antibodies against SMC5, hBUBR1, and GST were covalently coupled to Affi-Prep Protein A beads (Bio-Rad) and incubated with the supernatants for 2 hrs at 4˚C. After washing with buffer A, the proteins bound to the beads were dissolved in SDS sample buffer, boiled, separated by SDS-PAGE, and blotted with the indicated antibodies.

**Cell death quantification**

Cells were treated with the appropriate conditions and cell death was quantified in the following ways. Cells were stained with Hoechst 33258 (1:100, Molecular Probes) for 30 min at 37˚C. All cells (floating and adherent) were collected and washed in PBS. A portion of the cells was stained with trypan blue for 5 min. The number of blue cells (dead cells) was counted with a hemacytometer. At least 100 cells were counted for each condition in each experiment. The percentage of dead cells was then plotted. The stained nuclei

were also imaged for nuclear condensation.  The rest of the cells were lysed in

sample buffer, sonicated, boiled, and separated on SDS-PAGE.  The samples

were immunoblotted with anti-Asp214 cleaved PARP.

**Immunofluorescence**

Cells were plated in four-well chambered slides (Lab-Tek) and treated

according to experimental conditions.  Cells were washed with PBS followed by

fixation with 4% paraformaldehyde at 4˚C for 30 min.  The fixed cells were

washed with PBS and blocked and permeabilized in TBS containing 5% normal

donkey serum and 0.03% Triton X-100 for 30 min at room temperature.  After

blocking, the cells were incubated in the appropriate primary antibodies overnight

at 4˚C in TBS containing 1% normal donkey serum and 0.03% Triton X-100.  The

cells were then washed with TBS and incubated in fluorescent secondary

antibodies (Molecular Probes) in TBS containing 1% normal donkey serum and

0.03% Triton X-100 for 2-6 hrs at 4˚C.  After incubation, cells were washed with

TBS and nuclei were stained with Hoechst 33258 (1:10000) for 20 min at 4˚C.

Cells were again washed with TBS and mounted.  Cells were viewed with a 63x

objective on a Zeiss Axiovert 200M fluorescence microscope.  Images were

acquired with a CCD camera using Slidebook imaging software (Intelligent

Imaging Innovations).  Images examining the number of phospho-CHK2 (T68)

foci were taken at 0.2 μm intervals, deconvolved using the nearest neighbor

algorithm, and stacked to better resolve the number of foci. ATM/ATR phospho-substrate antibody intensities were measured using the Slidebook imaging software. For both measurements, at least 100 cells were counted for each condition in each experiment.

**Comet assay**

Comet assays were performed according to manufacture's protocol (Trevigen). Briefly, cells were collected after the indicated treatments, mixed with low melt agarose and spread onto slides. The cell/agarose pad was then allowed to harden at 4°C for 30 min. Cells were then lysed by immersing slides in cold lysis solution for 30 min at 4°C. After lysis, slides were immersed in alkaline solution (200 mM EDTA, pH 13) for 20 min at room temperature to unwind and denature the DNA and hydrolyze sites of damage. Slides were then washed two times with TBE for 5 min. Slides were then placed in a horizontal electrophoresis apparatus, equidistant from the electrodes in TBE. Voltage was applied for 10 min at 12V (1V per cm measured electrode to electrode). Slides were then immersed in 70% ethanol for 5 min and allowed to air dry at room temperature overnight. Slides were stained with SYBR Green 1 (Molecular Probes) for 10 min and then washed once in TBE. All incubations were performed in the dark to prevent unintended DNA damage. Slides were viewed using a 20X objective as described above. The percentage of cellular DNA in the

comet tails was calculated by subtracting the nuclear florescence intensity from

that of the entire cell.  At least 100 cells were scored in each condition over three

separate experiments.

**RESULTS**

**Human MMS21 is a subunit of the SMC5/6 complex**

We identified the human homologs of yeast NSE1 and MMS21 by searching the human EST database with the amino acid sequences of their RING-finger and SP-RING domains, respectively (Figure 2-1A). We cloned the full-length cDNAs of hNSE1 and MMS21 from a human fetal thymus cDNA library. The sequences of the hNSE1 and MMS21 genes that we isolated were identical to those reported previously (McDonald et al., 2003). Both human and yeast MMS21 proteins contain a SP-RING domain that is present in human PIAS1, a known SUMO ligase (Figure 2-1B). SP-RING domains are putative $Zn^{2+}$-binding motifs that contain five cysteine/histidine residues as $Zn^{2+}$-coordinating ligands (Johnson, 2004). Sequence alignment between human PIAS1 and MMS21 proteins from various species reveals the five conserved cysteine/histidine residues thought to be responsible for $Zn^{2+}$ coordination in the SP-RING domain (Figure 2-1B).

We next tested their interactions with SMC5. Both hNSE1 and MMS21 interacted with SMC5 in HeLa cells (Figure 2-1C). To examine the endogenous SMC5/6 complex, we raised antibodies against MMS21 and SMC5. The antibodies were shown to be specific using RNAi knockdown experiments of the endogenous proteins in HeLa cells (Figure 2-1D and E). Endogenous MMS21

protein was pulled down specifically by immunoprecipitation with anti-hSMC5, but not with controls anti-GST or anti-BUBR1 (Figure 2-1F). Therefore, MMS21 is likely the human ortholog of the yeast MMS21 and is a subunit of the SMC5/6 complex.

**MMS21 is a SUMO ligase *in vitro* and *in vivo***

We then tested whether MMS21 has SUMO ligase activity *in vitro*. Because several known SUMO ligases, such as PIAS1 and RanBP2, undergo efficient auto-sumoylation (Johnson and Gupta, 2001; Pichler et al., 2002), we first tested whether MMS21 was sumoylated in an *in vitro* sumoylation assay. Briefly, the $^{35}$S-labeled MMS21 protein translated in rabbit reticulocyte lysate was incubated with purified, bacterially expressed AOS1-UBA2, UBC9, and SUMO1 proteins in the presence of ATP. MMS21 efficiently formed high molecular weight conjugates on SDS-PAGE (Figure 2-2A). The appearance of these high molecular weight conjugates was dependent on the presence of ATP, AOS1-UBA2, UBC9, and SUMO1, since the removal of each of these components abrogated the laddering (Figure 2-2A). This suggested that MMS21 was sumoylated in this assay. Addition of recombinant GST-PIAS1 or the SUMO ligase domain of RanBP2, two known E3 SUMO ligases, did not enhance the sumoylation of MMS21 (Figure 2-3). In fact, addition of PIAS1 partially

suppressed MMS21 sumoylation (Figure 2-3), presumably due to competition

between MMS21 and PIAS1 for certain components in the SUMO reaction.

To verify that MMS21 is a SUMO ligase and not simply an efficient

SUMO substrate for UBC9, we mutated each of the five conserved

cysteine/histidine residues in the SP-RING domain of MMS21 and tested the

ability of these mutants to be sumoylated *in vitro*.  Mutations of cysteine/histidine

residues will not remove any potential SUMO-conjugation sites in MMS21, as

sumoylation occurs on lysines.  Consistent with MMS21 itself being a SUMO

ligase, mutation of any of the five conserved cysteines/histidines significantly

decreased the sumoylation of MMS21 (Figure 2-2B).  Although mutation of a

single cysteine/histidine in the SP-RING domain of MMS21 did not completely

prevent SUMO conjugation, it dramatically reduced the formation of high

molecular weight MMS21-SUMO1 conjugates (Figure 2-2B).  Therefore, this

indicates that sumoylation of MMS21 is dependent on its SP-RING domain.

We next performed *in vitro* sumoylation reactions using bacterially

purified GST-MMS21.  GST-MMS21 formed a high molecular weight ladder on

SDS-PAGE in reactions containing ATP, AOS1-UBA2, UBC9, SUMO1, and

GST-MMS21 (Figure 2-2C).  These high molecular weight species of GST-

MMS21 were absent in reactions lacking any given one component (Figure 2-2C).

To confirm that these high molecular weight GST-MMS21 species were indeed

GST-MMS21-SUMO1 conjugates, the same reaction mixtures were blotted with

anti-SUMO1. A similar high molecular weight ladder of SUMO1 was observed when all components of the SUMO reactions were included (Figure 2-2D). These results establish that MMS21 is sumoylated *in vitro* and this sumoylation is dependent on an intact SP-RING domain.

We next tested whether MMS21 was sumoylated in HeLa cells. Myc-tagged MMS21 was modified in the presence of untagged or GFP-tagged SUMO1 overexpression (Figure 2-4A). As reported previously (Gocke et al., 2005), GFP-SUMO1 was expressed at much higher levels, and was thus conjugated more efficiently to substrates than untagged or endogenous SUMO1 (Figure 2-4A). Modification of myc-MMS21 was significantly reduced by expression of SENP2, a SUMO isopeptidase (Figure 2-4A and B). In addition, modification of myc-MMS21 was not observed with the overexpression of SUMO1 ΔGG, a SUMO mutant incapable of conjugation (Figure 2-4B; Johnson, 2004). Finally, we performed immunoprecipitations of myc-MMS21 in HeLa cells followed by immunoblotting with anti-SUMO1. Expectedly, the major modified form of MMS21 contained SUMO1, indicating that MMS21 was indeed sumoylated in HeLa cells (Figure 2-4C). Furthermore, the myc-MMS21 C215A mutant was sumoylated to a much lesser extent in HeLa cells as was observed *in vitro* (Figure 2-4B and C). These findings establish that MMS21 is sumoylated *in vivo* and sumoylation of MMS21 requires an intact SP-RING domain, consistent with MMS21 being an SP-RING-type SUMO ligase.

## MMS21 enhances sumoylation of SMC6 and TRAX

To formally prove that MMS21 is a SUMO ligase, we need to show that MMS21 can stimulate the sumoylation of target proteins other than itself. To do so, we tested whether purified recombinant GST-MMS21 stimulated the sumoylation of the human SUMO substrates discovered in our IVEC screen in an *in vitro* sumoylation assay (Gocke et al., 2005). Among tens of substrates tested, only the sumoylation of TRAX was moderately ($2.8 \pm 0.2$ fold over three separate experiments) enhanced by GST-MMS21 (Figure 2-5A and data not shown). As a control, GST-MMS21 did not enhance the sumoylation of ETV1 (Figure 2-5A). We next tested whether MMS21 enhanced the sumoylation of TRAX and ten candidate proteins involved in DNA damage/repair pathways that were potential targets of MMS21 *in vivo* (Figure 2-5B and data not shown). As expected, MMS21 stimulated the sumoylation of TRAX in HeLa cells (Figure 2-5B). As compared to the *in vitro* assay, sumoylation of TRAX was significantly enhanced by MMS21 in HeLa cells. This could be due to the need for additional proteins from the SMC5/6 complex for the full activity of MMS21 *in vitro* as was shown previously for *S. cerevisiae* MMS21 (Zhao and Blobel, 2005). In addition, similar to the *S. pombe* NSE2, MMS21 efficiently enhanced the sumoylation of an alternatively spliced, N-terminal truncated SMC6 in HeLa cells (Figure 2-5B). Furthermore, the MMS21 C215A mutant did not stimulate the sumoylation of

TRAX or SMC6 (Figure 2-5B). To confirm that the high molecular weight

species of SMC6 and TRAX induced by the expression of MMS21 were SUMO1

conjugates, we performed immunoprecipitation of myc-SMC6 (Figure 2-5C) and

myc-TRAX (data not shown) followed by immunoblotting using anti-SUMO1.

We detected a high molecular weight ladder of SUMO1 conjugates when wild-

type MMS21, but not MMS21 C215A mutant, was coexpressed with SMC6 and

TRAX in HeLa cells (Figure 2-5C and data not shown). These results confirm

that MMS21 enhances SMC6 and TRAX sumoylation in HeLa cells. Therefore,

MMS21 is a SUMO ligase *in vivo*.

**The SUMO ligase activity of MMS21 is required for cellular DNA damage response**

To examine the role of MMS21 in DNA damage response, we transfected

HeLa cells with siRNA against MMS21 and then treated the cells with MMS.

There was only a slightly higher incidence of cell death in MMS21-RNAi cells in

the absence of DNA damage (Figure 2-6A), suggesting that a partial loss of

MMS21 did not cause cell lethality. In contrast, after exposure to a moderate

dose of MMS (0.015%) for 6 hrs, about 80% of the MMS21-RNAi cells had died

while only 20% of the control cells were dead (Figure 2-6A and B). Thus, as

compared to control cells, MMS21-RNAi cells were much more sensitive to

MMS. The MMS21-RNAi cells were also more sensitive to etoposide (VP-16), a

topoisomerase II inhibitor that induces DSBs (Figure 2-6B).  Therefore, consistent

with studies in yeast (Andrews et al., 2005; McDonald et al., 2003; Zhao and

Blobel, 2005), MMS21 is required for proper cellular responses to DNA damage

induced by multiple agents.

We next attempted to rescue the phenotypes of MMS21-RNAi cells with

ectopic expression of either wild-type MMS21 or its ligase-inactive mutant,

MMS21 C215A.  To avoid the knockdown of the ectopically expressed MMS21

proteins by RNAi, we first introduced silent mutations into the coding region of

the MMS21 gene that contains the sequence of the MMS21 siRNA.  Transfection

of these MMS21 plasmids restored the levels of MMS21 protein in MMS21-

RNAi cells (Figure 2-6D).  Significantly, expression of the wild-type MMS21

protein, but not MMS21 C215A, largely rescued the cell death phenotype of

MMS21-RNAi cells following MMS treatment (Figure 2-6C).  This indicates that

the ligase activity of MMS21 is required for its function in DNA damage

response.

To determine whether the increased cell death of MMS21-RNAi cells

following MMS treatment was due to apoptosis, we examined the nuclear

morphology of these cells.  As expected, after MMS treatment, MMS21 RNAi

caused an increased number of cells with hyper-condensed nuclei (data not

shown), a hallmark of apoptotic cells.  The number of cells with condensed nuclei

was greatly reduced by expression of the wild-type MMS21, but not the ligase-

inactive mutant, MMS21 C215A (data not shown). To further confirm that the observed cell death was indeed apoptosis, we examined the cleavage of a known caspase-3 substrate, PARP. PARP cleavage was observed in MMS21-RNAi cells treated with MMS (Figure 2-6D). Cleavage of PARP was prevented by expression of the wild-type MMS21, but not MMS21 C215A, in MMS21-RNAi cells (Figure 2-6D). These results indicate that MMS21-RNAi cells are more prone to undergo apoptosis in the presence of DNA damage, and the SUMO ligase activity of MMS21 is required for preventing DNA damage-induced apoptosis.

**RNAi-mediated depletion of MMS21 results in hyper-activation of ATM/ATR**

ATM and ATR are related protein kinases that are activated upon DNA damage and phosphorylate many cellular targets at Ser/Thr-Gln sites (Kim et al., 1999). To determine whether MMS21 is required for the DNA damage response through ATM/ATR, we stained control and MMS21-RNAi cells with an antibody that specifically recognizes phosphorylated Ser/Thr-Gln motifs (Figure 2-7A; DiTullio et al., 2002). The intensity of the antibody staining was quantified and used as a measure for the activity of ATM/ATR (Figure 2-7B; DiTullio et al., 2002). As expected, the level of phosphorylated ATM/ATR substrates increased upon DNA damage (Figure 2-7A and B). In the absence of MMS, the basal level

of ATM/ATR-mediated phosphorylation was higher in MMS21-RNAi cells.

After DNA damage, the MMS21-RNAi cells contained three-fold more

phosphorylated ATM/ATR substrates, as compared to control cells (Figure 2-7A

and B).

CHK2 is a key substrate of ATM and ATR (Kastan and Bartek, 2004).

Phosphorylation of CHK2 at Thr 68 after DNA damage requires ATM and ATR

(Melchionna et al., 2000).  Phosphorylated T68 CHK2 forms nuclear foci,

presumably at the sites of DNA damage (Ward et al., 2001).  We thus stained

control and MMS21-RNAi cells with a phospho-CHK2 (T68) antibody (Figure 2-

7C).  As compared to control cells, the MMS21-RNAi cells contained an

increased number of phospho-CHK2 nuclear foci after treatment with MMS

(Figure 2-7C).  The mean number of foci in control cells was around 8-9 per cell

while the mean number of foci in MMS21-RNAi cells was about 15-16 per cell

(Figure 2-7D).  Our data suggest that MMS21 is not required for ATM/ATR-

dependent DNA damage checkpoint response.  Instead, consistent with MMS21

playing a role in DNA repair, knockdown of MMS21 might lead to defective

DNA repair and an increased amount of unrepaired DNA lesions following DNA

damage, thus increasing the amount of ATM/ATR activity and the number of

phospho-CHK2 foci.


**Knockdown of MMS21 decreases repair of damaged DNA**

To determine whether knockdown of MMS21 resulted in an increased amount of unrepaired DNA lesions following DNA damage, we performed a single cell gel electrophoresis assay (comet assay; Collins, 2004). The comet assay is simple and widely used to evaluate the amount of DNA damage in cells. It is based on the ability of denatured, cleaved DNA fragments to migrate out of the cell when current is applied, whereas undamaged DNA migrates slower and remains within the confines of the nucleus (Collins, 2004).

We employed this assay to measure the amount of unrepaired DNA damage in control or MMS21-RNAi cells after MMS treatment. As expected, control and MMS21-RNAi cells had no comet tails without treatment of MMS (Figure 2-8A). To measure the ability of cells to repair damaged DNA, we treated cells with 0.015% MMS for 1 hr and then washed out MMS and allowed cells to repair the damaged DNA for 3 hr. The MMS21-RNAi cells, unlike control cells, were incapable of repairing their DNA lesions (Figure 2-8A). The amount of DNA that migrates out of the nucleus and forms a comet tail provides a quantitative measure of the amount of DNA damage in the cell (Collins, 2004). Quantitation of the amount of DNA in the comet tails showed a dramatic increase in the amount of unrepaired DNA lesions in the MMS21-RNAi cells (95%) as compared to control cells (25%; Figure 2-8B). To rule out the possibility that the increase in the amount of unrepaired DNA lesions was due simply to an increased number of apoptotic cells in the MMS21-RNAi culture as compared to the wild-

type culture, we performed the experiment in the presence of a pan-caspase

inhibitor, zVAD-fmk. Although zVAD-fmk could inhibit MMS-induced cell

death in MMS21-RNAi cells (Figure 2-9), addition of zVAD-fmk had no effect

on the amount of unrepaired DNA present in MMS21-RNAi cells (Figure 2-8A

and B). Finally, to rule out the possibility that MMS21-RNAi cells were more

susceptible to DNA damage than control cells, we treated cells with 0.015%

MMS for 1 hr without a period for repair. Treatment of both control and

MMS21-RNAi cells with MMS without recovery resulted in comet tails with

similar, large amounts of DNA damage lesions (Figure 2-8A and B). These

results suggest that knockdown of MMS21 results in a decreased ability of cells to

repair DNA lesions.

**DISCUSSION**

Studies in yeast have established a role for a chromatin-bound protein complex, containing SMC5, SMC6, MMS21, and other non-SMC proteins, in DNA repair. Here we show that, similar to yeast MMS21, human MMS21 is a functional SUMO ligase. The SUMO ligase activity of MMS21 is required for the prevention of apoptosis following DNA damage. We present evidence to further suggest that MMS21 is required for efficient DNA damage repair.

**The SUMO ligase activity of MMS21**

Studies of both *S. cerevisiae* MMS21 and *S. pombe* NSE2 have identified MMS21 as a SUMO ligase that autosumoylates. Our results concur with these previous findings and show MMS21 is a SUMO ligase that undergoes autosumoylation *in vitro* and *in vivo*. The *S. cerevisiae* MMS21 has been shown to stimulate the sumoylation of two substrate proteins, SMC5 and Ku70 (Zhao and Blobel, 2005). The *S. pombe* NSE2 stimulates the sumoylation of SMC6 and NSE3, but not SMC5 or NSE1 (Andrews et al., 2005). Consistent with the results in *S. pombe*, we show that MMS21 enhances sumoylation of SMC6. In addition, we also identify TRAX as a substrate of MMS21. The differences with respect to MMS21-mediated sumoylation of SMC5/6 in *S. pombe*, *S. cerevisiae*, and *H.*

*sapiens* could reflect interesting differences in the mechanism and regulation of the SMC5/6 complex in these organisms.

In fission yeast, SMC6 sumoylation is dependent on MMS21, indicating that SMC6 is a physiologically relevant substrate of MMS21 (Andrews et al., 2005). Like many SUMO substrates in mammalian cells, we were unable to detect the sumoylation of SMC6 or TRAX in the absence of SUMO1 overexpression, presumably due to the low steady-state levels of SUMO conjugates of these proteins. Upon overexpression of SUMO1, the SUMO1 conjugates of SMC6 and TRAX were observed in HeLa cells. Overexpression of MMS21 further enhanced the sumoylation of SMC6 and TRAX. However, we did not detect a decrease in the sumoylation of SMC6 or TRAX in MMS21-RNAi cells. This could be due to the incomplete knockdown of MMS21 by RNAi. Alternatively, sumoylation of SMC6 and TRAX in the presence of SUMO1 overexpression does not strictly require MMS21. It is also possible that other SUMO ligases can also mediate the sumoylation SMC6 and TRAX under these conditions. Therefore, our results indicate that MMS21 is capable of stimulating the sumoylation of SMC6 and TRAX in living cells. It remains to be established whether and how sumoylation of SMC6 and TRAX is important for DNA repair in human cells.

**Role of MMS21 and the SMC5/6 complex in DNA repair**

Down-regulation of the SMC5/6 complex in yeast and in mammalian cells (this study) renders cells more sensitive to a wide spectrum of DNA damaging agents (Fousteri and Lehmann, 2000; Fujioka et al., 2002; Hu et al., 2005; Lehmann et al., 1995; McDonald et al., 2003; Onoda et al., 2004; Pebernard et al., 2004; Prakash and Prakash, 1977a; Prakash and Prakash, 1977b).  It is possible that the SMC5/6 complex is directly involved in the repair of multiple types of DNA lesions.  On the other hand, components of the SMC5/6 complex are epistatic with RAD51 and RAD52, suggesting that the SMC5/6 complex may function in the repair of DSB through the RAD51- and RAD52-dependent HR pathway (Andrews et al., 2005; McDonald et al., 2003; Morikawa et al., 2004; Onoda et al., 2004; Pebernard et al., 2004).  Because many types of DNA damaging agents can indirectly lead to the generation of DSBs, it is also possible that a major function of the SMC5/6 complex is the repair of DSB through HR.

In addition to DNA repair, cohesin and condensin also play roles in the DNA damage checkpoint that delays cell cycle progression to allow time for DNA repair (Hagstrom and Meyer, 2003).  Though the SMC5/6 complex is not required for the initiation of the DNA damage checkpoint response in *S. pombe*, it is involved in the maintenance of the checkpoint (Harvey et al., 2004).  In this study, we show that ATM/ATR are activated to a greater extent in MMS21-RNAi cells, which is more consistent with SMC5/6 playing a role in DNA repair.  On the other hand, MMS21 RNAi does not completely deplete the cellular pool of the

MMS21 protein. It is possible that the residual amount of MMS21, though insufficient for DNA repair, is sufficient for DNA damage checkpoint signaling. In addition, MMS21-RNAi cells might be defective in checkpoint pathways that do not involve ATM/ATR.

**Role of sumoylation in DNA repair**

Through its reversible, covalent modification of target proteins, SUMO regulates diverse cellular processes, including transcription, chromatin remodeling, and DNA repair (Gill, 2004). Several proteins involved in DNA repair are SUMO substrates, including PCNA, WRN, XRCC1, KU70, KU80, and TRAX (Gill, 2004; Gocke et al., 2005; Zhao and Blobel, 2005). We show that a subunit of the SMC5/6 complex, MMS21, is a functional SUMO ligase. Furthermore, the SUMO ligase activity of MMS21 is essential for its function in protecting cells from apoptosis induced by DNA damage, thus further establishing a role of sumoylation in DNA repair. At present, we do not know the mechanism by which the ligase activity of MMS21 regulates DNA repair. However, we envision two non-exclusive possibilities. First, MMS21 might stimulate the sumoylation of other DNA damage checkpoint and repair proteins, such as TRAX, and mediate their recruitment to the sites of DNA damage. Consistent with this notion, sumoylation has been shown to alter the subcellular localization and/or kinetics of nucleocytoplasmic trafficking of certain target proteins (Gill,

2004; Johnson, 2004). However, we did not observe failure in the recruitment of

DNA damage checkpoint and repair proteins, such as BRCA1, BRCA2, CHK1,

CHK2, or RAD51, to nuclear foci after DNA damage in MMS21-RNAi cells

(Figure 2-7C and data not shown). In a second possibility, sumoylation of SMC6

by MMS21 might regulate its ATPase activity, thus affecting the loading and

unloading of the SMC5/6 complex onto chromatin. It will be interesting to

examine the possibility that SMC5/6 loading and unloading is also required for

DNA repair and how the SUMO ligase activity of MMS21 may regulate this

process during the cellular DNA damage response.

**A**

**B**

**C**

**D**

**E**

**F**
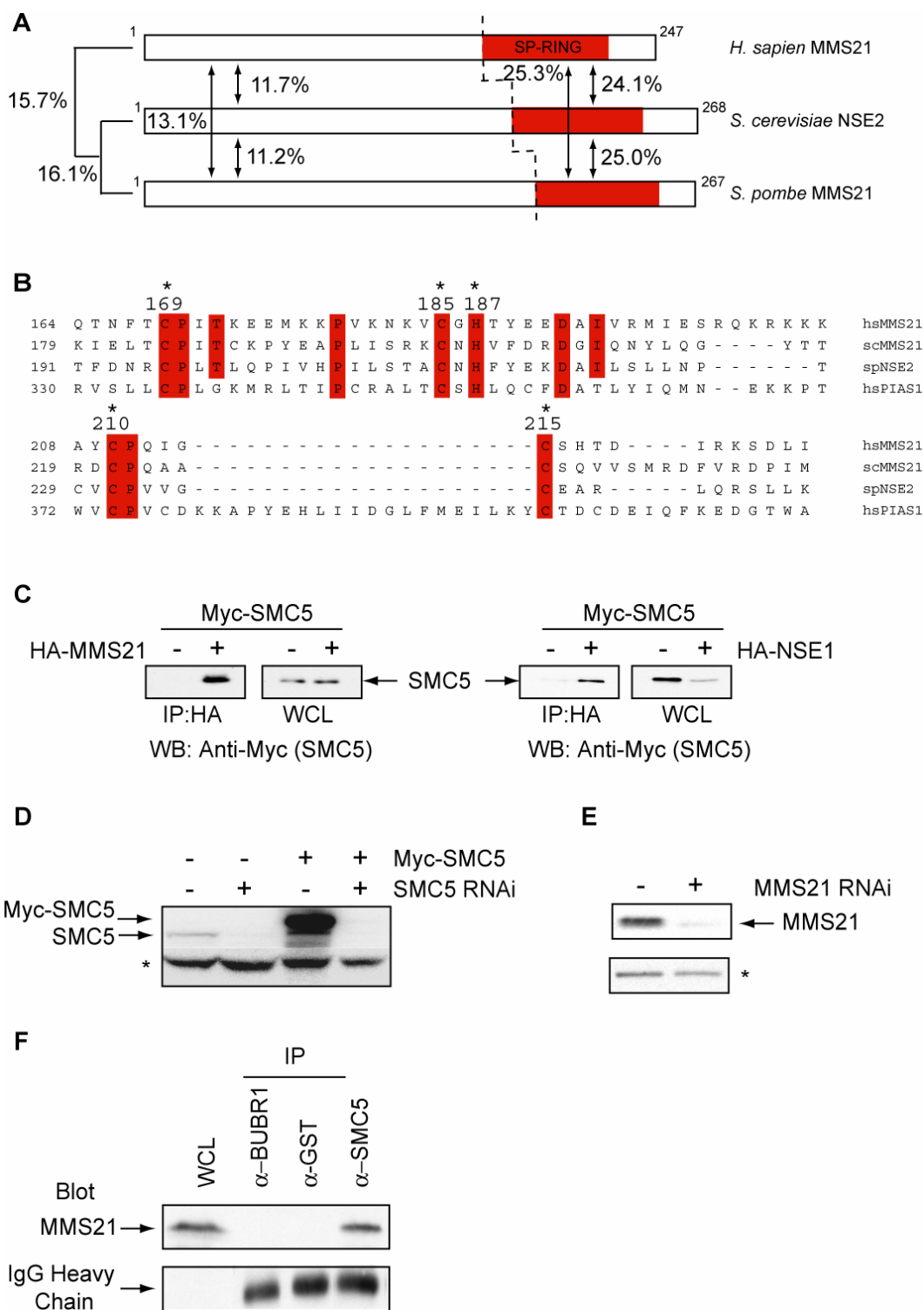
**Figure 2-1.  MMS21 is a subunit of the SMC5/6 complex**

(**A**) Sequence identities among MMS21 proteins of *H. sapien*, *S. cerevisiae*, and *S. pombe*.  The identities of the full-length MMS21, the N-terminal domain, and the C-terminal SP-RING domain (indicated by dashed lines) are shown.  (**B**) Sequence alignment of the SP-RING domains of PIAS1 and the MMS21 proteins from human (hs), *S. cerevisiae* (sc), and *S. pombe* (sp).  The conserved residues are shaded.  The putative $Zn^{2+}$-coordinating cysteines and histidines are indicated by asterisks.  Alignment was performed using ClustalW.  (**C**) MMS21 and hNSE1 interact with SMC5.  The pCS2-myc-hSMC5 plasmid was transfected into HeLa cells with or without co-transfection of plasmids encoding HA-tagged MMS21 or hNSE1.  Lysates of these cells were immunoprecipitated with anti-HA and blotted with anti-myc.  The whole cell lysates (WCL) were also blotted with anti-myc. (**D**) The SMC5 antibody recognizes endogenous SMC5 in HeLa cells.  HeLa cells were transfected with mock siRNA or SMC5 siRNA in the presence or absence of pCS2-myc-hSMC5.  Lysates of these cells were blotted with anti-hSMC5 antibody.  Asterisk indicates a nonspecific cross-reacting band that serves as a loading control.  (**E**) The MMS21 antibody recognizes endogenous MMS21 in HeLa cells.  HeLa cells were transfected with mock siRNA or MMS21 siRNA for 48 hrs.  Lysates of these cells were blotted with anti-MMS21.  Asterisk indicates a nonspecific cross-reacting band that serves as a loading control.  (**F**) Endogenous MMS21 interacts with SMC5 in HeLa cells.  HeLa cell lysates were immunoprecipitated with anti-GST, anti-BUBR1, or anti-hSMC5 and blotted with anti-MMS21.  IgG heavy chain was used as a loading control.
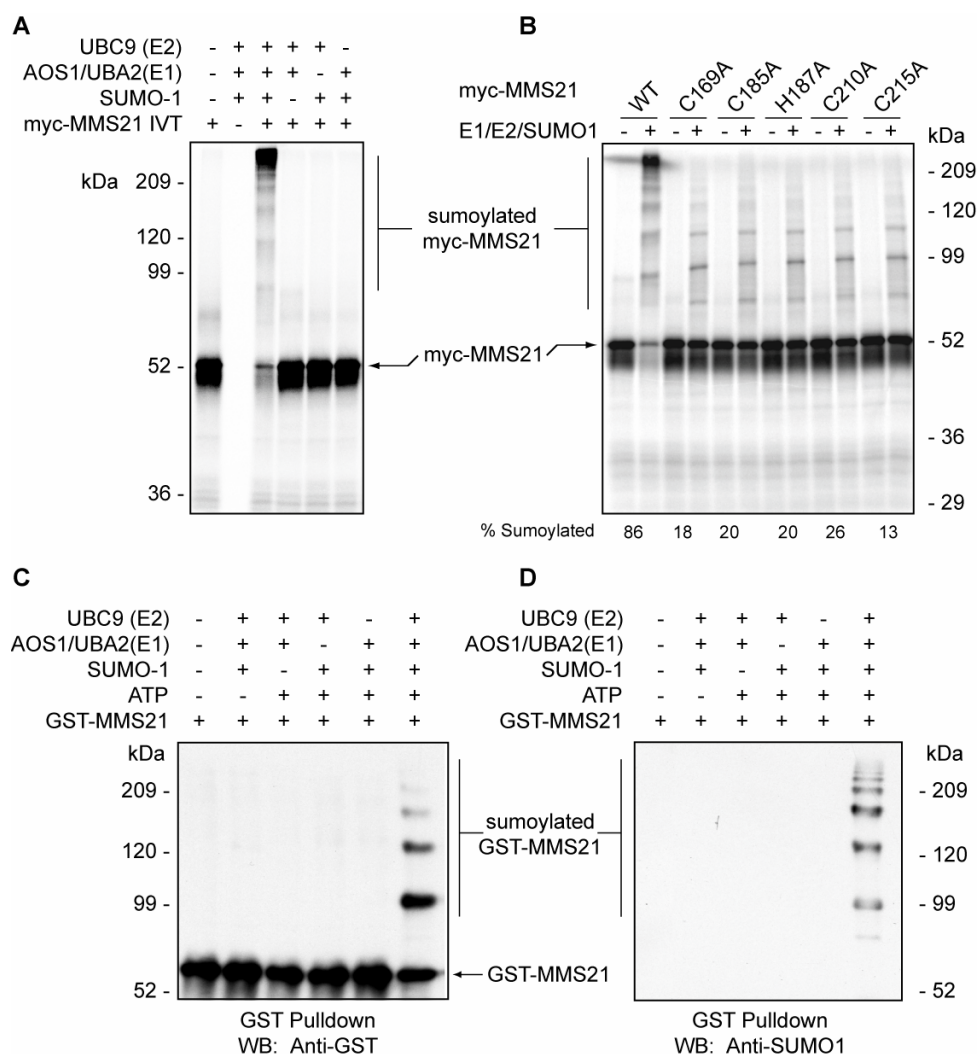
**Figure 2-2. MMS21 is sumoylated *in vitro***
(**A**) Myc-MMS21 was *in vitro* translated in the presence of ^{35}S-methionine and incubated with SUMO reaction mixtures containing the indicated components and analyzed by SDS-PAGE followed by autoradiography. (**B**) SUMO reactions were performed as in (A) using either wild-type or the indicated SP-RING domain mutants of MMS21. The percentage of MMS21 sumoylated was quantitated and is shown below the appropriate lanes. (**C**) *In vitro* SUMO reactions were performed using GST-MMS21 and the indicated components. GST-MMS21 was pulled down using glutathione-agarose beads followed by SDS-PAGE and immunoblotting with anti-GST. (**D**) The reactions described in (C) were immunoblotted with anti-SUMO1.
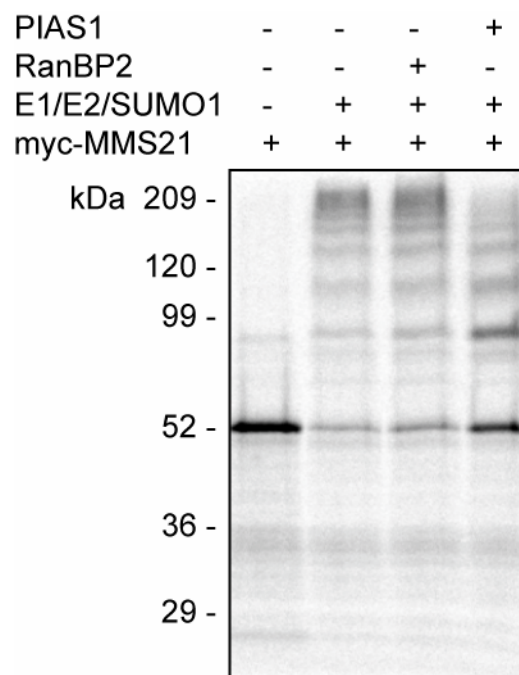
**Figure 2-3. RanBP2 and PIAS SUMO E3 ligases do not enhance MMS21 sumoylation**
MMS21 was *in vitro* translated in the presence of $^{35}$S-methionine and subjected to control or SUMO reactions containing the indicated proteins. Only the SUMO ligase domain of RanBP2 (RanBP2 ΔFG) was used in the assay (Pichler et al., 2002). The reactions were analyzed by SDS-PAGE followed by autoradiography.
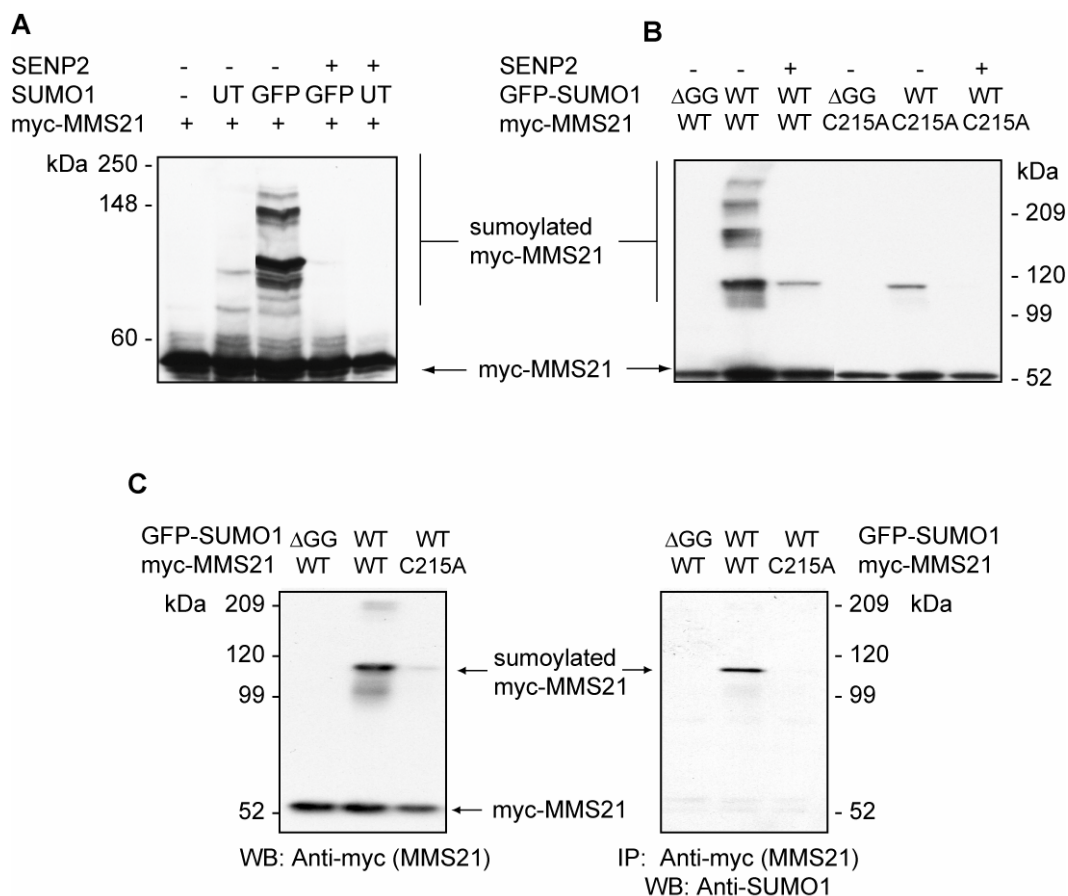
**Figure 2-4. MMS21 is sumoylated in HeLa cells**
(**A**) Myc-MMS21 was expressed in HeLa cells with or without untagged (UT) or
GFP-tagged (GFP) SUMO1 or the SUMO isopeptidase, SENP2. Whole cell
lysates were blotted with anti-myc. (**B**) Sumoylation of MMS21 *in vivo* requires
an intact RING domain. The wild-type (WT) or the C215A mutant of myc-
MMS21 was expressed in HeLa cells in the presence of wild-type (WT) or the
ΔGG mutant of GFP-SUMO1 and with or without SENP2. Whole cell lysates
were blotted with anti-myc. (**C**) MMS21 is conjugated to SUMO1 in HeLa cells.
HeLa cells were transfected as described in (B) with either wild-type (WT) or the
C215A mutant of myc-MMS21 in the presence of wild-type (WT) or ΔGG mutant
of GFP-SUMO1. Whole cell lysates were blotted with anti-myc (left panel) or
immunoprecipitated with anti-myc followed by immunoblotting with anti-
SUMO1 (right panel).
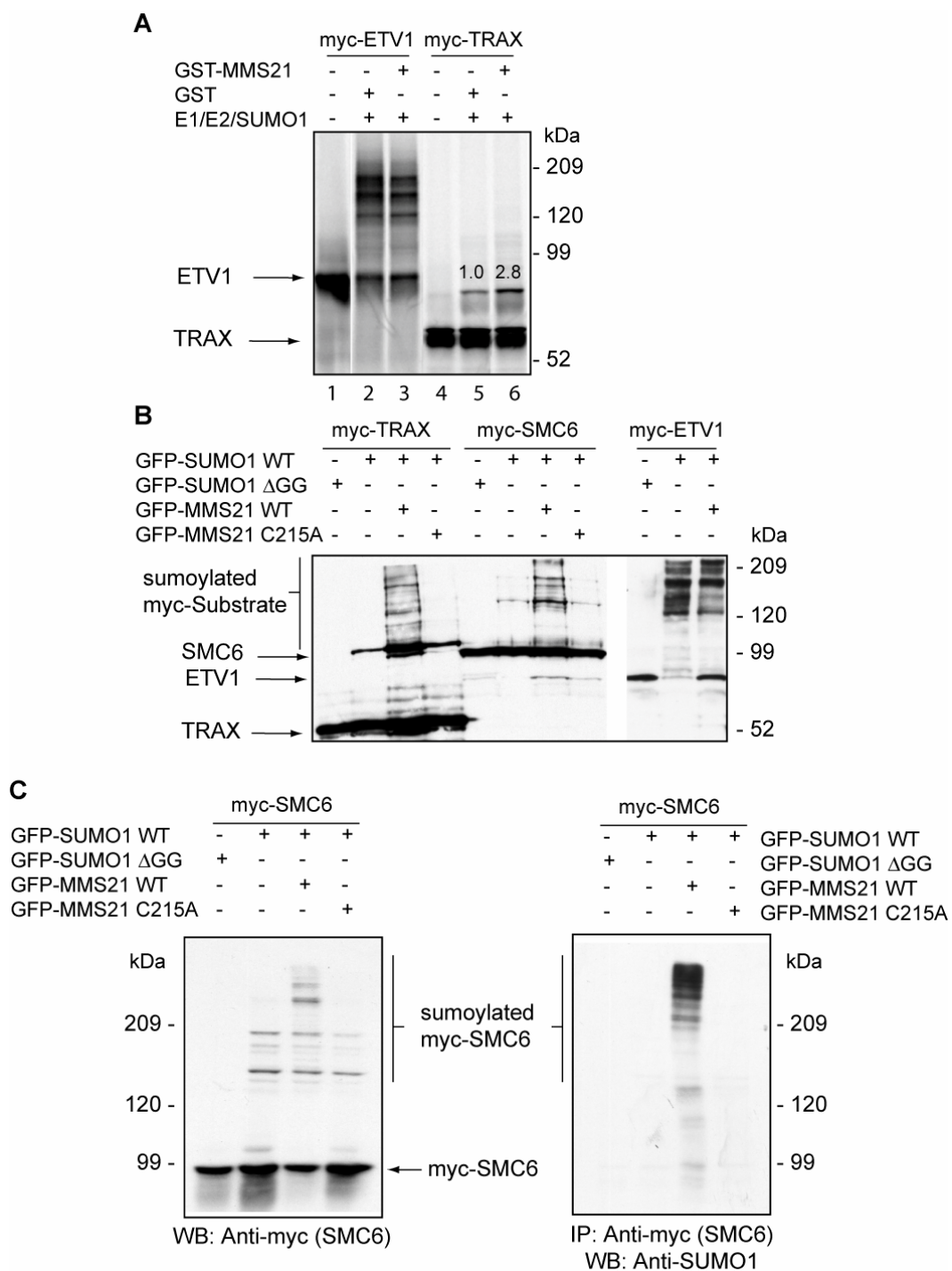
**Figure 2-5. MMS21 is a SUMO ligase that stimulates sumoylation of SMC6 and TRAX**

(**A**) Recombinant GST-MMS21 stimulates the sumoylation of TRAX, but not
ETV1, *in vitro*. ETV1 and TRAX were *in vitro* translated in the presence of $^{35}$S-
methionine and subjected to SUMO reactions in the presence of GST or GST-
MMS21. The reactions were analyzed by SDS-PAGE followed by
autoradiography. The fold increase of the mono-sumoylated TRAX in the
presence of GST-MMS21 is indicated. (**B**) Sumoylation of SMC6 and TRAX,
but not ETV1, is enhanced by MMS21 in HeLa cells. Myc-TRAX, myc-hSMC6,
or myc-ETV1 was expressed with GFP-SUMO1 wild-type (WT) or ΔGG in the
presence or absence of wild-type (WT) or the C215A mutant of GFP-MMS21 in
HeLa cells. The whole cell lysates were blotted with anti-myc. (**C**) MMS21
stimulates SUMO1 conjugation to SMC6 in HeLa cells. HeLa cells were
transfected as described in (B) and whole cell lysates were either immunoblotted
with anti-myc (left panel) or immunoprecipitated with anti-myc followed by
immunoblotting with anti-SUMO1 (right panel).
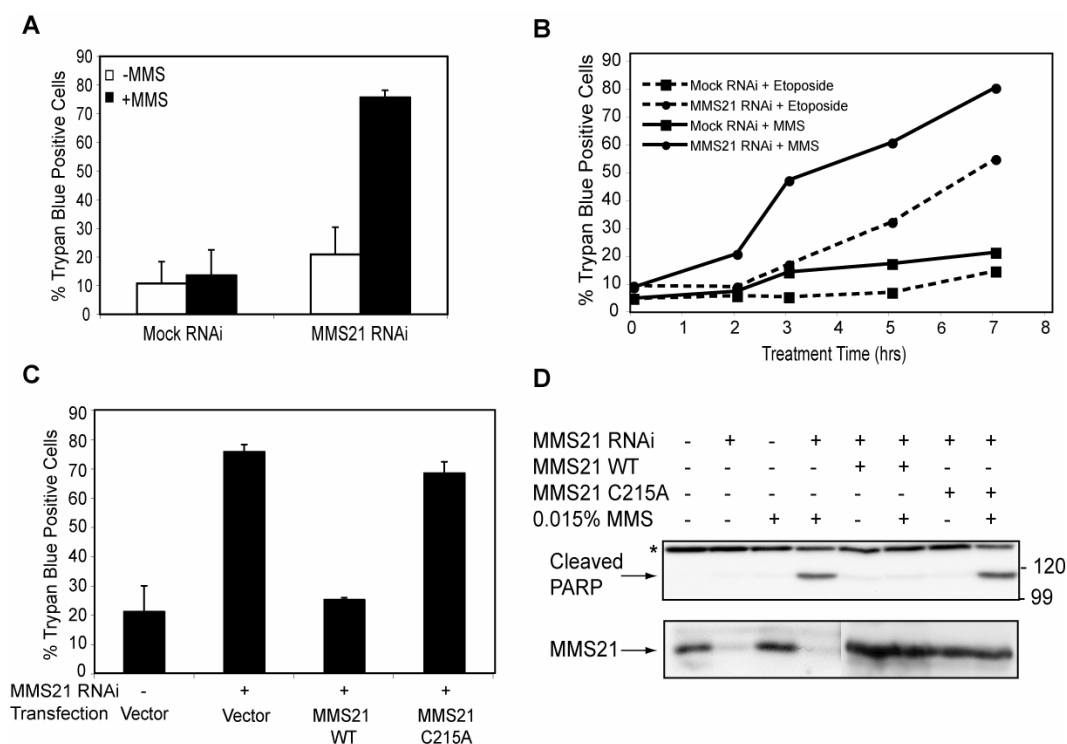
**Figure 2-6. The SUMO ligase activity of MMS21 is required to block DNA damage-induced apoptosis**
(**A**) MMS21-RNAi cells are more sensitive to MMS. HeLa cells were transfected with mock or MMS21 siRNA for 48 hrs and then either untreated or treated with 0.015% MMS for 6 hrs. The percentage of dead cells (trypan blue positive) is plotted. Results from three separate experiments are averaged with the standard deviation indicated. (**B**) Time course of cell death after MMS and etoposide treatment. Control (squares) or MMS21-RNAi (circles) cells were treated with 0.015% MMS (solid lines) or 40 µg/ml etoposide (dashed lines) for the indicated times and the percentage of dead cells was determined by trypan blue exclusion. (**C**) The wild-type (WT) MMS21, but not its ligase-inactive C215A mutant, rescues the sensitivity of MMS21-RNAi cells to MMS. Cells were transfected with mock or MMS21 siRNA for 24 hrs and then transfected with either empty vector or plasmids encoding wild-type or the C215A mutant of myc-MMS21. After 24 hrs, cells were treated with 0.015% MMS for 6 hrs. The percentage of dead cells (trypan blue positive) is plotted. Results from three separate experiments are averaged with the standard deviation indicated. (**D**) Whole cell lysates of cells from (C) were blotted with antibodies against cleaved PARP or anti-MMS21. Asterisk indicates a nonspecific cross-reacting band that serves as a loading control.
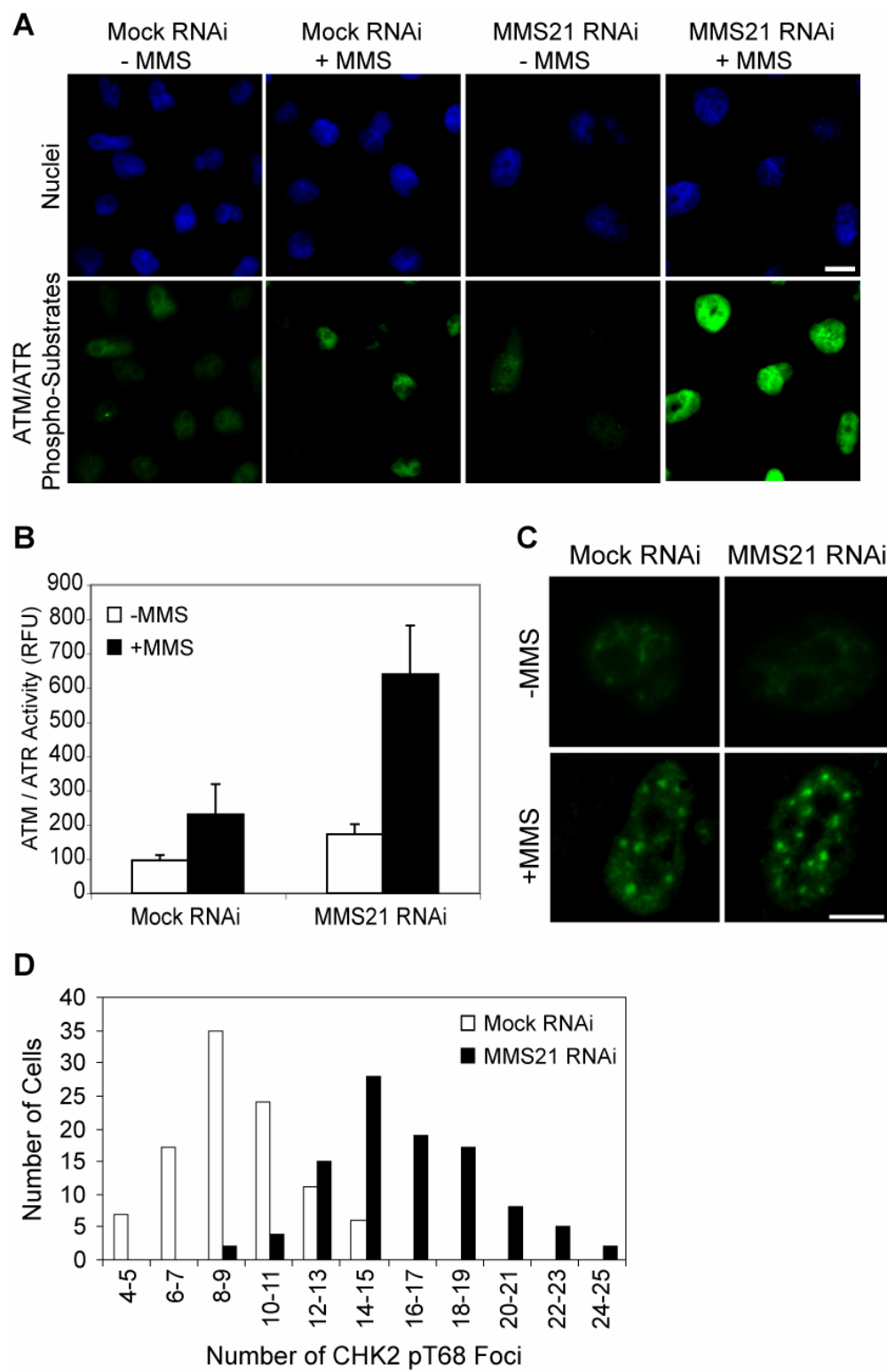
**Figure 2-7.  ATM/ATR are hyper-activated in MMS21-RNAi cells after DNA damage**
(**A**) HeLa cells were transfected with either mock or MMS21 siRNA for 48 hrs and were either untreated or treated with 0.015% MMS for 4 hrs.  Cells were fixed and stained with Hoescht 33258 (blue) or a phospho-specific antibody against ATM/ATR phosphorylation sites on its substrates (green).  Scale bar indicates 5 µm.  (**B**) Quantitation of the fluorescence intensities of the ATM/ATR phospho-substrate staining in (A).  Results from three separate experiments are averaged with the standard deviation indicated.  (**C**) Cells treated as in (A) were stained with a phospho-T68 CHK2 antibody (green).  Scale bar indicates 5 µm. (**D**) Histogram of cells in (C) with the indicated number of phospho-CHK2 foci.
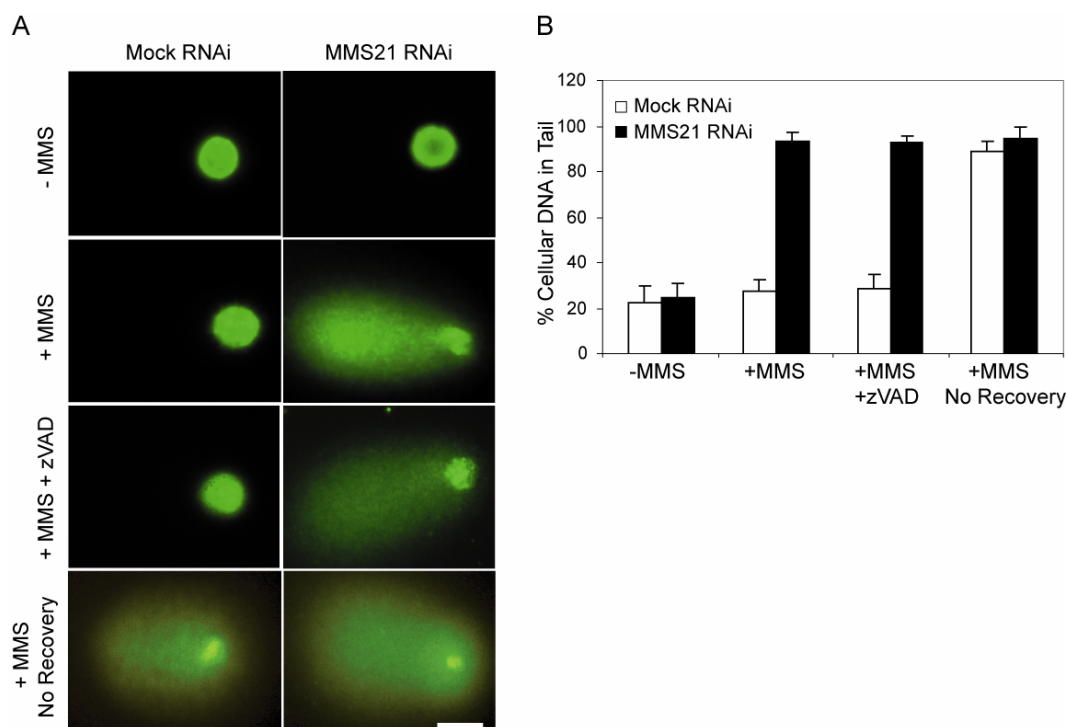
**Figure 2-8. MMS21 is required for efficient repair of damaged DNA**
(**A**) HeLa cells were transfected with mock or MMS21 siRNA and treated with
0.015% MMS for 0 hr (-MMS), 1 hr MMS treatment followed by a 3 hrs recovery
period without MMS (+MMS), 1 hr MMS treatment with 3 hrs recovery in the
presence of the pan-caspase inhibitor, zVAD-fmk (+MMS +zVAD), or 1 hr MMS
treatment without recovery (+MMS no recovery).  Cells were collected and
analyzed for unrepaired DNA lesions by the comet assay.  SYBR green staining
of DNA shows comet tails migrating out of the nucleus.  Scale bar indicates 10
μm.  (**B**) Quantitation of fluorescent intensities of cells in (A) to measure the
percentage of DNA migrated out of the nucleus into tails.  Results from three
separate experiments are averaged with the standard deviation indicated.
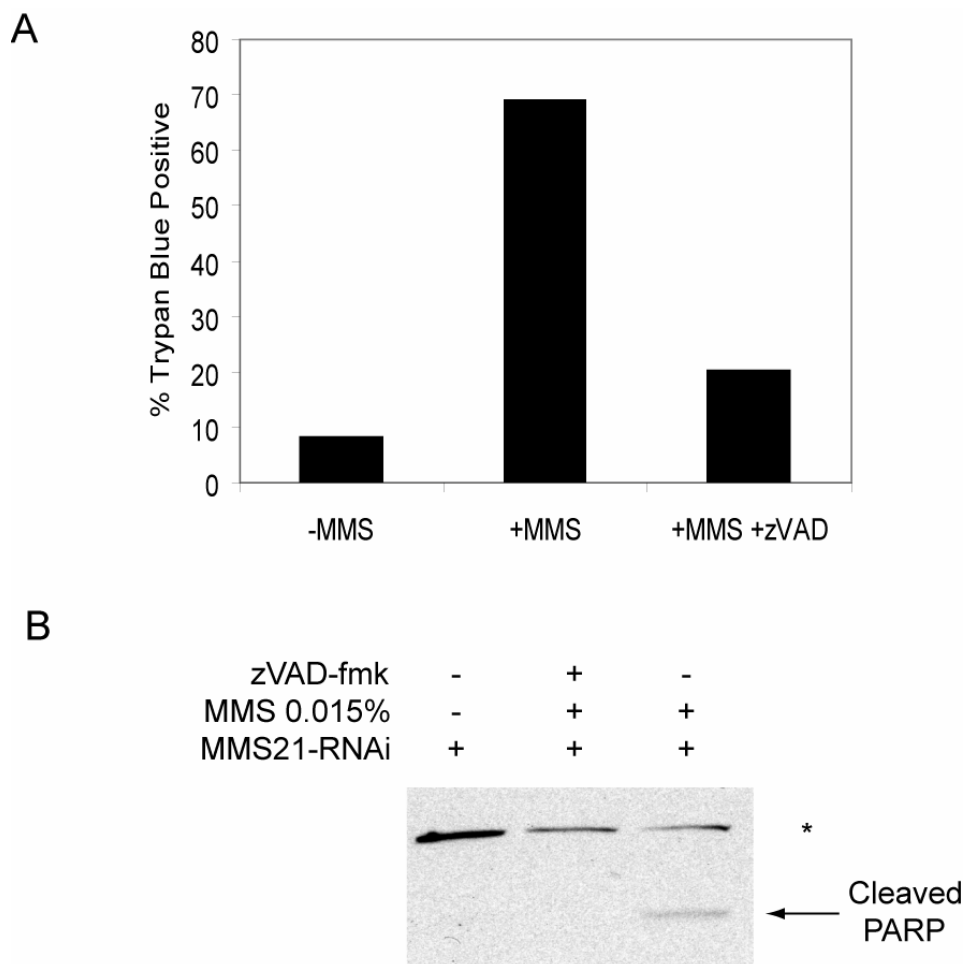
**Figure 2-9. zVAD-fmk prevents MMS-induced apoptosis in MMS21-RNAi cells**
(**A**) HeLa cells were transfected with either mock or MMS21 siRNA for 48 hrs. Cells were then either untreated or treated with 0.015% MMS for 6 hrs in the presence or absence of 50 µM zVAD-fmk. After treatment, cells were collected and the percentage of trypan blue positive cells was determined and plotted. (**B**) Lysates of cells in (A) were blotted with anti-cleaved PARP.

# CHAPTER III:  THE SMC5/6 COMPLEX PROMOTES SISTER CHROMATID HOMOLOGOUS RECOMBINATION

## INTRODUCTION

The Structural Maintenance of Chromosomes (SMC) proteins are essential for chromosomal architecture and organization (Hagstrom and Meyer, 2003; Hirano, 2002; Nasmyth and Haering, 2005b; Petronczki et al., 2003).  The eukaryotic SMC proteins form three heterodimers, SMC1/3, SMC2/4, and SMC5/6.  The SMC1/3 heterodimer forms the cohesin complex that maintains sister chromatid cohesion during mitosis (Hagstrom and Meyer, 2003; Hirano, 2002; Koshland and Guacci, 2000; Petronczki et al., 2003).  SMC2/4 forms the condensin complex that mediates chromosome condensation during mitosis (Hirano, 2005a; Swedlow and Hirano, 2003).  The SMC5/6 complex is involved in the cellular response to DNA damage (Fousteri and Lehmann, 2000; Hagstrom and Meyer, 2003; Hirano, 2002; Lehmann et al., 1995; Onoda et al., 2004).  Each SMC protein consists of an N-terminal Walker A box and a C-terminal Walker B box that are separated by a flexible linker region (Hirano, 2005b).  This linker region forms an intramolecular anti-parallel coiled-coil that brings the Walker A and B motifs into proximity, thus reconstituting a functional ATPase module (Haering et al., 2002a).  The SMC heterodimers of cohesin and condensin form V-shaped structures (Hagstrom and Meyer, 2003; Swedlow and Hirano, 2003).

The ATPase head domains can be linked by non-SMC proteins, called kleisins, to form rings (Nasmyth and Haering, 2005b).

The SMC1/3 cohesin complex is essential for maintaining cohesion between sister chromatids during mitosis to promote their equal segregation to daughter cells (Nasmyth, 2002). In addition, cohesin plays an important role in the repair of DNA double-strand breaks (DSBs; Hirano, 2005b; Lehmann, 2005). In yeast, mutations in the cohesin subunit SCC1/RAD21/MCD1 (referred to as SCC1 hereafter) are hypersensitive to DNA damaging agents (Birkenbihl and Subramani, 1992; Tatebayashi et al., 1998). Furthermore, chicken DT40 cells conditionally deficient in SCC1 show a decrease in sister chromatid exchanges (SCEs) induced by 4-nitroquinoline-1-oxide (Sonoda et al., 2001). It has been proposed that SMC1/3 facilitates DNA repair by holding sister chromatids together locally at DSBs to allow strand invasion and exchange with the sister chromatid repair template during HR (Schar et al., 2004; Sjogren and Nasmyth, 2001; Sonoda et al., 2001; Strom et al., 2004).

Studies in yeast have established that the normal replicative loading of the SMC1/3 cohesin complex on chromatin is insufficient to hold DSBs in close proximity, suggesting that the cohesin complex must be loaded post-replicatively at the vicinity of DSBs to facilitate sister chromatid HR (Strom et al., 2004). The cohesin complex has been shown to be recruited to DSBs in both yeast and human cells (Kim et al., 2002a; Strom et al., 2004; Unal et al., 2004). In yeast, the

recruitment of cohesin to HO endonuclease-induced DSBs requires MRE11 and the phosphorylation of the histone H2A variant H2AX at S139 (γH2AX; Unal et al., 2004). Additionally, the recruitment of cohesin to DSBs in yeast represents *de novo*, post-replicative loading of cohesin at DSBs that requires the SCC2/4 loading complex (Strom et al., 2004; Unal et al., 2004).

The SMC5/6 complex has primarily been studied in fission and budding yeasts. Cells harboring hypomorphic alleles of genes in the SMC5/6 complex show an increased sensitivity to DNA damage agents (Fousteri and Lehmann, 2000; Fujioka et al., 2002; Hu et al., 2005; Lehmann et al., 1995; McDonald et al., 2003; Morikawa et al., ; Onoda et al., 2004; Pebernard et al., 2004; Prakash and Prakash, 1977a; Prakash and Prakash, 1977b). Genetic analysis has shown that components of the SMC5/6 complex function together with RAD51 in the repair of DSBs through HR (Harvey et al., 2004; McDonald et al., 2003; Montelone and Koelliker, 1995; Onoda et al., 2004; Pebernard et al., 2004). Mutations in the SMC5/6 complex also exhibit defects in the maintenance of DNA damage checkpoint signals (Harvey et al., 2004; Verkade et al., 1999). In addition, plants in which the SMC6 ortholog has been disrupted show a defect in HR (Mengiste et al., 1999).

The yeast SMC5/6 complex contains several non-SMC elements (NSE), including NSE1, MMS21/NSE2 (hereafter referred to as MMS21 for simplicity), NSE3, NSE4, NSE5, and NSE6 (Fujioka et al., 2002; Hu et al., 2005; McDonald

et al., 2003; Morikawa et al., 2004; Pebernard et al., 2004; Pebernard et al., 2006; Sergeant et al., 2005; Zhao and Blobel, 2005). The MMS21 subunit functions as a SUMO ligase to sumoylate multiple components of the SMC5/6 complex, including SMC5, SMC6, and NSE3 (Andrews et al., 2005; Potts and Yu, 2005; Zhao and Blobel, 2005). Sumoylation of SMC6 by MMS21 is enhanced upon DNA damage, suggesting that the SUMO ligase activity of MMS21 is regulated by the cellular DNA damage response (Andrews et al., 2005).

We have recently shown that human cells deficient in SMC5/6 are hypersensitive to DNA damaging agents and have a decreased capacity to repair damaged DNA, suggesting that the SMC5/6 complex is required for DNA repair (Potts and Yu, 2005). Here we describe a mechanism by which the human SMC5/6 complex facilitates DNA repair. We show that SMC5/6 is required for HR repair using the sister chromatid as a template (inter-chromatid), but not for non-homologous end-joining (NHEJ) or HR repair using extra-chromosomal or intra-chromosomal DNA as the template. The SMC5/6 complex is recruited to nuclease-induced DSBs in human cells and is required for the recruitment of the SMC1/3 cohesin complex to DSBs.

## MATERIALS AND METHODS

**Cell culture, transfections, and siRNAs**

HeLa S3, HeLa Tet-On, 293/DR-GFP, 293/A658, and 293/1040 cells were grown in DMEM (Invitrogen) supplemented with 10% fetal bovine serum (Invitrogen), and 100 μg/mL penicillin and streptomycin (Invitrogen). At 40-50% confluency, plasmid or siRNA transfection was performed using the Effectene reagent (Qiagen) or the Oligofectamine reagent (Invitrogen), respectively, per manufacturer's protocols. 293 cells were transfected at 80-90% confluency with Lipofectamine 2000 (Invitrogen) when introducing both siRNA and plasmids for gene targeting, DR-GFP HR, and end-joining assays. The siRNA oligonucleotides against MMS21, SMC5, hSMC1, hSMC2, and SCC1 were chemically synthesized at an in-house facility or ordered from Dharmacon. The sequences of these oligonucleotides are listed in Table 3-1. The siRNA oligonucleotides against RAD51, KU70, and LACZ were obtained from the Dharmacon SMARTpool service. The annealing and transfection of the siRNAs were performed as previously described (Elbashir et al., 2001).

**Immunoblotting**

For determining efficiency of RNAi knockdown, 293 cells were lysed in SDS sample buffer, sonicated, boiled, separated by SDS-PAGE, and blotted with the indicated antibodies 2-3 days post-transfection of the desired siRNAs. Horseradish peroxidase-conjugated goat anti-rabbit or goat anti-mouse IgG (Amersham Biosciences) were used as secondary antibodies, and immunoblots

were developed using the ECL reagent (Amersham Biosciences) per

manufacturer's protocols.  The commercial antibodies used in this study are as

follows: anti-Myc (Roche, 11667203001, 1 µg/mL), anti-RAD51 (Santa Cruz

Biotechnology, sc-8349, 1:500), anti-SCC1 (Oncogene, NA-80, 1:250; Bethyl

Laboratory, A300, 1:500), anti-CD8-PE (Diatec, 3032, 1:15), anti-γH2AX

(Upstate, 07-164 and 05-636, 1:1000).  The production of polyclonal anti-MMS21

has been described previously (Potts and Yu, 2005).  Anti-SMC5 was kindly

provided by A. Lehmann (University of Sussex, United Kingdom).


**DR-GFP and gene targeting HR assays**

HR assays were performed as described previously (Pierce et al., 1999).

Briefly, we used a 293 cell line (293/DR-GFP) stably expressing a mutated *GFP*

gene (*SceGFP*) that had an insert containing in-frame stop codons and the 18-bp

I-SceI recognition sequence.  The DR-GFP repair substrate also contained an

internal fragment of *GFP* (*truncGFP*) down-stream of *SceGFP* (Pierce et al.,

1999).  Expression of neither *SceGFP* nor *truncGFP* could yield a functional GFP

protein.  To assay the rate of HR, 293/DR-GFP cells were transfected with an I-

SceI-encoding plasmid along with LACZ or MMS21 siRNA oligonucleotides.  To

determine the transfection efficiency, 293/DR-GFP cells were transfected with a

GFP-expression plasmid and either LACZ or MMS21 siRNA oligonucleotides.

The cells were then grown for 3 days.  The percentage of HR was determined by

measuring the percentage of GFP-positive cells using a FACScan flow cytometer (BD Biosciences) and normalizing to the transfection efficiency for each condition.

Gene targeting assays were performed essentially as described previously (Porteus and Baltimore, 2003). Briefly, we used a 293 cell line (293/A658) stably expressing a *GFP* gene that had an insert containing in-frame stop codons and a I-SceI recognition site (5'-TAGGATAACAGGGTAAT-3') at bp 327 of the *GFP* coding region. The expression of GFP was driven by a hybrid CMV/CBA promoter. This mutant *GFP* served as the artificial chromosomal gene target. The I-SceI/repair plasmid (A979) contained two cassettes: the first is an I-SceI expression cassette using the CMV/CBA promoter; the second is a 2100 bp repair substrate that contains a truncated *GFP* gene (*truncGFP*) followed by an additional 1300 bp of 3'-homology to the mutated *GFP* genomic target. Gene targeting was measured by transfecting 293/A658 cells with the I-SceI/repair plasmid and the indicated siRNA oligonucleotides. To normalize for differences in transfection efficiency, 293/A658 cells were also transfected with a GFP-expression plasmid and the indicated siRNAs. The cells were then grown for 3 days. The percentage of GFP-positive cells was measured by a FACScan flow cytometer and normalized to the transfection efficiency for each condition to give the gene targeting efficiency.

**Ligation-mediated quantitative PCR (LM-QPCR)**

293/A658D cells were transfected with siRNAs toward LACZ or MMS21.

Twenty-four hours after siRNA transfection, cells were transfected with a

CMV/CBA I-SceI expression construct.  Genomic DNA was collected, 0, 24, or

48 hrs after transfection with a DNAeasy extraction kit (Qiagen) per

manufacture's instructions.  I-SceI-induced 3' overhangs at DSBs were converted

to blunt ends by treatment of 5 µg genomic DNA with T4 DNA polymerase (New

England Biolabs) for 15 min at 12 ºC.  The resulting blunt-ended genomic DNA

was purified using a QIAquick spin column (Qiagen).  The asymmetric annealed

BW linker oligonucleotides (BW-1 and BW-2) were then ligated to the blunt-

ended genomic DNA at 16 ºC for 16 hrs as described previously (Curry et al.,

2005).  The resulting linker-ligated genomic DNA was purified using a QIAquick

spin column.  The presence of linker-ligated DSBs in the genomic DNA was

assayed by QPCR with 2X iTaq (Bio-Rad Laboratories) on an ABI-7500 (Applied

Biosystems) using primers spanning the linker region (linker #2) and *GFP* (*GFP*

#3).  Results were normalized for amount of genomic DNA in the samples using

primers toward *GFP* only (*GFP* #5).  The primer sequences used are listed in

Table 3-1.

**End-joining assay**

We used a 293 cell line (293/1040) stably expressing an end-joining reporter (Figure 3A) that contained a *GFP* gene flanked by I-SceI recognition sites driven by a CMV/CBA promoter for assaying end-joining. The *CD8α* gene was located downstream of the *GFP* gene and was not constitutively expressed due to the lack of an IRES. 293/1040 cells were transfected with the indicated siRNAs and either an I-SceI expression plasmid or an RFP expression plasmid as a transfection efficiency control. If I-SceI cuts both sites flanking *GFP* and end-joining occurs, GFP expression would be lost and CD8 expression would be gained. CD8 expression was measured by staining with phycoerytherin-conjugated anti-CD8 monoclonal antibody (Ditech). Cells were analyzed for the loss of GFP expression and gain of CD8 expression by FACS 3-5 days after transfection. The end-joining rate was determined by counting the percentage of GFP-CD8+ cells and normalizing to the transfection efficiency.

**Sister-chromatid exchange (SCE) assay**

293/A658 cells were transfected with the indicated siRNAs for 24 hrs. The cells were replated and incubated in the presence of 10 μM BrdU for 40 hrs (two cell divisions). Where indicated, 2.5 nM camptothecin was added during the BrdU labeling to induce a greater number of SCEs. Colcemid (150 ng/mL) was added during the final 30 minutes to enrich for mitotic cells. Cells were collected by trypsinization and washed in PBS. Cells were swelled in 75 mM KCl for 16

min at 37ºC, followed by centrifugation.  Cell pellets were resuspended in fixative

(3:1 solution of methanol:glacial acetic acid) and incubated for 20 min at 4ºC.

Cells were washed in fixative two more times.  After the final wash, cells were

resuspended in fixative and dropped onto cold slides.  Slides were allowed to air

dry in the dark for 2-3 days.  Chromosomes were then differentially stained for 5

min with 0.1 mg/mL acridine orange (Molecular Probes).  Slides were washed

extensively for 2 min under running water followed by 1-min incubation and

mounting in Sorenson Buffer, pH 6.8 (0.1M $Na_2HPO_4$, 0.1M $NaH_2PO_4$).  Slides

were immediately viewed with a 63x objective on a Zeiss Axiovert 200M

fluorescence microscope.  Images were acquired with a CCD camera using

Slidebook imaging software (Intelligent Imaging Innovations).  Images were

analyzed for the number of SCE by counting the number of crossover events per

metaphase.  A minimum of 50 metaphases were scored for each experiment over

three independent experiments.


**Long tract sister-chromatid recombination (LTGC/SCR) assay**

LTGC/SCR assays using the U2OS/SCR cells (kindly provided by Dr.

Ralph Scully, Boston, MA) were essentially described previously (Puget et al.,

2005).  Briefly, U2OS/SCR cells were transfected with the indicated siRNAs for

24 hrs and subsequently transfected with an I-SceI expression plasmid for 24

additional hours.  Cells were then collected and replated at 50,000, 100,000, and

200,000 cells per 10cm$^2$ dish in duplicates. Cells were incubated for four days

before addition of blasticidin (Invitrogen, 5 μg/mL). Fourteen days after

continual selection, blasticidin resistant (BsdR+) cells were fixed and stained with

crystal violet before counting. The percentage of cells undergone LTGC/SCR

was normalized to the plating and transfection efficiency of the LACZ-RNAi and

MMS21-RNAi cells. Plating efficiency was determined by plating 200 cells per

60 cm$^2$ dish in quadruplicates after RNAi and I-SceI transfection. Cells were

incubated as describe above except in the absence of blasticidin. Transfection

efficiency was determined by transfection of GFP-expression plasmid followed

by flow cytometry.

For determining the percentage of unequal, short tract gene conversion

and intrachromatid recombination, we treated U2OS/SCR cells with RNAi for 24

hrs followed by transfection of I-SceI. Cells were analyzed four days later by

flow cytometry for the number of GFP-positive cells. Results were normalized to

transfection efficiencies.

**Comet assay**

Comet assays were performed according to manufacturer's protocol

(Trevigen) and as previously described (Potts and Yu, 2005). Briefly, cells were

collected after the indicated treatments, mixed with low melt agarose and allowed

to harden on slides. Cells were then incubated in lysis buffer followed by

incubation in alkaline buffer. Slides were then washed in TBE and then placed in

a horizontal electrophoresis apparatus and voltage was applied for 10 min at 12V.

Slides were then immersed in 70% ethanol and then allowed to air dry at room

temperature overnight. Slides were stained with SYBR Green 1 (Molecular

Probes) for 10 min and then washed once in TBE. All incubations were

performed in the dark to prevent unintended DNA damage. Slides were viewed

using a 20X objective as described above. The percentage of cells displaying a

comet tail was calculated. At least 100 cells were scored in each condition over

three independent experiments.


**Chromatin immunoprecipitation (ChIP) assay**

293/A658 cells ($5x10^7$ cells per ChIP) were transfected with vector control

or CMV/CBA I-SceI expression plasmid for 24 hrs. In experiments involving

siRNA, cells were transfected with siRNAs for 24 hrs prior to transfection with

the I-SceI expression plasmid. ChIP was performed as described previously

(Aparicio et al., 2005). Cells were crosslinked in 0.37% formaldehyde and the

reaction was quenched with 0.3 M glycine. The cells were washed in TBS and

MC lysis buffer (10 mM Tris-Cl, pH 7.5, 10 mM NaCl, 3 mM $MgCl_2$, and 0.5%

NP-40). The nuclear pellet was then resuspended in sonication buffer (10 mM

Tris-Cl, pH 7.5, 200 mM NaCl, 3 mM $MgCl_2$, 1 mM $CaCl_2$, 4% NP-40, 1% SDS,

3 mM PMSF, and 1X protease inhibitor cocktail (Roche)). Cells were sonicated

at 60% duty cycle, four times for 30 sec continuously in an ice water bath with 2 min breaks between sonications. The fragmented chromatin was then cleared by centrifugation and the soluble fraction diluted 1:5 in FA lysis buffer (50 mM HEPES-KOH, pH 7.5, 150 mM NaCl, 1 mM EDTA, 1% Triton X-100, 0.1% sodium deoxycholate, 0.1% SDS, 2 mM PMSF, and 1X protease inhibitor cocktail). The diluted chromatin was then precleared with protein A-Sepharose beads (Bio-Rad). One percent of the resulting precleared chromatin was used as the input sample. To the remaining precleared chromatin, 2 μg of the indicated antibodies were added and incubated rotating overnight at 4ºC. The chromatin bound beads were washed in FA lysis buffer, ChIP wash buffer (10 mM Tris-Cl, pH 8.0, 0.25 M LiCl, 1 mM EDTA, 0.5% NP-40, and 0.5% sodium deoxycholate), and TE. Chromatin was then eluted from the beads by incubation in ChIP elution buffer (50 mM Tris-Cl, pH 7.5, 10 mM EDTA, and 1% SDS) at 65ºC for 10 min. The chromatin was then decrosslinked and proteins degraded. The DNA was then purified over a QIAquick spin column, per manufacturer's instructions. Conventional semi-quantitative PCR was performed on the resulting purified DNA after ChIP using with 25-30 cycles of amplification. Quantitative real-time PCR (QPCR) was performed as described above using validated primers toward the 5' side of the DSB (*GFP #5*) or the 3' side of the DSB (*GFP#7*) and *GAPDH* as a normalization control. The sequences of the primers used are listed in Table 3-1.

**RESULTS**

**The SMC5/6 complex is not required for all forms of homologous recombination**

To investigate the mechanism by which the SMC5/6 complex promotes DNA repair, we tested whether SMC5/6 is required for the repair of a single DSB in human cells induced by the rare-cutting I-SceI endonuclease (Pierce et al., 1999). A repair substrate containing a direct repeat green fluorescent protein (DR-GFP) reporter was stably integrated into the genome to create 293/DR-GFP cells. Both copies of the *GFP* genes within DR-GFP are mutated: *SceGFP* contains in-frame stop codons and the 18 bp I-SceI recognition site while *truncGFP* is an internal fragment of *GFP* (Figure 3-1A). Without HR, neither *SceGFP* nor *truncGFP* encodes functional GFP proteins, and the cells remain GFP-negative. Expression of I-SceI results in a chromosomal DSB in the *SceGFP* gene. Four mechanisms can be used to repair this DSB (Moynahan et al., 2001): 1) HR between the two tandem copies of the mutated GFP genes within the same chromatid (intra-chromatid recombination), 2) HR between *SceGFP* on one chromatid and *truncGFP* on the sister chromatid (unequal sister chromatid recombination), 3) HR between *SceGFP* on one chromatid and *SceGFP* on the sister chromatid (equal sister chromatid recombination), and 4) NHEJ (Figure 1A). Intra-chromatid recombination and unequal sister chromatid

recombination, but not equal sister chromatid recombination or NHEJ, will reconstitute a functional *GFP* gene, resulting in GFP-positive cells. The percentage of GFP-positive cells is determined by flow cytometry.

As expected, about 2% of cells were GFP-positive after the co-transfection of a plasmid encoding I-SceI and LACZ siRNA (LACZ-RNAi; Figure 3-1B and D). Knockdown of a critical HR component, RAD51 greatly reduced the amount of GFP-positive cells (Figure 3-1D). Surprisingly, the percentage of GFP-positive cells increased by 2-fold in cells transfected with MMS21 or SMC5 siRNA (Figure 3-1B and D). Depletion of MMS21 was confirmed by western blotting (Figure 3-1C). The increase in GFP-positive cells in MMS21-RNAi cells was abrogated by RAD51-RNAi (Figure 3-1D), suggesting that the increase caused by MMS21-RNAi is through a RAD51-dependent HR pathway. Inactivation of proteins generally required for all forms of HR, such as RAD51, BRCA1, and BRCA2, leads to a reduction of GFP-positive cells in this type of assay (Moynahan et al., 1999; Moynahan et al., 2001). Since the DSB generated by I-SceI can be repaired by multiple pathways, there may be active competition for the repair of the DSB by these pathways. Therefore, one explanation for the increase in GFP-positive cells in MMS21-RNAi or SMC5-RNAi cells is that knockdown of the SMC5/6 complex selectively blocks HR through equal sister chromatid recombination or NHEJ (pathways that do not generate GFP-positive

cells), thus shunting the repair of the DSBs down the other two HR pathways that will yield GFP-positive cells.

**Inactivation of the SMC5/6 complex enhances gene targeting in human somatic cells**

We next tested whether down-regulation of SMC5/6 affected the rate of HR using a gene targeting assay that measured the frequency of HR between a chromosomal locus and an episomal repair plasmid (Porteus and Baltimore, 2003). Briefly, an artificial gene target (A658), containing a mutated *GFP* gene with in-frame stop codons and an I-SceI recognition site inserted, is stably integrated at a single genomic locus of 293 cells (293/A658). The 293/A658 cells are transfected with an I-SceI/repair plasmid that contains the *I-SceI* gene and a truncated *GFP* gene. In the absence of HR, neither *SceGFP* (the mutated *GFP* gene integrated in the genome) nor *truncGFP* (the truncated *GFP* gene on the I-SceI/repair plasmid) will express functional GFP, and the cells remain GFP-negative (Porteus and Baltimore, 2003). Expression of I-SceI introduces a DSB within the integrated *GFP* locus, which can be repaired by three major pathways: 1) HR between the integrated *SceGFP* chromosomal locus and the episomal repair plasmid (gene targeting), 2) HR between the two sister chromatids, and 3) NHEJ (Figure 3-2A). Only gene targeting, but not NHEJ or HR between sister

chromatids, reconstitutes a functional *GFP* gene and results in GFP-positive cells. The number of GFP-positive cells is determined by flow cytometry (Figure 3-3).

If SMC5/6 complex is specifically required for HR between sister chromatids, down-regulation of SMC5/6 by RNAi should increase the frequency of gene targeting. We transfected 293/A658 cells with LACZ, RAD51, MMS21, or SMC5 siRNAs together with the I-SceI/repair plasmid. Depletion of these proteins was confirmed by western blotting (Figure 3-2B and data not shown). As expected, RNAi against RAD51 decreased the frequency of gene targeting (episomal recombination) by 80% (Figure 3-2C). Interestingly, knockdown of either MMS21 or SMC5 by RNAi showed about 4-fold increase in the frequency of gene targeting (Figure 2C). RAD51-RNAi reversed the stimulatory effects of MMS21-RNAi or SMC5-RNAi (Figure 3-2C), indicating that the enhanced gene targeting is dependent on RAD51. We next restored expression of MMS21 in MMS21-RNAi cells by transfecting in an MMS21 expression plasmid that contained silent mutations in the siRNA-targeting region. As expected, ectopic expression of MMS21 in MMS21-RNAi cells largely diminished the increase in gene targeting of MMS21-RNAi cells (Figure 3-2D). This confirmed that the increase in gene targeting is due to the specific knockdown of MMS21.

We next examined the efficiency of I-SceI to induce DSBs in control or MMS21-RNAi cells by ligation-mediated quantitative PCR (LM-QPCR; Figure 2E) and Southern blotting (Figure 3-4). Both assays suggested a slight decrease

in the number of DSBs in the MMS21-RNAi cells (Figure 3-2E and 3-4).

Therefore, the increase in HR in cells depleted for MMS21 or SMC5 in the DR-

GFP or gene targeting assays is not due to an increase in the number of DSBs in

cells with defective SMC5/6.

We next tested the effects on gene targeting by knocking down the

SMC1/3 cohesin complex that had been shown to be specifically required for

sister chromatid HR.  Treating 293/A658 cells with SMC1-RNAi or SCC1-RNAi

resulted in a four-fold increase in the percentage of GFP-positive cells after the

expression of I-SceI (Figure 3-2F).  This increase in gene targeting was inhibited

by RAD51-RNAi (Figure 3-2F).  As a control, RNAi against the condensin

subunit, SMC2, did not significantly increase the percentage of GFP-positive cells

(Figure 3-2F).  To confirm that the increase in gene targeting by MMS21-RNAi

was not due to a decrease in cohesin protein levels, we examined the levels of

SCC1 in MMS21-RNAi cells.  As expected, MMS21-RNAi did not affect SCC1

or RAD50 protein levels (Figure 3-3).  These results suggest that, like the

SMC1/3 cohesin complex, SMC5/6 may be specifically required for the repair of

DSBs through sister chromatid HR.


**The SMC5/6 complex is not required for NHEJ**

An alternative explanation for the increase in gene targeting is that

knockdown of SMC5/6 blocks another DSB repair pathway, such as NHEJ,

thereby resulting in a general increase in HR. To test whether SMC5/6 is required for the repair of DSBs through NHEJ, we used an end-joining reporter cell line that measures the number of end-joining events. 293 cells (293/1040) were stably integrated with an end-joining substrate (1040) that contained a CMV/CBA promoter driving the expression of a *GFP* gene which is flanked by I-SceI recognition sites (Figure 3-5A). The *CD8α* gene is downstream of the *GFP* gene and is not expressed because it lacks a promoter or an internal ribosome entry site (IRES). Therefore, cells are normally GFP-positive and CD8-negative (GFP+CD8-). Upon the transfection of I-SceI, two DSBs will be generated, resulting in the deletion of *GFP*. Ligation of the two ends through NHEJ will result in CD8 expression (Figure 3-5A), which can be monitored with a fluorescent CD8 antibody. The rate of end-joining was determined by calculating the percentage of GFP-CD8+ cells.

Approximately 5% of the control LACZ-RNAi cells were GFP-CD8+ after I-SceI expression (Figure 3-5B). Knockdown of an NHEJ protein, KU70, resulted in an approximately 70% decrease in the number of GFP-CD8+ cells, validating the assay (Figure 3-5B). In contrast, MMS21-RNAi increased the number of GFP-CD8+ cells by about 2-fold (Figure 3-5B). Similarly, SCC1-RNAi resulted in a 2-fold increase in end-joining (Figure 3-5B). Knockdown of hSMC2 did not affect the end-joining efficiency. These findings indicate that the SMC5/6 and SMC1/3 cohesin complexes are not required for NHEJ. The

increase in end-joining upon depletion of SMC5/6 or cohesin complexes is

consistent with a shift in the choice of DSB-repair pathway from sister chromatid

HR to end-joining. Therefore, the increase in gene targeting in SMC5- and

MMS21-RNAi cells is most likely due to a blockade of sister chromatid HR.


**The SMC5/6 complex is required for sister chromatid HR**

To directly examine the function of the SMC5/6 complex in the repair of

DSBs by sister chromatid HR, we tested whether it is required for sister chromatid

exchange (SCE), a form of sister chromatid HR that requires a crossing-over

event during the resolution of double Holliday junctions. SCE can be monitored

by the incorporation of the bulkier thymidine analog, bromo-deoxyuridine

(BrdU), for two cell cycles, resulting in sister chromatids with either one or both

of its DNA strands containing BrdU (Wolff, 1977). This asymmetric labeling can

be visualized by using a DNA-intercalating dye, acridine orange, which is

excluded from chromatids with both strands incorporated with BrdU. HR events

will result in sister chromatids that show a gap in staining on one chromatid with

a gain of staining in the corresponding region of its sister chromatid (Figure 3-

6A).

We first measured the number of spontaneous SCEs per metaphase in cells

treated with either LACZ, MMS21, or SCC1 siRNAs. MMS21- and SCC1-RNAi

cells contained about half the number of SCEs per metaphase than LACZ-RNAi

cells (Figure 3-7). The low level of spontaneous SCEs during a normal cell cycle can be greatly stimulated by the addition of the topoisomerase inhibitor, camptothecin, during BrdU labeling (Degrassi et al., 1989). Similar to spontaneous SCEs, MMS21-RNAi and SCC1-RNAi cells contained approximately half the number of camptothecin-induced SCEs per metaphase than LACZ-RNAi cells, $20.80 \pm 3.52$ and $18.05 \pm 3.23$ versus $38.66 \pm 4.17$, respectively (Figure 3-6A and B).

We next used a previously described reporter assay to measure long tract gene conversion sister chromatid recombination (LTGC/SCR; Johnson and Jasin, 2000; Puget et al., 2005). The HR reporter in this assay is integrated into U2OS cells and contains a *GFP* gene with a stop-I-SceI site and an upstream truncated *GFP* gene as the recombination substrate upon I-SceI-induced DSB (Figure 3-6C). In addition, the LTGC/SCR reporter contains two halves of the *BsdR* gene that confers resistance to blasticidin. Cells that are not transfected with I-SceI are sensitive to blasticidin, as the two halves of the *BsdR* gene are in the wrong orientation and do not produce a functional protein. Upon I-SceI-induced unequal LTGC/SCR, the *BsdR* gene is duplicated. The presence of splice donor and acceptor sites then allows splicing to reconstitute a functional *BsdR* gene. The frequency of LTGC/SCR can be measured by counting the number of blasticidin-resistant clones.

We observed a 75% reduction in the number of blasticidin-resistant cells after treatment with MMS21-RNAi as compared to LACZ-RNAi, 0.25% ± 0.04 and 1.02% ± 0.08, respectively (Figure 3-6D, red bars, and Figure 3-7). The percentage of blasticidin-resistant cells was normalized to the plating and transfection efficiencies of these cells in the absence of blasticidin. This decrease in LTGC/SCR is similar that that observed for H2AX-/- ES cells (Xie et al., 2004). We also measured the frequency of intrachromatid HR and short tract, unequal HR by examining the percentage of GFP-positive cells after I-SceI transfection in either control or MMS21-RNAi cells. We observed a two-fold increase in the number of GFP-positive cells in MMS21-RNAi cells (Figure 3-6D, green bars). This is consistent with the two-fold increase in the number of GFP-positive cells observed in MMS21-RNAi cells using the DR-GFP reporter in 293 cells (Figure 1). In contrast, the number of GFP-positive cells decreased in H2AX-/- ES cells (Xie et al., 2004). This is consistent with the notion that H2AX is required for all forms of HR whereas the SMC5/6 complex is only required for sister chromatid HR.

We observe a significant decrease in both SCE (that measures sister chromatid recombination involving crossing over) and LTGC (that measures unequal sister chromatid recombination) in MMS21-RNAi cells. These results indicate that the SMC5/6 complex is specifically required for sister chromatid HR, but not intrachromatid HR. Thus, the enhanced episomal HR (gene

targeting), intrachromatid HR, and end-joining upon depletion of subunits of the SMC5/6 complex is due to the impaired ability of these cells to repair I-SceI-induced DSBs by sister chromatid HR.

**The SMC5/6 complex is required for DNA repair in cells after DNA replication**

One prediction of the results described above is that the SMC5/6 complex should only be required for the repair of damaged DNA in cells that contain sister chromatids. To test this hypothesis, we determined the ability of MMS21-RNAi cells to repair MMS-induced damaged DNA when either arrested at the G1/S-boundary (without sister chromatids) or cells that had progressed through S phase (with sister chromatids). HeLa S3 cells treated with mock, MMS21, or KU70 siRNAs for 36 hrs were arrested at G1/S-boundary by thymidine for 16 hrs. One group of cells was then released into S phase to allow DNA replication for two hrs. Both groups of cells were then treated with 0.015% methyl-methane sulfate (MMS) for one hr to induce DNA damage. The cells were then allowed to recover in the absence of MMS for three hours either still arrested at G1/S-boundary or released (Figure 3-8A). Cells were analyzed by flow cytometry to confirm their appropriate cell cycle stages (Figure 3-9A). The amount of unrepaired DNA damage was measured by the comet assay (Figure 3-8B; Collins, 2004).

Cells treated with mock siRNA were competent to repair the MMS-induced damaged DNA in the presence (S/G2) or absence (G1/S-boundary) of sister chromatids (Figure 3-8B and C). As predicted, MMS21-RNAi cells were capable of efficient repair of damaged DNA in cells with no sister chromatids (G1/S-boundary), but not in cells that contained sister chromatids (S/G2), 6.6% ± 9.1 and 85.3% ± 6.3 cells with comet tails, respectively (Figure 3-8B and C). To ensure that both G1/S-boundary and S/G2 cells were equally susceptible to MMS-induced DNA damage, we treated cells with MMS for one hr without allowing additional time for repair of the damaged DNA. Approximately 95% of both G1/S-boundary and S/G2 cells displayed comet tails after MMS treatment (data not shown), confirming that both G1/S-boundary and S/G2 cells are susceptible to MMS-induced DNA damage. Contrary to MMS21-RNAi cells, KU70-RNAi cells were competent to repair MMS-induced damaged DNA in S/G2 cells, but were incapable of repairing the damaged DNA in G1/S-boundary cells (Figure 3-8B and C). These results suggest that MMS21 is specifically required for the repair of MMS-induced DNA damage in S/G2 cells, but not in G1/S-boundary cells.

We next determined whether MMS21 is required for the repair of IR-induced DSBs in S/G2 cells. Mock-RNAi or MMS21-RNAi cells arrested at G1/S-boundary or released into S-phase were treated with 10 Gy of IR to induce DSBs. Cell lysates were collected at 0, 4, and 24 hrs after irradiation and the

repair efficiency of the cells was measured. Because H2AX phosphorylation is dramatically induced by IR-induced DSBs and its dephosphorylation is coupled with repair of those DSBs (Rothkamm et al., 2003), the amount of γH2AX (phosphorylated H2AX) provides a measure of unrepaired DSBs. MMS21-RNAi cells were competent to repair IR-induced DSBs in G1/S-boundary cells, but not in S/G2 cells (Figure 3-8D). These results suggest that MMS21 is specifically required for the repair of damaged DNA in cells that utilize sister chromatid HR (S/G2 cells), but not in cells that primarily rely on NHEJ for repair (G1/S-boundary cells).

These results demonstrate the preference for the use of NHEJ in G1/S-boundary cells and the preference for sister chromatid HR in S/G2 cells as reported previously (Rothkamm et al., 2003). We have shown that gene targeting is increased in cells arrested at S/G2, but decreased in cells treated with aphidicolin (Figure 3-9C). To confirm that the increase in gene targeting in the MMS21-RNAi cells (Figure 3-2) is not merely a result of cell-cycle arrest at S/G2, we determined the cell cycle profile of MMS21-RNAi cells by flow cytometry. We observed no significant differences in the cell cycle profile of asynchronous cultures of HeLa cells treated with either MMS21 siRNA or mock siRNA for 48 hrs (Figure 3-9B). Additionally, we determined the long-term viability and proliferative capacity of MMS21-RNAi cells by colony formation assays. We observed no significant differences in the ability of MMS21-RNAi

cells to form colonies as compared to LACZ-RNAi cells, 3.4 ± 1.4% and 2.1 ± 1.1% respectively (data not shown). Therefore, the increased gene targeting efficiency in MMS21-RNAi cells and their decreased ability to repair DNA damage in S/G2 is due to a defect in sister chromatid HR in these cells, rather than a secondary effect of an arrest at S/G2.

**The SMC5/6 complex is recruited to I-SceI-induced DSBs**

Many proteins involved in the repair of DSBs, such as ATM, RAD51, MRE11/RAD50/NBS1 (MRN), and cohesin complexes, are recruited to DSBs to facilitate repair in functionally distinct ways (Lisby and Rothstein, 2005). To investigate whether the SMC5/6 complex is also recruited to DSBs, we used our gene targeting cell line (293/A658) that contained an I-SceI endonuclease recognition site in the *GFP* gene. Upon transfecting I-SceI, we monitored the recruitment of proteins to a single DSB by performing chromatin immunoprecipitation (ChIP) using primers directed toward *GFP*. The SMC5/6 complex was recruited to I-SceI-induced DSBs in cells transfected with I-SceI (Figure 6A). In cells transfected with a mock expression plasmid, no SMC5/6 was present at the *GFP* locus, showing that these proteins were not constantly associated with the locus (Figure 3-10A). Expectedly, the cohesin complex (hSCC1) and γH2AX were present at the I-SceI-induced DSBs (Figure 3-10A). Importantly, this recruitment was specific to the DSB locus (*GFP*), as they were

not recruited to other genomic loci, such as *GAPDH* (Figure 3-10A). The *GFP*

PCR product was specific to the DSB, as 293 cells not integrated with the *GFP*

construct did not produce a PCR product (Figure 3-11). Our PCR analysis of the

DSB was in the linear range and the chromatin from these cells was sheared to a

proper size of 300–1000 bp (Figure 3-11). To examine the fold-enrichment of the

SMC5/6 complex at I-SceI-induced DSBs, we performed quantitative, real-time

PCR (QPCR). Using two different validated primer sets, we observed a 15-20-

fold enrichment of MMS21, SMC5, SCC1, and γH2AX at the DSB (Figure 3-10B

and 3-11), comparable to the up to 16-fold enrichment of RAD51 at I-SceI-

induced DSBs (Rodrigue et al., 2006). These data show that the SMC5/6

complex is recruited to DSBs.


**The SMC5/6 complex is required for the recruitment of the cohesin complex
to DSBs**

We tested whether depletion of both the SMC5/6 and SMC1/3 complexes

had a synergistic effect in the SCE assay. Western blotting confirmed efficient

depletion of MMS21 and SCC1 together or alone (data not shown). Knockdown

of both complexes by siRNAs towards MMS21 and SCC1 did not further

decrease the number of SCEs compared to knockdown of either one alone (Figure

3-12A). This suggested that the SMC5/6 and cohesin complexes may function in

a common pathway to promote sister chromatid HR.

Since both complexes are recruited to DSBs, we tested whether one complex is required for the recruitment of the other to DSBs by ChIP. Although SCC1 was significantly depleted from the DSBs, the accumulation of MMS21 at DSBs was only slightly reduced (Figure 3-12B). Thus, recruitment of the SMC5/6 complex to DSBs appears to be independent of cohesin. Remarkably, knockdown of the SMC5/6 complex blocked the recruitment of SCC1 to DSBs, although the phosphorylation of γH2AX was not altered (Figure 3-12C). As revealed by QPCR analysis, there was a severe defect in the recruitment of either hSMC1 or SCC1 to the DSB in both MMS21- or SMC5-RNAi cells. To determine whether this requirement for SMC5/6 in cohesin recruitment was specific for the DSB, we examined the effects of SMC5/6 depletion on cohesin loading at another genomic locus, AluSx on the X-chromosome (Hakimi et al., 2002). We measured the fold-enrichment of both SCC1 and hSMC1 at this locus in LACZ-, MMS21-, or SMC5-RNAi cells (Figure 3-12E). Depletion of either SMC5 or MMS21 did not affect the loading of either hSMC1 or SCC1 at this genomic locus. These results suggest that the SMC5/6 complex is not essential for cohesion loading throughout the genome. Instead, it is specifically required at DSBs. Thus, one mechanism by which the SMC5/6 complex facilitates sister chromatid HR is to promote the recruitment of cohesin to DSBs.

**DISCUSSION**

**Role of SMC5/6 in sister chromatid HR**

Studies in yeast, plants, and humans (this study) support a role of the SMC5/6 complex in DNA repair by promoting HR between sister chromatids. Both cohesin and condensin are also required for efficient DNA repair (Hagstrom and Meyer, 2003). It has been suggested that cohesin promotes DNA repair by maintaining the close proximity of sister chromatids at damage sites, thus facilitating homology-directed DNA repair using the opposing sister chromatid as template (Hagstrom and Meyer, 2003; Jessberger, 2002; Lehmann, 2005).

Cohesin loaded during S phase is insufficient to maintain sister chromatid cohesion at DSBs to facilitate sister chromatid HR (Strom et al., 2004). It is well-established that cohesin is recruited *de novo* to DSBs, which requires the MRN complex, γH2AX, and the SCC2/4 complex (Kim et al., 2002a; Strom et al., 2004; Unal et al., 2004). In this study, we show that an additional level of regulation exists, at least in human cells, in the recruitment of cohesin to DSBs. The SMC5/6 complex is necessary for cohesin recruitment to DSBs whereas cohesin is not required for the recruitment of the SMC5/6 complex to DSBs. These results are consistent with the following model (Figure 3-13). In this model, the SMC5/6 complex localizes to sites of DNA damage and promotes the recruitment of cohesin to the DSB. This SMC5/6-facilitated recruitment of cohesin to the

DSB holds the sister chromatids in close proximity to permit RAD51-dependent strand invasion and exchange using the sister chromatid as the repair template.

The exact mechanism by which the SMC5/6 complex recruits the cohesin complex to DSBs is unclear. We have so far failed to detect a direct physical interaction between the SMC5/6 and cohesin complexes (data not shown). However, MMS21 stimulates the sumoylation of two cohesin complex subunits, SCC1 and SA2, in cells (Figure 3-14). The functional significance of MMS21-induced sumoylation of cohesin remains to be determined. It will be interesting to test whether and how sumoylation of the cohesin complex regulates its recruitment and loading onto chromatin around a DSB.

The cohesin and condensin complexes form a ring-shaped structure that has been proposed to trap chromatin inside (Nasmyth and Haering, 2005b). Based on the homology of SMC5/6 complex with the cohesin and condensin complexes, it is plausible that the SMC5/6 complex also forms a ring structure and holds DNA (Nasmyth and Haering, 2005b). An alternative and not mutually exclusive mechanism by which the SMC5/6 complex promotes sister chromatid HR is that both the SMC5/6 and SMC1/3 complexes directly hold sister chromatids together in a similar manner as the cohesin complex in a ring-shaped structure. Additionally, a third related complex, the MRN complex, exists at DSBs and is proposed to hold the broken ends of the DSB together. It will be interesting to examine the interplay between these three complexes.

**Sister chromatid HR and gene targeting**

Gene targeting can be used to correct genetic mutations in human somatic cells. However, its experimental and therapeutic applications have been hindered by the low rate of spontaneous gene targeting in these cells (Porteus and Carroll, 2005). Intense effort has been focused on developing ways to increase the rate of gene targeting. It has been shown that gene targeting can be greatly enhanced by introducing DSBs in the target gene, therefore promoting HR (Jasin, 1996). To create sequence-specific DSBs within the human genome, we and others have developed zinc-finger nucleases that contain both zinc finger DNA-binding domains and endonuclease domains (Porteus and Baltimore, 2003). Another obstacle to achieving efficient gene targeting is the existence of multiple pathways of HR. Even after the introduction of DSBs in the target gene, these DSBs can be readily repaired through HR with the opposing sister chromatid as the template, instead of the episomal repair plasmid, thus minimizing the rate of gene targeting. This effect may be quite substantial as it is likely that most DSBs repaired by HR use the sister chromatid as a template.

We show that inactivation of the human SMC5/6 complex increases the efficiency of gene targeting by about 4 fold. This increase in episomal recombination is due to a specific decrease in the ability of the cells to promote sister chromatid HR, as shown directly by the SCE and LTGC/SCR assays. In

addition, we show that the increase in gene targeting and the decrease in SCE in cells with a compromised SMC5/6 function are similarly observed in cells depleted of the SMC1/3 cohesin complex that is implicated in sister chromatid HR. Furthermore, the increase in gene targeting upon inhibition of the SMC5/6 complex is not due to a defect in NHEJ. These results support the model that inhibition of the SMC5/6 or cohesin complexes reduces sister chromatid HR, therefore shifting the DSB repair pathway to NHEJ or HR with an episomal template (gene targeting). Our results further suggest that other strategies aimed at blocking HR between sister chromatids are expected to improve the efficiency of gene targeting. The challenge is to inhibit sister chromatid HR transiently without disturbing overall sister chromatid cohesion that can lead to genomic instability. This may ultimately lead to new strategies for genomic manipulations in mammalian somatic cells for both research and therapeutic purposes.

In summary, our results suggest that the SMC5/6 complex promotes DSB repair specifically through sister chromatid HR by facilitating the recruitment of cohesin to DSBs. Our study also identifies a novel strategy to improve the rate of gene targeting by blocking sister chromatid HR.
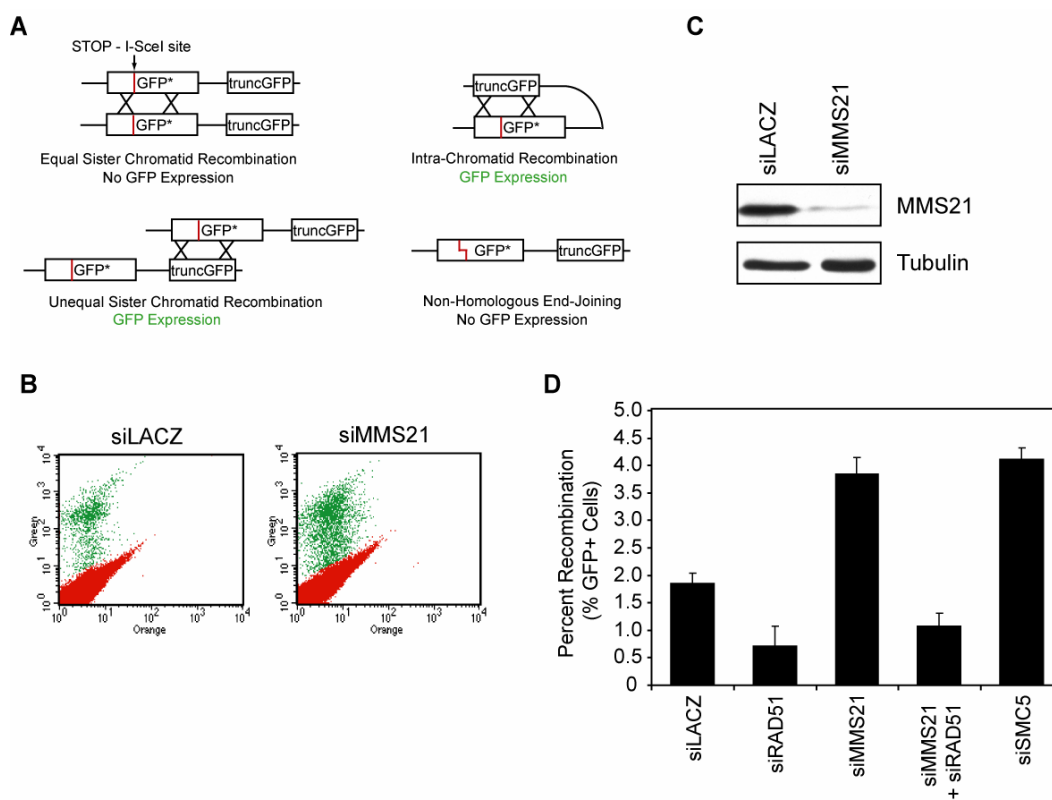
**Figure 3-1. The SMC5/6 complex is not required for all types of homologous recombination**

 (**A**) Schematic drawing of the homologous recombination assay.  The direct repeat GFP (DR-GFP) repair substrate contains a mutated *GFP* gene with an in-frame stop codon and an I-SceI site inserted (shown as red line) and a truncated *GFP* gene.  The four major types of repair of the DSB produced by I-SceI that can occur in this system are shown.  (**B**) 293/DR-GFP cells were transfected with an I-SceI-encoding plasmid along with the indicated siRNA oligonucleotides and analyzed 3 days later by flow cytometry.  GFP-positive cells are gated and shown in green.  Experiments are performed in triplicates.  Only one set of representative samples is shown.  (**C**) Western blotting showing the efficiency of siRNA knockdown 3 days after transfection in 293/DRGFP cells.  (**D**) Quantitation of the percentage of GFP-positive cells shown in (B).  Results from three separate samples are averaged with the standard deviation indicated.
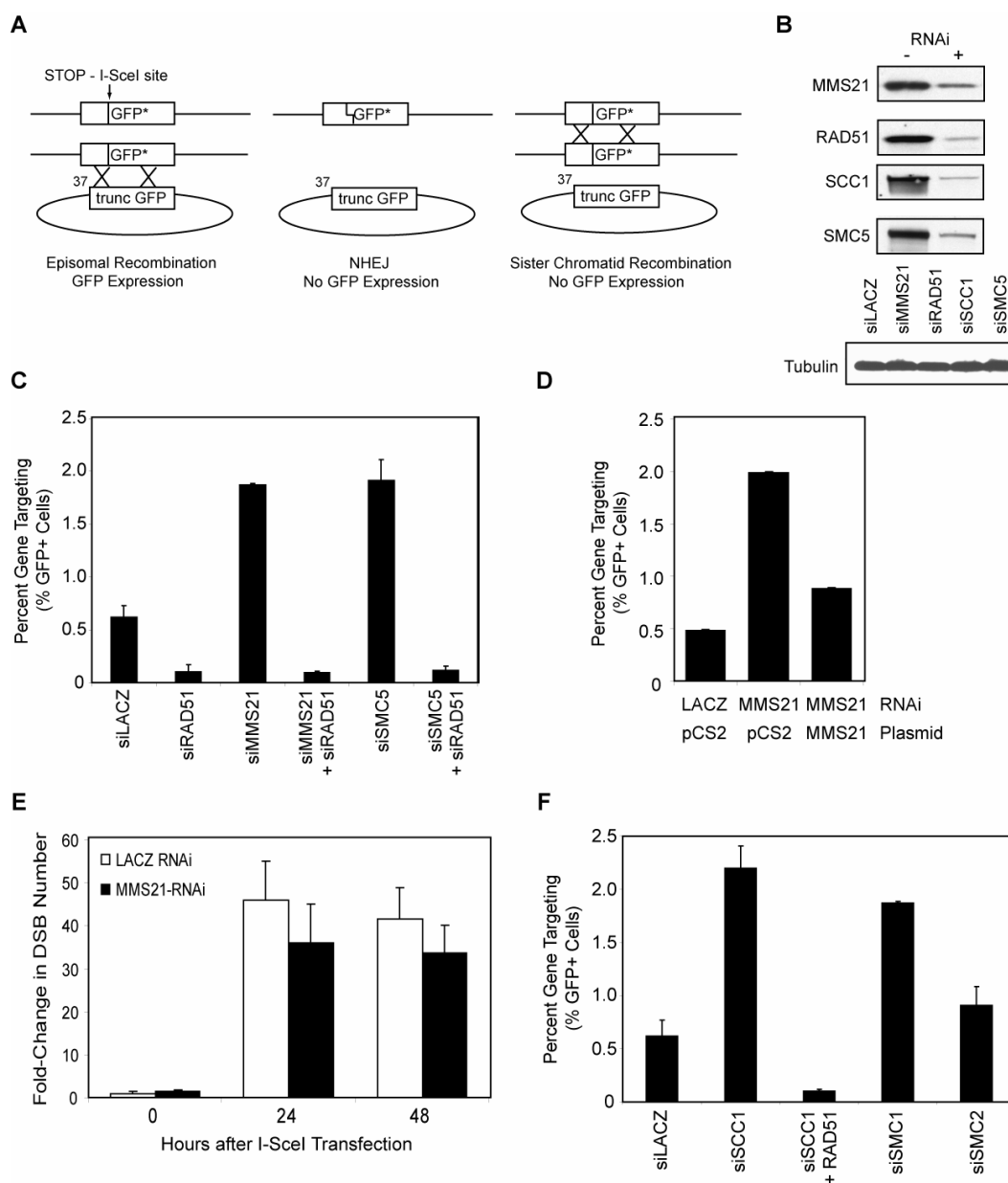
**Figure 3-2. Down-regulation of the SMC5/6 or cohesin complexes enhances gene targeting**

(**A**) Schematic drawing of the *GFP* gene targeting assay. A *GFP* gene containing an insert with an in-frame stop codon and an I-SceI site is stably integrated into 293 cells. The stop-I-SceI site is indicated by a red line. Gene targeting is accomplished by expression of an I-SceI/repair plasmid that contains a truncated *GFP* (*truncGFP*) gene and an I-SceI expression cassette. Expression of I-SceI

introduces a DSB at the stop-I-SceI site in the cells.  The three major repair pathways that repair the I-SceI-induced DSB are shown.  (**B**) Western blot analysis showing the efficiency of RNAi knockdown 3 days after transfection in 293/A658 cells.  The siRNA and antibody used for western blot are indicated to the left.  Tubulin was used as the loading control.  (**C**) 293/A658 cells were transfected with the repair plasmid along with the indicated siRNA oligonucleotides and analyzed 3 days later by flow cytometry.  Quantitation of the percentage of GFP-positive cells is shown.  Results from three separate samples are averaged with the standard deviations indicated.  (**D**) 293/A658 cells were transfected with the indicated siRNA oligonucleotides and expression plasmids and experiments were carried out as described in (C).  (**E**) 293/A658 cells were transfected with an I-SceI expression plasmid for the indicated times.  Genomic DNA was collected and the number of DSBs was quantitated by ligation-mediated quantitative PCR (LM-QPCR).  (**F**) 293/A658 cells were treated with the indicated siRNA oligonucleotides and experiments were carried out as described in (C).
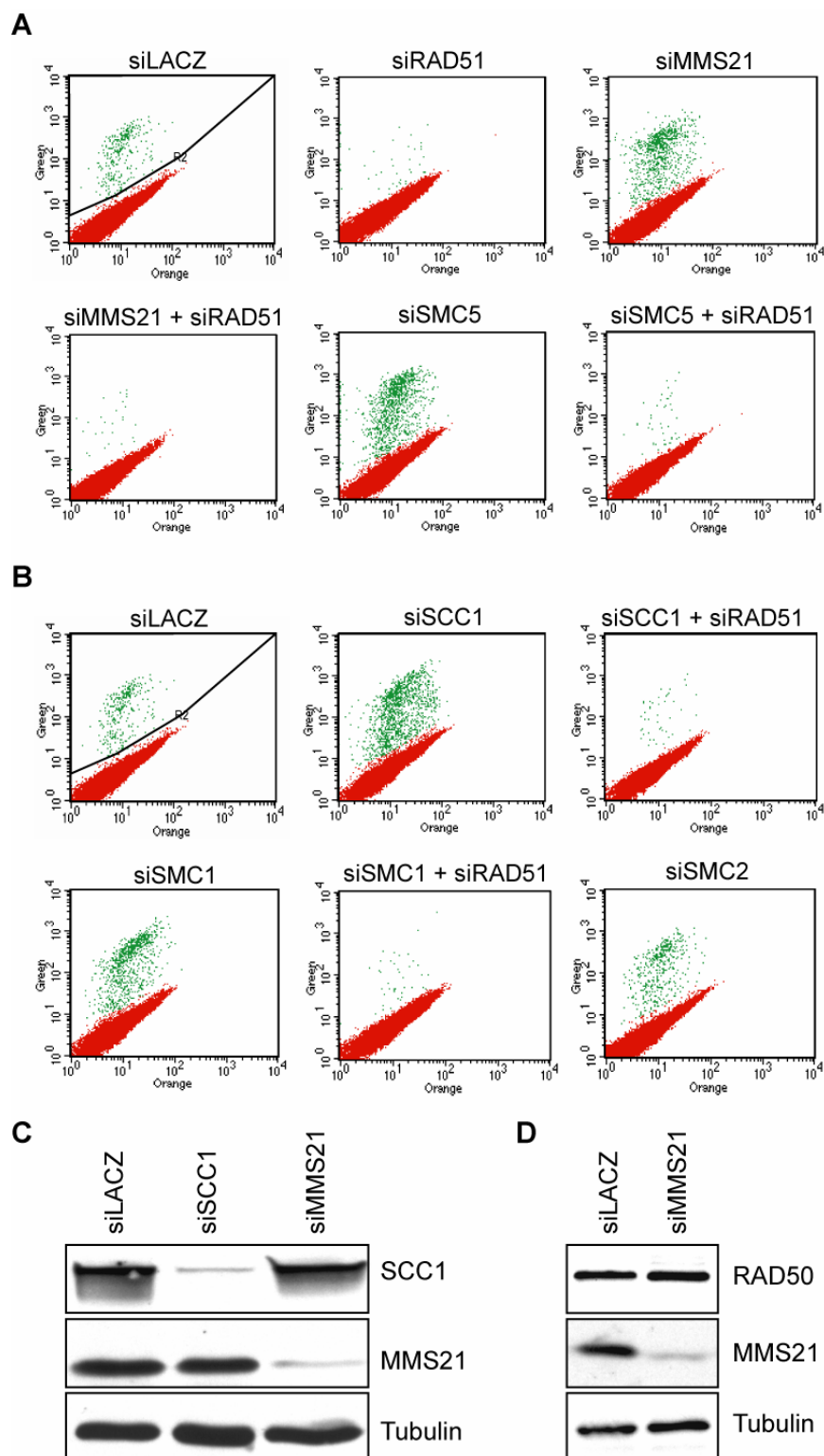
**Figure 3-3.  Knockdown of the SMC5/6 or cohesin complexes increases the efficiency of gene targeting**
(**A and B**) 293/A658 cells were transfected with the repair plasmid along with the indicated siRNA oligonucleotides and analyzed three days later by flow cytometry.  GFP-positive cells are gated and shown in green.  Experiments are performed in triplicates.  Only one set of samples is shown.  (**C and D**) 293/A658 cells were transfected with the indicated siRNA and blotted with the indicated antibodies.
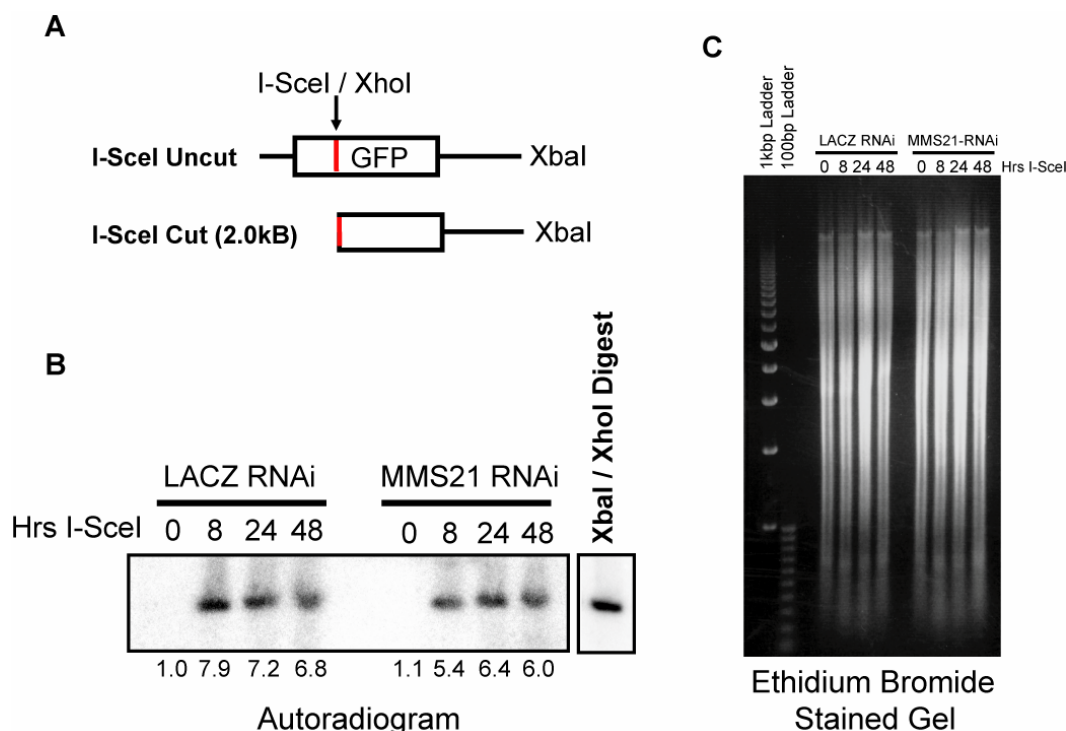
**Figure 3-4. I-SceI endonuclease activity is unaltered by MMS21-RNAi**
(**A**) Schematic drawing of the integrated target in 293/A658 cells. The *GFP* gene
contains an I-SceI recognition site followed by an XhoI recognition site. An XbaI
recognition site is located 2.0kb downstream of the I-SceI recognition site. Upon
I-SceI-induced DSB and digestion of genomic DNA with XbaI, a 2.0kB product
is obtained that indicates I-SceI activity. (**B**) 293/A658 cells were transfected
with the indicated siRNAs. Twenty-four hours after RNAi, an I-SceI expression
plasmid was transfected into the cells. Genomic DNA was collected at the
indicated times after I-SceI transfection. Genomic DNA was digested with XbaI
and southern blot analysis was performed to determine the amount of I-SceI-
induced DSBs in the cells. A fragment of the A658 plasmid was used as the
hybridization probe. As a control for I-SceI digestion, A658 plasmid containing
the stop-I-SceI-*GFP* was digested with XbaI and XhoI to mimic an I-SceI-
induced DSB. The 2.0kB I-SceI cut band is shown in the autoradiogram.
Quantitation of the relative intensities of the bands is shown. Image is a
representative sample of multiple experiments. (**C**) Ethidium bromide stained gel
before southern blot hybridization, shown in (B), to illustrate the equal loading of
DNA across samples. Image is a representative sample of multiple experiments.
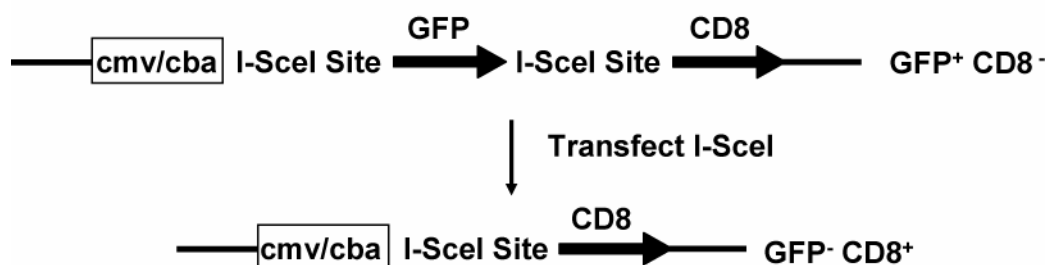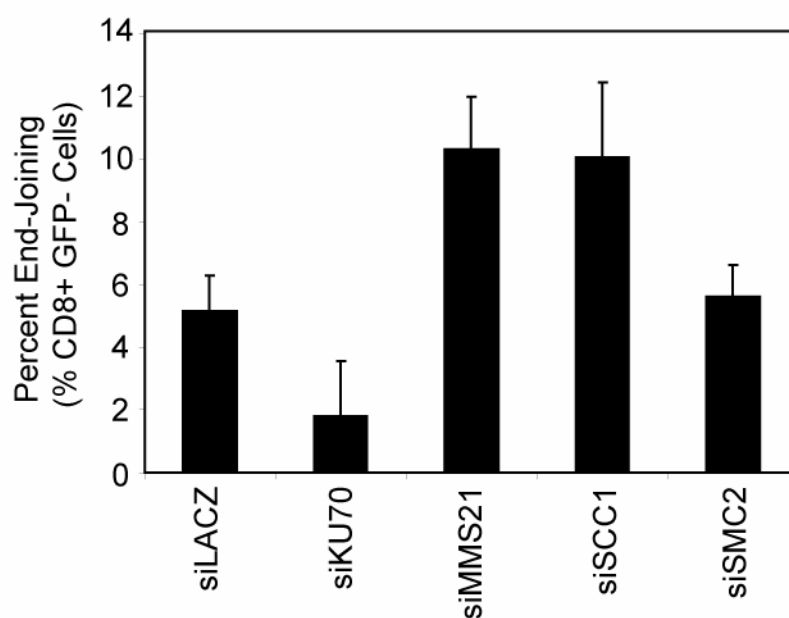
**Figure 3-5. The SMC5/6 complex is not required for end-joining**
(**A**) Schematic drawing of the end-joining assay.  293/1040 cells containing the integrated substrate shown are GFP+ CD8- prior to transfection.  If end-joining occurs upon transfection of I-SceI, the cells will become GFP- CD8+ because the *GFP* gene will be lost and the *CD8* gene will be driven by the CMV/CBA promoter.  (**B**) 293/1040 cells were transfected with the I-SceI plasmid and the indicated siRNA for four days.  Quantitation of the percentage of CD8+ GFP- cells is shown.  Results from three separate samples are averaged with the standard deviations indicated.
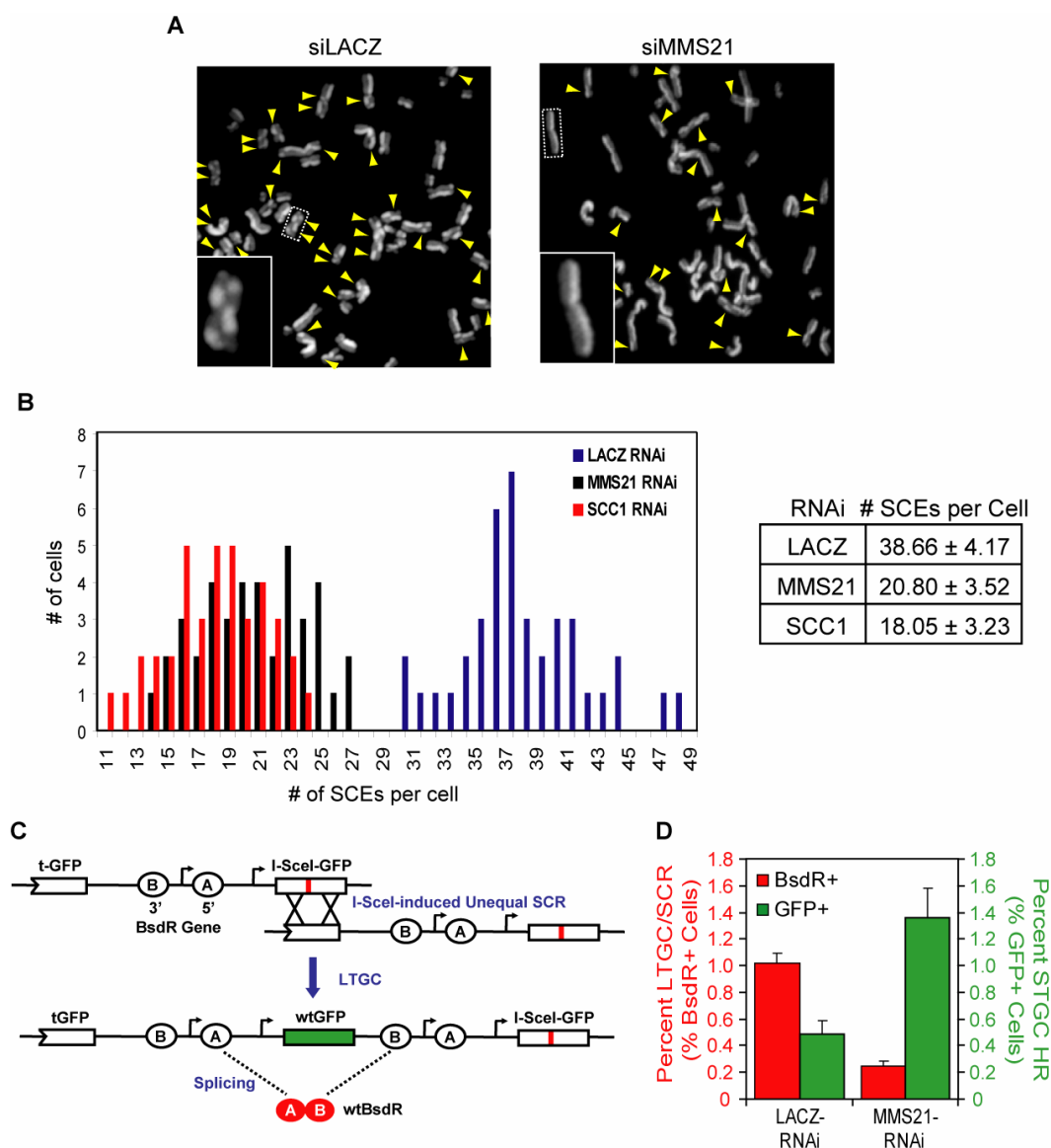
**Figure 3-6.  The SMC5/6 complex is required for sister chromatid HR**
(**A**) 293/A658 cells transfected with the indicated siRNA for 24 hrs were labeled with 10 µM BrdU in the presence of 5 µM camptothecin for 40 hrs (two cell divisions).  Chromosome spreads were stained with acridine orange to distinguish sister chromosomes.  Arrowheads indicate recombination events.  (**B**) Histogram of cells in (A) with the indicated number of sister chromatid recombination events per cell.  Results from three separate samples are averaged with the standard deviations indicated in the table to the right.  (**C**) Schematic illustration of the HR substrate integrated into U2OS cells.  A stop-I-SceI containing *GFP* gene is

located downstream of a truncated *GFP*. Two halves of the *BsdR* gene (A and B) that confers blasticidin resistance is present in between the two *GFP* genes. Upon I-SceI transfection, a DSB is produced that can be repaired by unequal sister chromatid HR. If long-tract gene conversion (LTGC) occurs, the *BsdR* genes will be duplicated, therefore allowing the production of a functional *BsdR* gene by splicing, due to the presence of splice donor and acceptor sites. Cells that have undergone LTGC/SCR are selected by blasticidin. (**D**) U2OS/SCR cells were transfected with the indicated siRNAs for 24 hrs followed by transfection of an I-SceI expression plasmid for an additional 24 hrs. For measuring LTGC/SCR (red bars), cells were replated and those that had undergone LTGC/SCR events were selected by 5 μg/mL blasticidin for fourteen days. Colonies were fixed and counted. For measuring short tract gene conversion (STGC; green bars), cells were analyzed by flow cytometry for GFP-positive cells four days after I-SceI transfection. Results from two separate experiments are averaged with the standard deviations indicated.

**A**



LACZ RNAi

MMS21 RNAi

**B**



| RNAi | # SCEs per Cell |
|------|-----------------|
| LACZ | 2.92 ± 1.56 |
| MMS21 | 1.56 ± 1.36 |
| SCC1 | 1.63 ± 1.40 |

**C**



LACZ RNAi

MMS21 RNAi
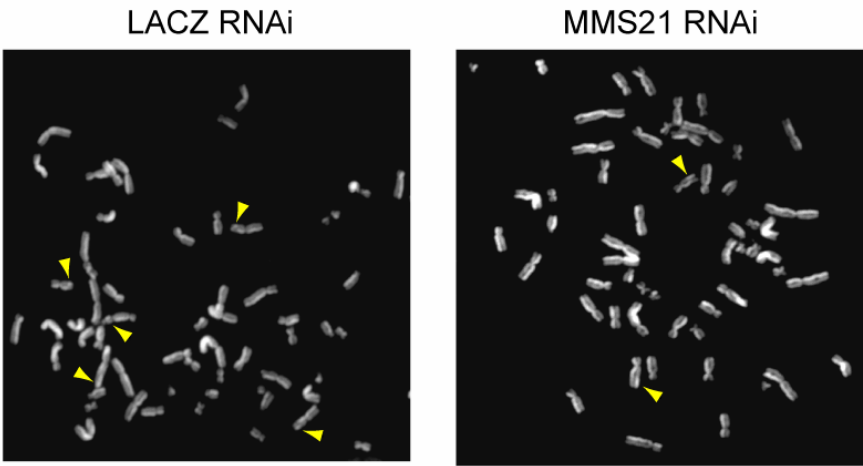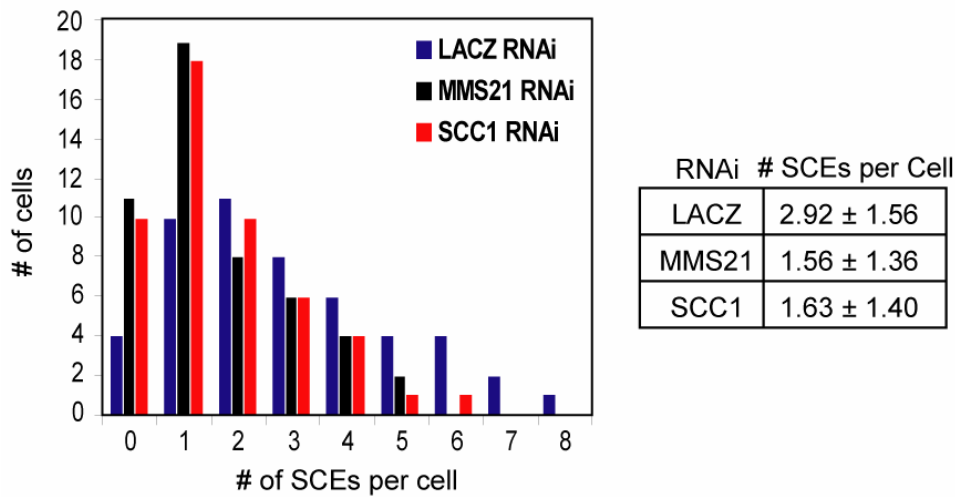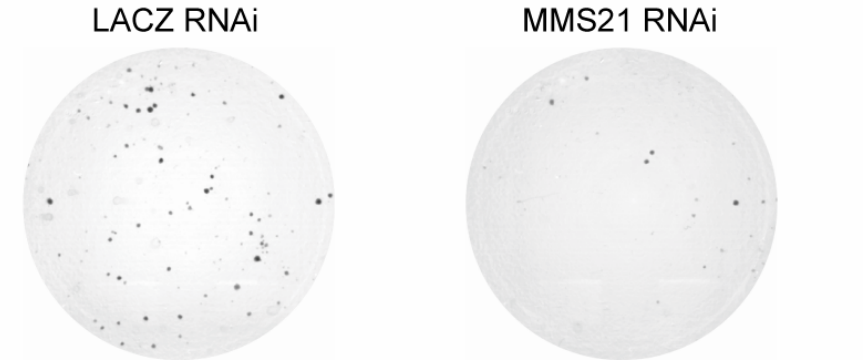
**Figure 3-7.  Knockdown of the SMC5/6 or cohesin complexes decreases the number of spontaneous SCEs**

(**A**) 293/A658 cells transfected with the indicated siRNA for 24 hrs were labeled with 10 µM BrdU for 40 hrs (two cell divisions).  Chromosome spreads were stained with acridine orange to distinguish sister chromosomes.  Arrowheads indicate recombination events.  Images are a representative sample of multiple experiments.  (**B**) Histogram of cells in (A) with the indicated number of sister-chromatid recombination events per cell.  Results from three separate samples are averaged with the standard deviation indicated in the table to the right.  (**C**) Images of colony formation assays described and quantitated in Figure 3-6C and D.  Images are a representative sample of multiple experiments.
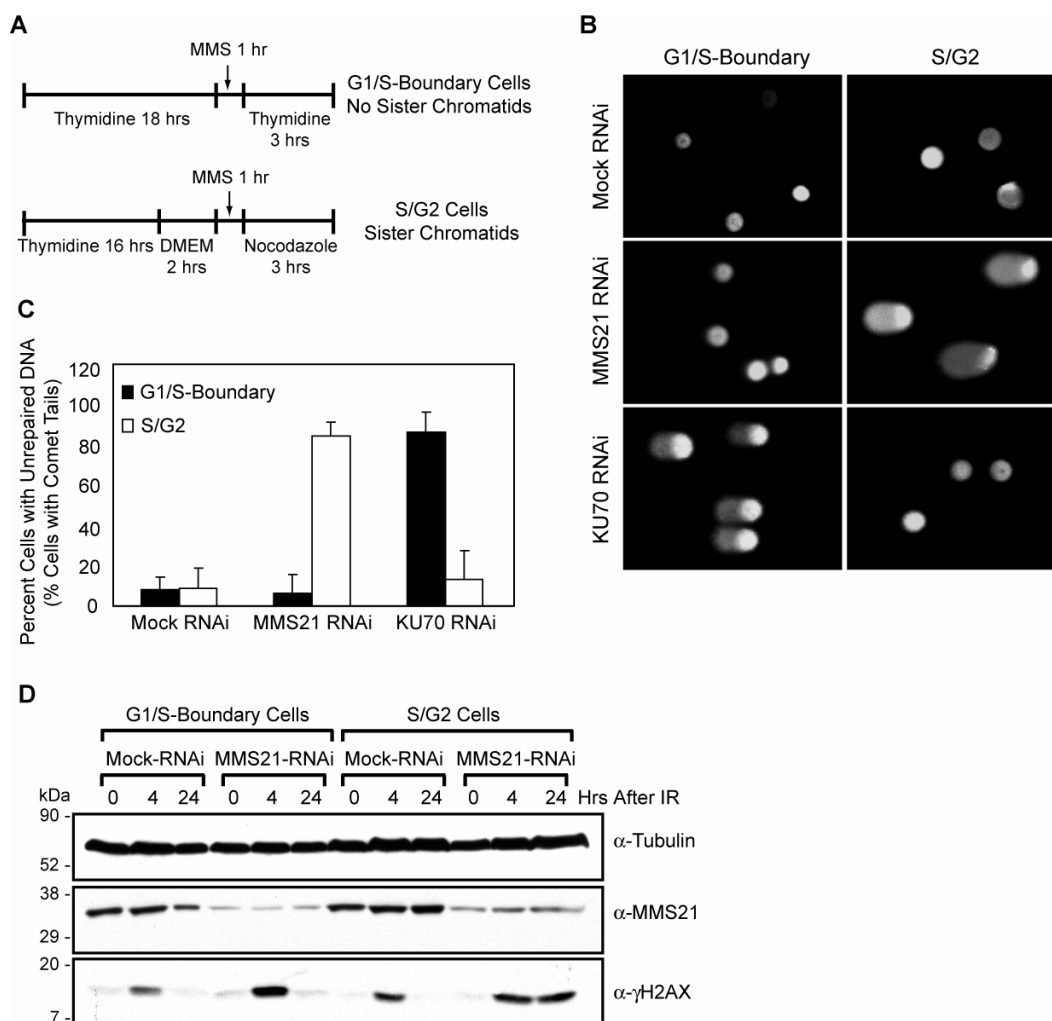
**Figure 3-8. The SMC5/6 complex is only required for efficient repair of damaged DNA in cells with sister chromatids**

(**A**) Timeline of the experimental design. Cells were transfected with the indicated siRNA for 36 hrs before treatment with 2 mM thymidine as shown. One half of the cells were released from G1 and, two hours later, both released and G1-arrested cells were treated for one hour with 0.015% MMS. Cells were then allowed to recover for three hours either arrested in G1 with thymidine or in S/G2/M with 0.1 µg/mL nocadozole. The presence of unrepaired damaged DNA was then measured by the comet assay. (**B**) Cells described in (A) were analyzed for the presence of unrepaired damaged DNA by the comet assay. SYBR green staining of DNA shows comet tails migrating out of the nucleus. Images are a representative sample of multiple experiments. (**C**) Quantitation of the percentage of cells shown in (B) with comet tails, representing unrepaired

damaged DNA.  Results from three separate samples are averaged with the standard deviations indicated.  (**D**) Mock-RNAi or MMS21-RNAi cells arrested at the G1/S-boundary or released into S-phase were treated with 10 Gy IR.  Cell lysates were collected at 0, 4, and 24 hrs after IR.  Western blots are shown for Tubulin (loading control), MMS21 (RNAi efficiency), and γH2AX (unrepaired DNA damage).
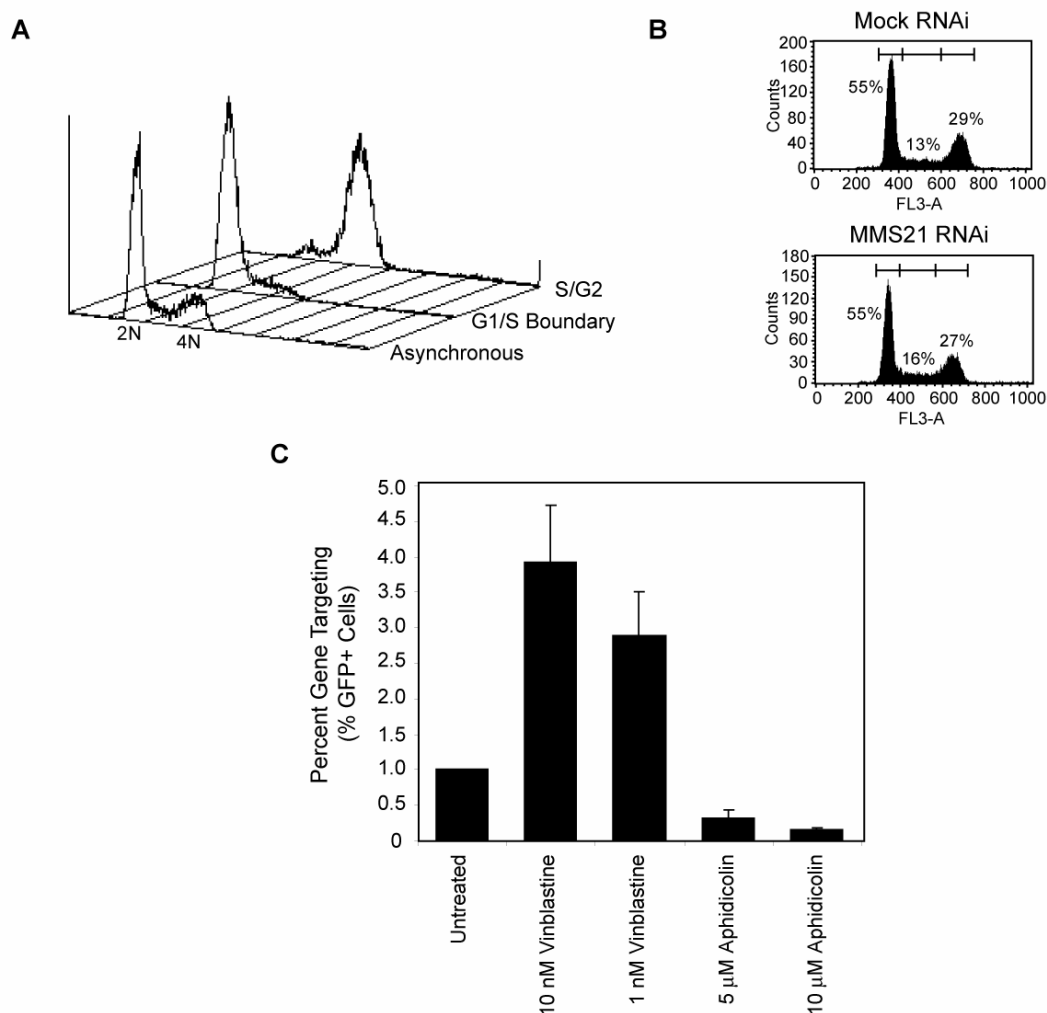
**Figure 3-9.  Gene targeting is increased in cells arrested at G2/M**
(**A**) FACS analysis of cells described in Figure 3-8A.  (**B**) HeLa S3 cells were transfected with mock or MMS21 siRNA for 48 hrs.  Cell cycle profile of each sample was analyzed by FACS.  The percentages of cells in G1, S, and G2/M are shown.  (**C**) 293/A658 cells were transfected with a ponasterone-inducible I-SceI vector for 24 hrs.  Cells were then incubated with varying concentrations of vinblastine or aphidicolin for 3 hrs before the addition of ponasterone for 21 hrs to induce I-SceI expression.  Cells were washed after the induction period to remove ponasterone and vinblastine or aphidicolin.  Cells were allowed to recover and express GFP for 2-3 days before FACS.  The percentage of GFP-positive cells is shown.  Results are an average from at least three separate experiments and the standard deviations are indicated.
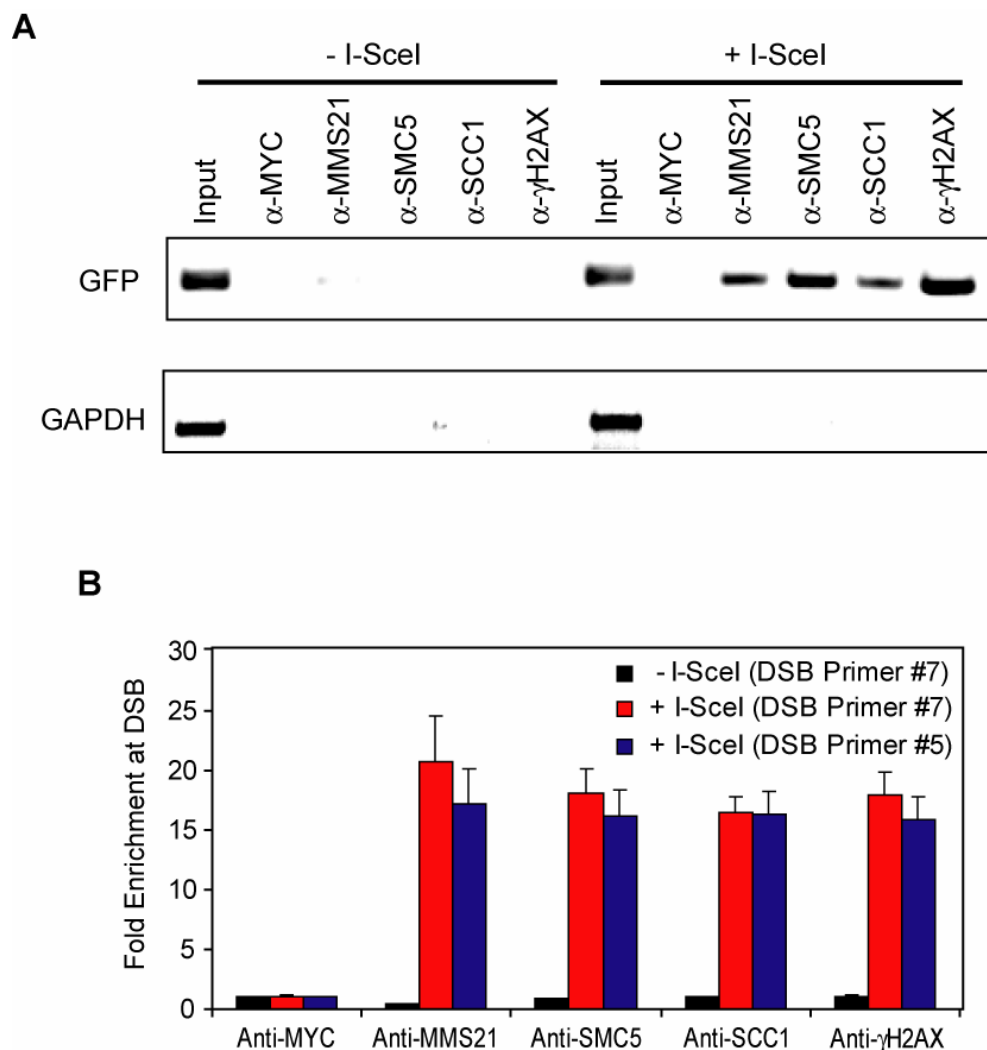
**Figure 3-10.  The SMC5/6 complex is recruited to DSBs**
(**A**) 293/A658 cells with integrated *GFP* gene containing a stop-I-SceI site were
transfected with either control or I-SceI expression plasmids.  Chromatin
immunoprecipitations (ChIP) were performed 24 hrs later with the indicated
antibodies.  The immunoprecipitated DNA was then analyzed by PCR using
control primers (*GAPDH*) and primers near the DSB (*GFP*).  Images are a
representative sample of multiple experiments.  (**B**) Quantitative real-time PCR
(QPCR) analysis of the ChIP samples described in (A).  The average fold-
enrichment of proteins at DSBs (*GFP* normalized to the control locus *GAPDH*)
represents enrichment compared to the anti-MYC control ChIP.  Results from two
separate samples using *GFP* primers #7 or #5 (+I-SceI only) performed in
triplicates are averaged with the standard deviations indicated.

**A**

293T/A658D · 293T

| µL Input DNA | 1 | 2 | 3 | 4 | 1 | 2 | 3 | 4 |

GFP

GAPDH

**B**

100 bp Ladder · -I-SceI Chromatin · +I-SceI Chromatin

900bp
700bp
500bp

300bp

100bp
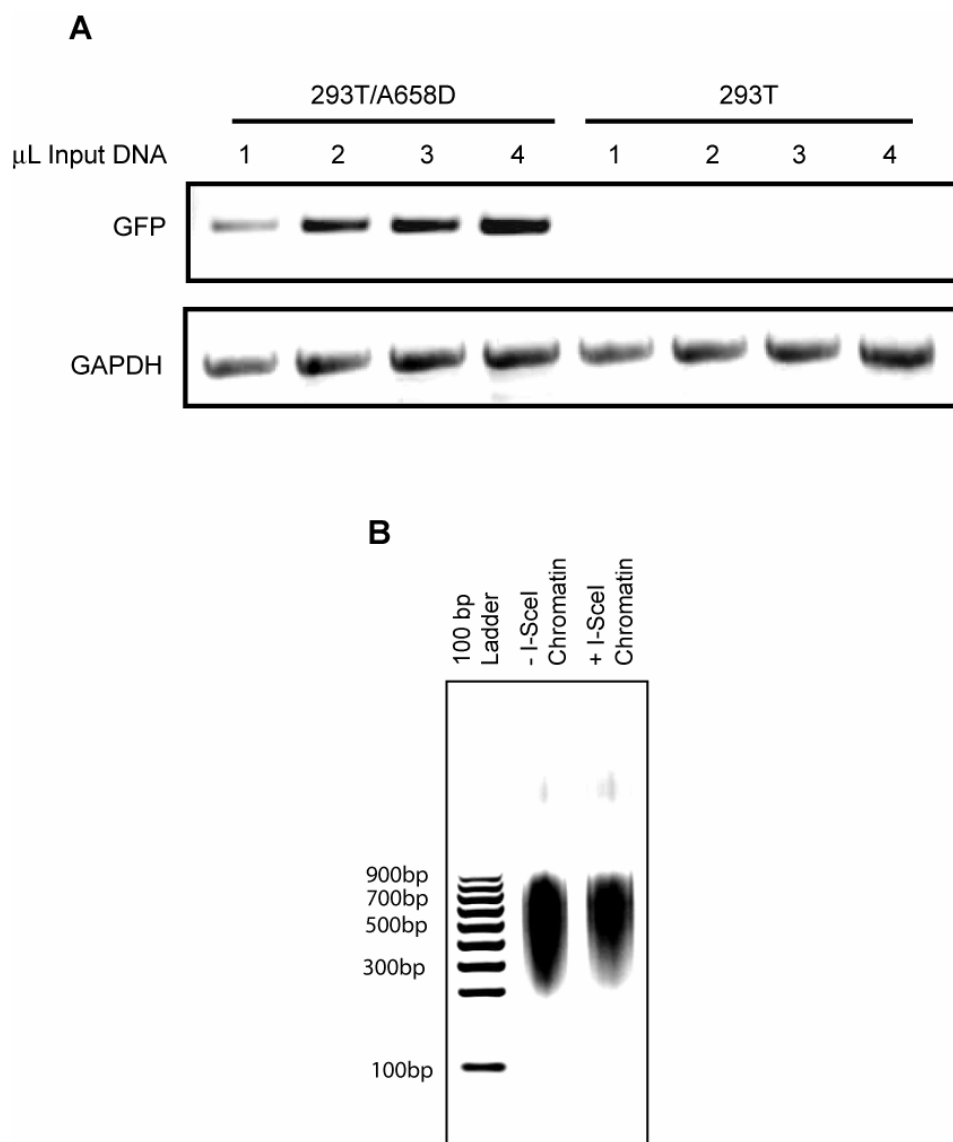
**Figure 3-11. Validation of chromatin immunoprecipitation (ChIP) experiments**
(**A**) The PCR products using the *GFP* primers are specific to *GFP* and the PCR reactions are in the linear range.  PCR reactions with varying amounts of input genomic DNA from either 293/A658 cells with the integrated gene targeting locus containing the *GFP* gene with the Stop-I-SceI site or wild-type 293 cells were performed.  (**B**) The sonicated fragments of DNA for ChIP were separated on agarose gel and stained with ethidium bromide.
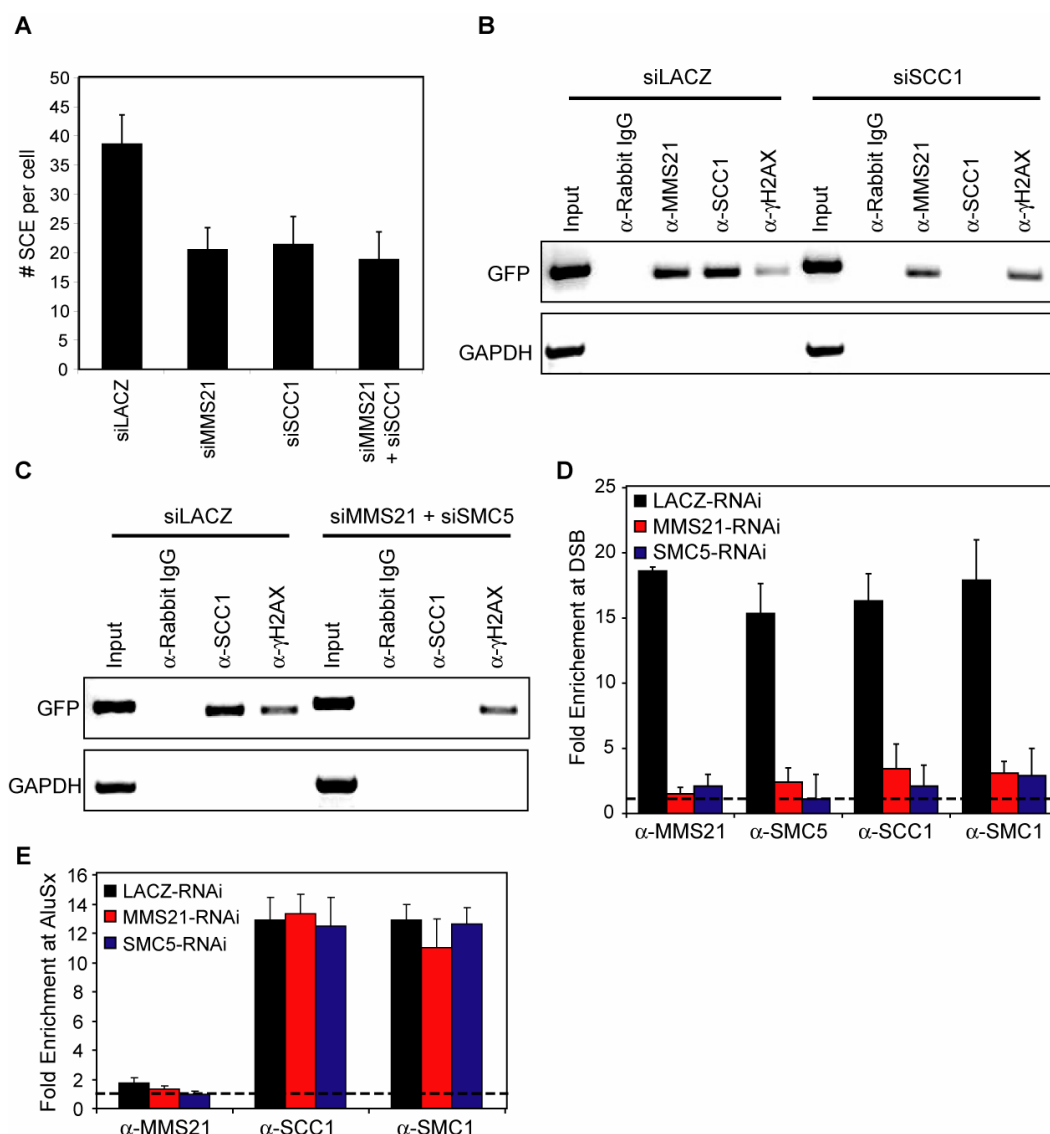
**Figure 3-12. Recruitment of cohesin to DSBs requires the SMC5/6 complex**
(**A**) Knockdown of both MMS21 and SCC1 does not further decrease the number
of SCEs per cell as compared to knocking down either one alone. The number of
SCEs per cell was determined as described in Figure 3-6A. Results from three
separate samples are averaged with the standard deviations indicated. (**B**) ChIP
was performed as described in Figure 3-10A except that 293/A658D cells had
been transfected with control LACZ siRNA or SCC1 siRNA for 24 hrs before
transfection of an I-SceI expression plasmid. Images are a representative sample
of multiple experiments. (**C**) ChIP was performed on 293/A658 cells that had
been transfected with control LACZ siRNA or MMS21 and SMC5 siRNA for 24

hrs before transfection of an I-SceI expression plasmid.  Images are a representative sample of multiple experiments.  (**D**) ChIP was performed as described in (C) with the indicated siRNAs and antibodies.  QPCR was performed using primers toward the DSB.  The dashed line indicates the background from rabbit IgG ChIP.  Results are shown as the average fold enrichment with the standard deviation indicated.  (**E**) ChIP was performed as described in (C) with the indicated siRNAs and antibodies.  QPCR was performed using primers toward the AluSx genomic locus.  The dashed line indicates the background from rabbit IgG ChIP.  Results are shown as the average fold enrichment with the standard deviation indicated.
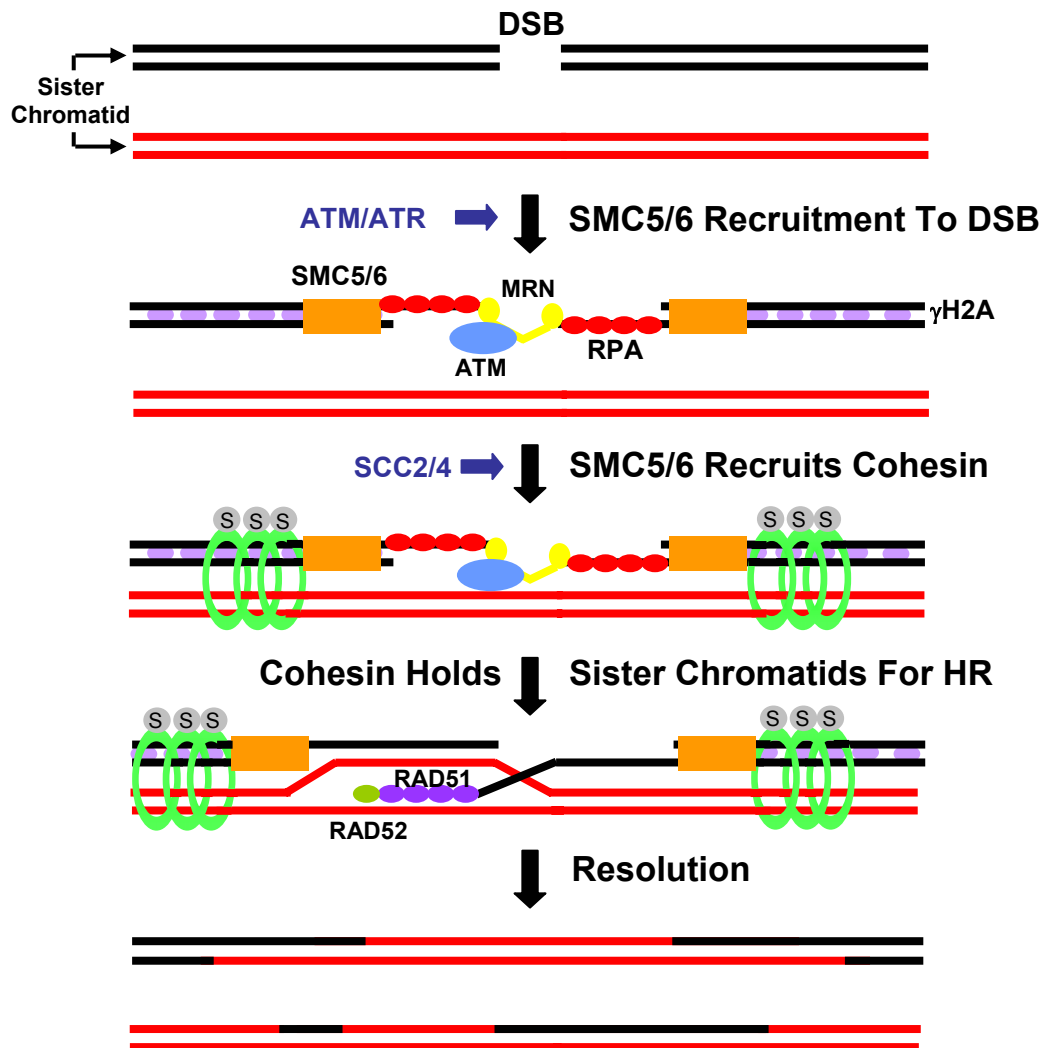
**Figure 3-13. Model for SMC5/6 function in sister chromatid HR**
SMC5/6 is recruited to DSBs in an ATM/ATR-dependent manner. It facilitates the recruitment of the cohesin complex to DSBs, possibly by sumoylation of the SCC1/SA2 cohesin subunits. Loading of the cohesin complex at DSBs is also dependent on the SCC2/4 chromatin loading complex. The post-replicative loading of cohesin at the DSB brings sister chromatids in close proximity to allow strand invasion and exchange during sister chromatid HR. The MRN complex has been speculated to hold the free ends of the DSB together to facilitate repair.
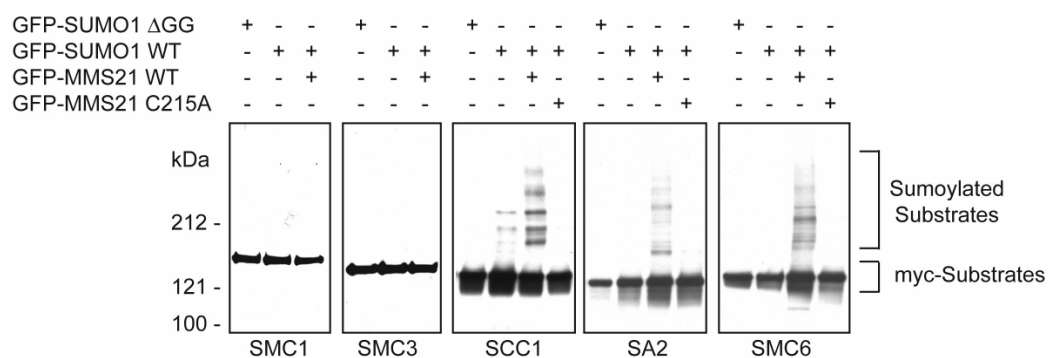
**Figure 3-14. MMS21 stimulates the sumoylation of cohesin subunits, SCC1 and SA2**

HeLa Tet-On cells were transfected with Myc-tagged cohesin subunits separately with or without GFP-MMS21 wild-type or C215 SUMO ligase mutant in the presence of GFP-SUMO1 wild-type or ΔGG conjugation mutant.  Cell lysates were collected 24 hrs after transfection and blotted with anti-Myc.

**Table 3-1.  Sequences of the oligonucleotides used**

| | |
|---|---|
| Primers for Conventional PCR and QPCR | |
| GFP #1 F | 5'-CGT CCA GGA GCG CAC CAT CTT CTT-3' |
| GFP #1 R | 5'-ATC GCG CTT CTC GTT GGG GTC TTT-3' |
| GFP #5 F | 5'-GTG ACC ACC TTC ACC TAC GG-3' |
| GFP #5 R | 5'-AAG TCG TGC TGC TTC ATG TG-3' |
| GFP #7 F | 5'-ACA TGG TCC TGC TGG AGT TC-3' |
| GFP #7 R | 5'-CTT GTA CAG CTC GTC CAT GC -3' |
| GAPDH F | 5'-GAC CCC TTC ATT GAC CTC AAC TAC A-3' |
| GAPDH R | 5'-GGT CTT ACT CCT TGG AGG CCA TGT-3' |
| AluSx F | 5'-AAA TGT GCT TTG AAC AAA GGA GTC-3' |
| AluSx R | 5'-AGT TTC AGG TCT CTT GGA GAG TG-3' |

| | |
|---|---|
| Primers for LM-PCR | |
| BW-1 | 5'-GCG GTG ACC CGG GAG ATC TGA ATT C-3' |
| BW-2 | 5'-GAA TTC AGA TC-3' |
| Linker-2 | 5'-ACC CGG GAG ATC TGA ATT C-3' |
| GFP #3 R | 5'-AGT TCA CCT TGA TGC CGT TC-3' |

| | |
|---|---|
| Oligonucleotides for RNA interference | |
| MMS21 | 5'-CUC UGG UAU GGA CAC AGC UTT-3' |
| SMC5 | 5'-GAA GCA AGA UGU UAU AGA ATT-3' |
| hSMC1 | 5'-CAA GCG GCG UAU UGA UGA ATT-3' |
| hSMC2 | 5'-AAA CGU CGA UAC ACU AUA ATT-3' |
| hSCC1 | 5'-GCC CAU GUG UUC GAG UGU ATT-3' |
| LACZ | Dharmacon SMARTpool Service |
| hRAD51 | Dharmacon SMARTpool Service |
| hKU70 | Dharmacon SMARTpool Service |

# CHAPTER IV:  THE SMC5/6 COMPLEX MAINTAINS TELOMERE LENGTH IN ALT CANCER CELLS

## INTRODUCTION

Telomeres are proteinaceous, repetitive DNA elements (TTAGGG in humans) that comprise 5-15 kilobases (kb) of the ends of each chromosome (Blackburn, 2001).  These sequences are shortened after every cell division due to the end-replication problem of the lagging strand (Harley et al., 1990).  Critically short telomeres result in cellular senescence (Bodnar et al., 1998).  Therefore, telomeres have been proposed to act as a counting mechanism for cellular proliferation (Bodnar et al., 1998).  Telomerase is the enzyme responsible for synthesis of new telomeric repeats (Smogorzewska and de Lange, 2004).  Normal human somatic cells repress telomerase to limit their own proliferative capacity (Cong et al., 2002).  Cancer cells overcome this limited proliferative potential generally by transcriptional upregulation of telomerase (Shay and Bacchetti, 1997).  However, telomerase is not activated in a subset of tumors, including many sarcomas, astrocytomas, and Li-Fraumeni syndrome tumors (Bryan et al., 1997; Henson et al., 2005).  Cells in a portion of these tumors rely on an alternative mechanism to lengthen telomeres, termed alternative lengthening of telomeres (ALT; Bryan et al., 1995; Henson et al., 2002; Muntoni and Reddel,

2005).  While telomerase synthesizes telomeric repeats using an RNA template, ALT relies on homologous recombination (HR) between telomeric sequences to elongate telomeres (Dunham et al., 2000; Londono-Vallejo et al., 2004; Lundblad and Blackburn, 1993).  A hallmark of ALT cells is the extreme heterogeneity in telomere length (<1 to >20 kb) as a result of HR (Rogan et al., 1995).  Another defining feature of ALT cells is the localization of telomeres in promyelocytic leukemia (PML) bodies, termed ALT-associated PML bodies (APBs; Yeager et al., 1999).  However, some ALT cells do not display these hallmarks, suggesting the potential existence of multiple ALT pathways (Muntoni and Reddel, 2005).

APBs appear upon the activation of ALT and disappear when it is repressed (Perrem et al., 2001; Yeager et al., 1999).  The recruitment of telomeres to PML bodies is enriched in cells with sister chromatids, i.e. cells in late S/G2 (Grobelny et al., 2000).  A number of proteins involved in DNA repair are present in APBs, including RAD51, RAD52, RPA, MRE11, NBS1, BRCA1, RAD9, BLM, and WRN (Johnson et al., 2001; Nabetani et al., 2004; Yankiwski et al., 2000; Yeager et al., 1999; Zhu et al., 2000).  The recruitment of factors involved in the repair of DNA double-strand breaks (DSBs) to APBs is distinct from their recruitment to irradiation-induced nuclear foci (Wu et al., 2003).  Recent studies have suggested that NBS1, a subunit of the MRE11/RAD50/NBS1 (MRN) complex, is required for APB formation (Jiang et al., 2005; Wu et al., 2003).  It has been proposed that APBs are the sites of telomere recombination that

elongates telomeres to allow unlimited proliferative potential, although the molecular mechanisms for this process are largely unknown.

The structural maintenance of chromosomes (SMC) family of proteins (SMC1-6) form three multi-subunit protein complexes that regulate chromosomal dynamics (Hirano, 2005b). The cohesin complex consists of the SMC1/3 heterodimer that promotes the proper segregation of sister chromatids to daughter cells during mitosis (Koshland and Guacci, 2000). The condensin complex consists of the SMC2/4 heterodimer that promotes condensation of chromosomes during mitosis (Swedlow and Hirano, 2003). The SMC5/6 complex is required for the efficient repair of DNA damage (Lehmann, 2005; Lehmann et al., 1995; Verkade et al., 1999). It is also required for the proper segregation of the repetitive DNA elements of ribosomal DNA (rDNA) in yeast (Torres-Rosell et al., 2005b).

The SMC5/6 complex consists of the SMC5/6 heterodimer and at least six non-SMC element (NSE1-6) proteins (Lehmann, 2005). MMS21/NSE2 (herein referred as MMS21 for simplicity) is a small ubiquitin-like modifier (SUMO) ligase that promotes the covalent attachment of SUMO to proteins (Lee and O'Connell, 2006). Sumoylation often results in the alteration of protein-protein interactions, subcellular localization, or transcriptional repression (Muller et al., 2001). The SUMO ligase activity of MMS21 is required for proper DNA damage repair (Lee and O'Connell, 2006; Potts and Yu, 2005; Zhao and Blobel). The

SMC5/6 complex is recruited to DSBs and promotes sister chromatid HR by facilitating the recruitment of cohesin to DSBs (De Piccoli et al., 2006; Lindroos et al., 2006; Onoda et al., 2004; Potts et al., 2006).  In addition to its localization to DSBs, the SMC5/6 complex also localizes to repetitive DNA elements, such as rDNA and telomeres in yeast (Lindroos et al., 2006; Torres-Rosell et al., 2005b; Zhao and Blobel, 2005).  Mutation of MMS21 in yeast impairs clustering of telomeres during meiosis (Zhao and Blobel, 2005).  In this study, we investigate the function of the human SMC5/6 complex in telomere recombination and maintenance.

## MATERIALS AND METHODS

### Cell culture, transfections, siRNAs, and flow cytometry

All cell lines were maintained in DMEM (Invitrogen) supplemented with

10% (v/v) fetal bovine serum (Gemini), and 100 $\mu$g mL$^{-1}$ penicillin and

streptomycin (Invitrogen). At 40-50% confluency, cells were transfected with

plasmids or siRNAs with either Effectene (Qiagen) or Oligofectamine

(Invitrogen), respectively, according to manufacturers' instructions. The siRNA

oligonucleotides used in this study are:  LACZ (5'-

GCGCCGAAAUCCCGAAUCUdTdT-3'), Luciferase (5'-

CUUACGCUGAGUACUUCGAdTdT-3'), human MMS21 (5'-CUCUGG

UAUGGACACAGCUdTdT-3'), mouse MMS21 (5'-

GGAGUUGACGAAGAUAUGAdTdT-3'), NBS1 (5'-

AAGAAGCAGCCTCCACAAAdTdT-3'), RAD50 (5'-

GGAUCUUCAGACAGGAUUCdTdT-3'), SMC5 (5'-

GAAGCAAGAUGUUAUAGAAdTdT-3'), and SMC6 (5'-

AGAGCGGCTTACTGAACTAdTdT-3'). RAD51 siRNAs were obtained from

Dharmacon's SMARTpool service. Knockdown efficiency of at least 75% with

these oligonucleotides was confirmed as previously described (Potts et al., 2006;

Potts and Yu, 2005). For cell cycle arrest in G1/S or G2/M, cells were treated for

24 hrs with 2 mM thymidine or media lacking methionine for four days,

respectively. Flow cytometry analysis of cell cycle profile was performed as previously described (Potts and Yu, 2005).

**Immunofluorescence, immunoblotting, immunoprecipitation, and antibodies**

For immunofluorescence, cells were plated in 4-well chamber slides (LabTek) and treated as indicated. Cells were washed in PBS and fixed in 1% (w/v) paraformaldehyde for 15 min at room temperature. The fixed cells were washed in PBS and then permeabilized and blocked for 20 min at 4 ºC in incubation buffer (PBS containing 0.2% (v/v) Triton X-100 and 3% (w/v) bovine serum albumin). After blocking, cells were incubated in primary antibody (2 μg mL$^{-1}$) for 1 hr at room temperature in incubation buffer. Cells were then washed with PBS and incubated in fluorescent secondary antibodies (Alexa Fluor 488 or 647, Molecular Probes) in incubation buffer for 30 min at room temperature. After incubation, cells were washed with PBS and their nuclei were stained with 4'-6-diamidino-2-phenylindole (DAPI; 1 μg mL$^{-1}$). Slides were mounted and viewed with a 63x objective on a Zeiss Axiovert 200M fluorescence microscope. Images were acquired with a CCD camera using the Slidebook imaging software (Intelligent Imaging Innovations). All images were taken at 0.5 μm intervals, deconvolved using the nearest neighbor algorithm, and stacked to better resolve foci. For quantitation, multiple, random fields were captured and 50-100 cells were counted in each of three independent experiments.

For immunoblotting, cells were lysed in SDS sample buffer, sonicated, boiled, separated by SDS-PAGE, and blotted with the indicated antibodies. Horseradish peroxidase-conjugated goat anti-rabbit or goat anti-mouse IgG (Amersham Biosciences) were used as secondary antibodies, and immunoblots were developed using the ECL reagent (Amersham Biosciences) per manufacturer's protocols.

For immunoprecipitation, whole cell lysate was made by lysing cells in NP-40 lysis buffer (50 mM Tris-HCl, pH 7.7, 150 mM NaCl, 0.5% (v/v) NP-40, 1 mM DTT, and 1X protease inhibitor cocktail) on ice for 15 min, sonicated three times, followed by centrifugation at 16,000g for 15 min at 4 ˚C. Anti-FLAG affinity gel (Sigma) was incubated with the supernatants for two hours at 4 ˚C. The beads were then washed five times with the NP-40 lysis buffer. The FLAG-tagged proteins bound to the beads were eluted with FLAG-peptide (Sigma), dissolved in SDS sample buffer, boiled, separated by SDS-PAGE, and blotted with the indicated antibodies as described above.

The commercial antibodies used in this study are as follows:  anti-FLAG M2 (Sigma, F1804), anti-γH2AX (Upstate, 05-636), anti-Myc (Roche, 11667203001), anti-p21 (Santa Cruz, SC-6246), anti-PML (Santa Cruz, SC-5621 or SC-966), anti-RAD50 (GeneTex, GTX70228), anti-SCC1 (Bethyl Laboratory, A300-080A), anti-SMC1 (Bethyl Laboratory, A300-055A), anti-SMC5 (Bethyl Laboratory, A300-236A), anti-SMC6 (Bethyl Laboratory, A300-A237A), and

anti-TRF2 (Calbiochem, OP129 or Upstate, 05-521).  The production of

polyclonal anti-MMS21 has been described previously (Potts and Yu, 2005).


**Telomeric sister chromatid exchange and quantitative telomeric FISH**

For telomere sister chromatid exchange (CO-FISH) analysis, human

SUSM1 or G5 mTERC$^{-/-}$ WRN$^{-/-}$ RAS$^{v12}$ MEF ALT cells (a kind gift from Dr.

Sandy Chang, M.D. Anderson Cancer Center, Houston, TX; Laud et al., 2005)

were transfected with the indicated siRNAs for 48 hrs before addition of 3:1

BrdU:BrdC (7.5 µM:2.5 µM) for 16 hrs.  Chromosome spreads were prepared as

previously described (Potts et al., 2006).  Chromosome spreads were treated with

0.5 mg mL$^{-1}$ RNAse A at 37 ºC for 10 min.  Slides were then incubated in 2X

SSC containing 10 µg mL$^{-1}$ Hoescht 33258 for 15 min followed by exposure to

365 nm UV light (Stratalinker 1800) for 30 min.  Nicked DNA was then degraded

by incubation of slides in 1.6% (v/v) ExoIII (Promega) for 10 min.  Slides were

then treated with 5 µg mL$^{-1}$ pepsin for 7.5 min at 37 ºC and washed in PBS.

Chromosome spreads were then dehydrated through an ethanol series (70% (v/v),

85% (v/v), and 100% ethanol).  Slides were allowed to air dry in the dark before

incubation with a FITC-G-rich, telomeric, peptide nucleic acid (PNA) probe

(NH$_2$-FITC- TTAGGGTTAGGGTTAGGG-COOH; Panagene) for one hour at

room temperature.  Slides were then washed in PBS containing 0.02% (v/v)

Tween-20 followed by incubation in CY3-C-rich, telomeric PNA probe (NH$_2$-

CY3- CCCTAACCCTAACCCTAA-COOH; Applied Biosystems) for one hour at room temperature.  Slides were then washed in PBS containing 0.02% (v/v) Tween-20 for 20 min at 57 ºC and stained in 1 μg mL$^{-1}$ of DAPI in 2X SSC containing 0.02% (v/v) Tween-20 for five min followed by mounting. Chromosomes were imaged as described above with the number of T-SCEs quantitated in 50 cells in multiple experiments by counting the frequency of unequal exchange events resulting in unequal signal intensity of both FITC and CY3 on both sister telomeres.  Chromosomes with closely associated or indistinguishable sister telomeres were not counted.  Control experiments were performed to ensure signals generated were not due to unintended denaturation of DNA and were dependent on BrdU/C incorporation.

For quantitative telomere length analysis (Q-FISH), SUSM1 cells were treated with the indicated siRNAs for the indicated number of population doublings.  Cells were treated with siRNAs every third day and passaged as needed.  For making stable knockdown of the SMC5/6 complex in HCT116 cells, cells were transfected with pSuperior-neo plasmid (Oligoengine) containing either shRNA sequences for Luciferase, MMS21, or SMC6 (as described above) followed by selection with G418.  Colonies were expanded and analyzed for efficiency of knockdown by western blot analysis.  Cells were maintained in culture under selection of G418 for up to 120 population doublings.  Chromosome spreads from either SUSM1 siRNA transfected or HCT116 shRNA stable cell

lines were made as described previously (Potts et al., 2006). Slides were treated

with pepsin, washed, and dehydrated as described above. Telomeres were stained

with a CY3-telomere PNA probe by incubation at 70 ºC for seven minutes

followed by 60 min incubation at room temperature. Slides were washed and

processed after probe incubation as described above. Slides were imaged as

described above with the intensity of telomeres quantitated in 50 cells in multiple

experiments. Additionally, the number of chromosomes containing telomere

signal free ends and end-to-end fusions were quantitated.

For telomere restriction fragment analysis, SUSM1 cells were transfected

with siRNAs for the indicated number of population doublings as described

above. Genomic DNA was collected and digested with HinfIII and RsaI for eight

hours. The digested DNA along with a radiolabeled DNA ladder was run on a 25

cm, 0.7% (w/v) agarose gel for 18 hrs. The gel was then denatured and dried for

one hour at 50 ºC. The dried gel was then neutralized followed by

prehybridization for one hour at 42 ºC in hybridization solution (5X SSC, 5X

Denhardt Solution, 10 mM $Na_2HPO_4$, 1 mM $Na_2H_2P_2O_7$). After prehybridization,

the gel was incubated overnight at 42 ºC in hybridization solution containing [32]P-

end labeled $(TTAGGG)_4$ oligonucleotide. The gel was then washed for 15 min in

2X SSC followed by three times for 10 min each in 0.1X SSC containing 0.1%

(w/v) SDS. The gel was exposed overnight to phosphor screen and scanned on

Fuji Imager.  Approximate telomere lengths were quantitated using ImageQuant

software (Molecular Dynamics) and TELORUN.

**Senescence-associated β-galactosidase assay (SA-β-gal)**

Cells were transfected with the indicated siRNAs for the indicated number

of population doublings as described above and then plated in chamber slides for

24 hrs.  Slides were washed in PBS and fixed in PBS containing 2% (v/v)

formaldehyde and 0.2% (v/v) glutaraldehyde for 5 min, followed by extensive

washing in PBS.  Cells were incubated in X-gal staining solutions (40 mM citric

acid/sodium phosphate pH 6.0, 1 mg mL-1 X-gal, 5 mM potassium ferricyanide, 5

mM potassium ferrocyanide, 150 mM NaCl, and 2 mM MgCl2) for 16 hrs at 37

ºC.  Slides were washed extensively and mounted.  Slides were imaged as

described above.  The number of SA-  -gal-positive cells was quantitated by

counting the percentage of blue cells in random fields from multiple experiments.

**RESULTS**

**The SMC5/6 complex localizes to PML bodies in ALT cells**

To determine whether the SMC5/6 complex forms nuclear foci coinciding with DSBs, we treated U2OS cells with 10 gray of irradiation and stained the cells for SMC5, SMC6, and γH2AX (a DSB foci marker). To our surprise, a subset of cells exhibited SMC5/6 nuclear foci in the absence of DNA damage and these foci did not overlay with γH2AX in the presence or absence of irradiation (Figure 4-1A). To determine the nature of these SMC5/6 nuclear bodies, we stained U2OS cells with antibodies against the components of the SMC5/6 complex (SMC5, SMC6, and MMS21) and markers of other known nuclear structures, such as centromeres and PML nuclear bodies. We observed a specific colocalization of the SMC5/6 complex with PML nuclear bodies in U2OS cells (Figure 4-1B and data not shown). Approximately 75% of PML foci contained the SMC5/6 complex (Table 4-1). Because only a subset of U2OS cells exhibited colocalization of the SMC5/6 complex in PML bodies, we speculated that the recruitment of the SMC5/6 complex might be regulated during the cell cycle. We arrested U2OS cells in G1/S with thymidine or enriched cells in G2/M by methionine-deprivation and determined the colocalization of the SMC5/6 complex with PML bodies. Flow cytometry analysis confirmed that thymidine treatment resulted in the enrichment of G1/S cells and methionine-deprivation

resulted in the enrichment of G2/M cells (Figure 4-2D).  In cells arrested in G1,

the SMC5/6 complex failed to localize to PML bodies and exhibited diffuse

nuclear staining (Figure 4-1C and data not shown).  The percentage of cells with

colocalization of the SMC5/6 complex and PML bodies dramatically increased in

cells enriched in G2/M (Figure 4-1C), suggesting a cell cycle regulated

recruitment of the SMC5/6 complex to PML.

Next, we examined whether the SMC5/6 complex localized to PML

bodies in other cell types.  Surprisingly, we discovered that the SMC5/6 complex

localized to PML bodies in only a subset of cell lines (Table 4-2).  The

localization of the SMC5/6 complex to PML bodies did not depend on the cell

type, tissue of origin, or immortalization technique (Table 4-2, Figure 2, and data

not shown).  The only correlation of whether the SMC5/6 complex localized to

PML bodies was the telomere length maintenance mechanism (Table 4-2).  The

SMC5/6 complex localized to PML bodies in cells in which the telomeres were

maintained by recombination (ALT cells), but not in telomerase-positive cells.

To confirm that the localization of the SMC5/6 complex to PML bodies was

indeed due to ALT, we examined the localization of SMC6 in SW26 and SW39

cells.  These cells were derived from the same parental cell line (IMR90 primary

lung fibroblast), but rely on either ALT (SW26) or telomerase (SW39) to

maintain telomere length (Wright et al., 1989).  As expected, SMC6 only formed

nuclear foci corresponding to PML bodies in SW26 cells, but not in SW39 cells

(Figure 4-3). Therefore, the SMC5/6 complex specifically localizes to PML

bodies in cells that use telomere recombination to elongate telomeres (ALT), but

not in telomerase-positive cells.

It has previously been demonstrated that telomeres are recruited to PML

bodies in ALT, but not telomerase-positive, cells. To determine whether the PML

bodies that contained the SMC5/6 complex also contained telomeres, we stained

U2OS ALT cells for the SMC5/6 complex and the telomere-binding protein,

TRF2. Approximately 50% of TRF2 foci indeed colocalized with the SMC5/6

complex (Figure 4-1D and Table 4-1). We also examined whether SMC5

colocalized with telomeres in generation five (G5) mTERC$^{-/-}$ WRN$^{-/-}$ RAS$^{v12}$

MEF ALT cells (Laud et al., 2005). These cells were previously shown to display

ALT characteristics, such as elevated telomere recombination, telomere length

heterogeneity, and APB formation (Laud et al., 2005). SMC5 indeed colocalized

with a subset of telomeres in these MEF ALT cells (Figure 4-2C). These results

suggest that the SMC5/6 complex localizes to PML bodies in which telomeres are

present (referred to as APBs hereafter).

**The SMC5/6 complex is required for telomere recombination**

ALT cells rely on recombination of telomeric sequences to elongate and

maintain telomere length (Muntoni and Reddel). Previously, we demonstrated

that the SMC5/6 complex was specifically required for sister chromatid HR (Potts

et al., 2006). To determine whether the SMC5/6 complex was required for telomere HR, we examined the frequency of telomere HR using the chromosome orientation fluorescence in situ hybridization (CO-FISH) assay in G5 mTERC$^{-/-}$ WRN$^{-/-}$ RAS$^{v12}$ MEF ALT cells (Laud et al., 2005). These cells were previously shown to display substantial levels of telomere recombination (Laud et al., 2005). When using differentially labeled fluorescent probes that recognize the telomere leading strand sequence (G-rich, CY3 probe) or the lagging strand sequence (C-rich, FITC probe), CO-FISH yields opposing telomere signals on each sister chromatid (Figure 4-4A, top). However, if telomere sister chromatid exchange (T-SCE) occurs, leading and lagging strand sequence will be exchanged, typically in unequal portions, resulting in an overlap of G-rich and C-rich telomeric sequences (Figure 4-4A, bottom). Treatment of G5 mTERC$^{-/-}$ WRN$^{-/-}$ RAS$^{v12}$ MEF ALT cells with siRNAs toward MMS21 resulted in substantial knockdown of MMS21 (Figure 4-4B). We observed an approximately 80% reduction in the number of unequal T-SCE events in cells treated with MMS21 siRNA (Figure 4-4C and D). In addition to examining the requirement of the SMC5/6 complex for telomere recombination in mouse ALT cells, we examined whether the SMC5/6 complex is required for recombination of telomeres in the classical human SUSM1 ALT cell line that displays robust T-SCE activity. Treatment of SUSM1 cells with siRNAs toward SMC5 resulted in substantial knockdown of both SMC5 and MMS21, suggesting that MMS21 requires binding to SMC5 for its

stability (Figure 4-4E), a common observation for multisubunit complexes.

Knockdown of MMS21, SMC5, or SMC6 resulted in approximately 75%

reduction of telomere recombination (Figure 4-4F).  These results suggest that the

SMC5/6 complex is required for T-SCE in ALT cells.

**Inhibition of the SMC5/6 complex disrupts APB formation**

A hallmark of ALT cells is the association of some of their telomeres with

PML bodies (APBs; Yeager et al., 1999).  It has been suggested that APBs are the

site of telomere recombination in ALT cells.  Inhibition of APB formation causes

progressive telomere shortening in ALT cells (Jiang et al., 2005).  Due to the

striking localization of the SMC5/6 complex to telomeres and PML bodies in

ALT cells (Figure 4-1) and the requirement of the SMC5/6 complex for telomere

recombination (Figure 4-4), we examined whether the SMC5/6 complex is

required for the recruitment of telomeres to PML bodies in ALT cells.

Knockdown of MMS21, SMC5, or SMC6 by RNAi blocked the recruitment of

telomeres to PML bodies in U2OS cells (Figure 4-5A and B).

It has previously been reported that inhibition of NBS1, a component of

the MRN complex that facilitates HR, disrupts APBs (Jiang et al., 2005; Wu et

al., 2003).  To determine whether the requirement for the SMC5/6 complex in

APB formation was indirectly due to its role in HR, similar to NBS1, we

determined the effect of inhibiting the essential HR factor, RAD51, on APB

formation. U2OS cells treated with RAD51 siRNA resulted in substantial

knockdown of the RAD51 protein (Figure 4-3C), but did not alter APB formation

(Figure 4-5A and B). Importantly, this level of knockdown has previously been

shown to inhibit HR (Potts et al., 2006). Therefore, APB formation is not

disrupted by inhibition of any HR protein.

Previously, we have shown that the SMC5/6 complex is required to recruit

the cohesin complex to DSBs (Potts et al., 2006). We thus examined whether the

SMC5/6 complex also recruited cohesin to PML bodies. We immunostained

U2OS cells for endogenous or Myc-tagged SMC1 and SCC1, two cohesin

subunits. In either case, we failed to observe localization of the cohesin complex

to PML bodies (Figure 4-6), suggesting that the SMC5/6 complex might facilitate

APB formation using a cohesin-independent mechanism.

**MMS21 sumoylates components of the telomere-binding shelterin complex**

To gain insights into the mechanism by which the SMC5/6 complex

promoted APB formation, we tested whether the SUMO ligase activity of

MMS21 was required for APB formation. Expectedly, MMS21-RNAi cells were

defective in APB formation (Figures 4-5B and 4-7A and B). Cells treated with

MMS21 siRNA were transfected with wild-type or SUMO ligase-dead mutant

(C215A) MMS21 plasmids that also contained silent mutations in the siRNA-

binding site to prevent knockdown of the transgenes. Overexpression of wild-

type MMS21 substantially rescued APB formation in MMS21-RNAi cells (Figure 4-7A and B). Although the SUMO ligase-dead mutant of MMS21 was still recruited to PML bodies in ALT cells (data not shown), it did not efficiently restore APB formation in MMS21-RNAi treated cells (Figure 4-7A and B). These results strongly suggest that the SUMO ligase activity of MMS21 is required for APB formation.

We next tested whether MMS21 stimulated the sumoylation of the telomere-binding proteins, TRF1, TRF2, TIN2, TPP1, POT1, and RAP1. These proteins are components of the shelterin/telosome complex (Figure 4-7C) that protects telomeres from being recognized as DSBs and prevents telomere HR (de Lange, 2005). Overexpression of MMS21 in HeLa cells stimulated the sumoylation of four of the six ectopically expressed shelterin components, including TRF1, TRF2, TIN2, and RAP1 (Figure 4-8A). This was striking as we had shown previously that MMS21 only stimulated the sumoylation of two out of 30 SUMO substrates identified in an *in vitro* expression cloning (IVEC) screen (Gocke et al., 2005; Potts and Yu, 2005). The MMS21-induced sumoylation of TRF1, TRF2, TIN2, and RAP1 was not further enhanced by irradiation (Figure 4-8A), suggesting that this activity was not regulated by DNA damage. To test the specificity of sumoylation of the shelterin complex by MMS21, we transfected cells with Myc-TRF1 in the presence of various SUMO ligases, such as MMS21, PIAS1, PIASxβ, or PIASy. We observed a dose-dependent increase of TRF1

sumoylation in the presence of wild-type MMS21, but not its SUMO ligase-dead

C215A mutant or other SUMO ligases (Figure 4-7D). Overexpression of the

SUMO isopeptidase, SENP2, or the use of a SUMO mutant (SUMO-ΔGG)

incapable of conjugation, greatly reduced the amounts of slow-migrating TRF1

species, confirming their identity as SUMO conjugates (Figure 4-7D). These

results suggest that MMS21 is sufficient to sumoylate several shelterin

components in the telomerase-positive HeLa cell line. We next examined

whether these shelterin components were sumoylated in U2OS ALT cells without

the overexpression of MMS21. Indeed TRF1, TRF2, and RAP1 were sumoylated

in ALT cells without overexpression of MMS21 (Figure 4-7E and data not

shown). We next determined whether sumoylation of TRF2 or RAP1 in ALT

cells was dependent on MMS21 by knocking down MMS21 by RNAi.

Knockdown of MMS21 substantially decreased the sumoylation of both TRF2

and RAP1 in U2OS ALT cells. This decreased sumoylation of TRF2 and RAP1

was rescued by expression of an siRNA-resistant wild-type MMS21, but not

SUMO ligase-dead MMS21 C215A (Figure 4-7E). Therefore, the SUMO ligase

activity of the SMC5/6 complex component, MMS21, is required for APB

formation and is necessary and sufficient for the sumoylation of multiple subunits

of the shelterin complex.


**TRF1 and TRF2 sumoylation is required for APB formation**

Previous studies have shown that sumoylation controls the recruitment of several proteins (such as DAXX) to PML bodies (Lin et al., 2006). This sumoylation-dependent recruitment of proteins to PML bodies was shown to be dependent on the conserved SUMO-binding motif of PML (Lin et al., 2006). We examined whether sumoylation of shelterin subunits is required for their recruitment to APBs. Sumoylation often occurs on lysines within a loosely defined consensus motif, ΨKXE (Ψ, a hydrophobic residue; X, any residue; Rodriguez et al., 2001). TRF1 contained two such potential sumoylation sites with multiple lysines in each (Figure 4-9A). We mutated both motifs by replacing the lysines with arginines. Although mutation of either sumoylation motif (TRF1 M1 or M2) alone was not sufficient to decrease sumoylation, mutation of both (TRF1 ΔSUMO) appreciably inhibited MMS21-induced sumoylation of TRF1 (Figure 4-9B). Mutation of all six lysines in M1 and M2 to arginines (TRF1 ΔSUMO) did not disrupt TRF1 localization to telomeres or binding to TIN2 (Figure 4-8B and C). Strikingly, TRF1 ΔSUMO failed to localize to PML bodies whereas wild-type or single SUMO site mutant TRF1 did (Figure 4-9C and D). Therefore, sumoylation of TRF1 is required for its recruitment to PML bodies.

We next asked whether sumoylation of other shelterin components was required for their recruitment to APBs. We identified three potential sumoylation sites (Figure 4-10A) in another shelterin component, TRF2 (Figure 4-7C). Mutation of all three potential sumoylation sites (TRF2 ΔSUMO) substantially

decreased MMS21-induced sumoylation of TRF2 (Figure 4-10B and data not

shown).  As observed for TRF1 ΔSUMO, TRF2 ΔSUMO also failed to localize to

PML bodies (Figure 4-10C and D).  These results suggest that the sumoylation of

multiple subunits of the shelterin complex is required for APB formation in ALT

cells.


**The SMC5/6 complex is required for telomere maintenance**

To determine whether the reduction in telomere recombination and APB

formation in SMC5/6-RNAi ALT cells affected telomere length, we examined

chromosomes for telomere signal free ends, end-to-end fusions, and telomere

length by quantitative FISH (Q-FISH) and telomere restriction fragment (TRF)

analysis.  SUSM1 cells were transfected with siRNAs toward Luciferase,

MMS21, or SMC5 every three days for a total of 36 population doublings.

Knockdown level of MMS21 was confirmed during the course of siRNA

treatment (Figure 11A).  We observed an increase in the percentage of both

telomere signal free ends and chromosomal end-to-end fusions in MMS21- or

SMC5-RNAi SUSM1 ALT cells at late population doubling (Table 4-3).  In

addition, we observed progressive shortening of telomeres over time in SUSM1

ALT cells treated with MMS21- or SMC5-RNAi by both TRF and Q-FISH

analysis (Figure 4-11A and B and Figure 4-12B).  This decrease in telomere

length was similar to that observed in cells treated with RAD50-RNAi (Figure 4-

11B), a known regulator of telomere length in ALT cells (Jiang et al., 2005; Wu et al., 2003). Consistent with the Q-FISH and TRF analysis, we observed an increased number of telomeres colocalizing with γH2AX, a marker of DSBs, in MMS21-RNAi ALT cells (Figure 4-12C), although this result could also be attributed to the increased number of unrepaired DSBs in MMS21-RNAi cells (Potts et al., 2006). These findings suggest that the SMC5/6 complex is required to maintain telomere length in ALT cells.

To examine whether this progressive shortening of telomeres in SMC5/6-RNAi ALT cells was specific to ALT cells, we generated stable HCT116 telomerase-positive cell lines in which MMS21 or SMC6 were knocked down by short hairpin RNAs (shRNAs). shMMS21 or shSMC6 HCT116 cells contained markedly reduced levels of MMS21 or SMC6 even after 120 population doublings (Figure 4-12D). Unlike ALT cells, these telomerase-positive SMC5/6-RNAi cells did not exhibit alterations in telomere lengths, signal free ends, or chromosomal end-to-end fusions (Figure 4-11C, 4-12E and Table 4-3). Previous findings in yeast also support our results that the SMC5/6 complex has minimal role in telomere length maintenance in telomerase-positive cells (Xhemalce et al., 2007; Zhao and Blobel, 2005).

Critically short telomeres results in cellular senescence (Bodnar et al., 1998). We next examined whether the shortened telomeres in SMC5/6-RNAi ALT cells led to cellular senescence. To do so, we determined whether these cells

exhibited senescence-associated β-galactosidase (SA-β-Gal) activity, a classical

marker of cellular senescence. Knockdown of the SMC5/6 complex in SUSM1

ALT cells caused a progressive increase in the number of SA-β-gal-positive cells

over time (Figure 4-11D and E). This increase correlated with the substantial

decrease in telomere lengths in these cells (Figure 4-11A and B). ALT cells

treated with SMC5/6-RNAi exhibited other expected senescence phenotypes,

such as morphological changes and an upregulation of the cyclin-dependent

kinase inhibitor, p21 (Figure 4-10F, 4-11, and data not shown). Therefore, these

results suggest that, in the absence of the SMC5/6 complex, telomeres undergo

progressive shortening in ALT cells, leading to cellular senescence.

**DISCUSSION**

The molecular mechanisms underlying the ALT pathway for telomere homologous recombination and telomere lengthening are largely unknown. Our results support a role for the SMC5/6 complex in telomere maintenance in ALT cells. More interestingly, the MMS21 SUMO ligase within the SMC5/6 complex stimulates the sumoylation of multiple subunits of the shelterin complex and this sumoylation is required for APB formation.

**SMC5/6 and APB formation**

The recruitment of telomeres to PML bodies (APBs) is a hallmark of ALT cells (Yeager et al., 1999). PML bodies are nuclear structures composed of PML aggregates and a diverse set of other proteins (Maul et al., 2000). These nuclear bodies are very dynamic in nature with transient recruitment and release of proteins (Borden, 2002). PML bodies have been proposed to be involved in numerous cellular processes (Borden, 2002). Though the roles of PML nuclear bodies in most of these processes are not clearly established, they are thought to facilitate post-translational modifications and localization of proteins to sites of action (Borden, 2002). APBs are a specialized type of PML bodies that contain telomeres as well as factors involved in DNA repair (Henson et al., 2002; Yeager et al., 1999). Disruption of APBs results in progressive shortening of telomeres,

suggesting that they promote telomere elongation in ALT cells (Jiang et al., 2005).

We observed the localization of the SMC5/6 complex to APBs in ALT cells. Similar to other HR proteins in ALT cells (Grobelny et al., 2000; Wu et al., 2000), the SMC5/6 complex localized with PML bodies in cells with sister chromatids, i.e. cells in late S/G2 phases of the cell cycle. The mechanism for cell cycle regulated localization of the SMC5/6 complex and other HR proteins to APBs is unclear at present. However, extensive evidence suggests that the recruitment of HR proteins to APBs is functionally linked with telomere HR. Thus, the fact that telomeres and HR proteins only localize to PML bodies after replication of telomeres suggests that the majority of telomere HR occurring in APBs is through uneven sister chromatid HR, instead of inter- or intra-chromatid telomere HR. The mechanism by which APB formation is restricted to ALT (telomerase-negative) cells is also unclear.

Previously, we reported that the SMC5/6 complex facilitates sister chromatid HR by promoting the recruitment of the cohesin complex to DSBs (Potts et al., 2006). We did not observe localization of cohesin to APBs in ALT cells. This may not be unexpected since telomeres assemble into specialized t-loop structures resembling Holliday junctions that can potentially undergo replication-induced HR, resulting in elongation (Henson et al., 2002). The proposed function of cohesin in HR is to promote strand invasion and exchange

(Holliday junction formation) through holding sister chromatids in close proximity. Therefore, cohesin may not be required for telomere HR, although this remains to be formally tested.

**MMS21-dependent sumoylation of shelterin and APB formation**

Sumoylation is a post-translational modification that involves the covalent conjugation of SUMO to lysine residues on protein substrates (Muller et al., 2001). Many components of PML nuclear bodies are sumoylated (Seeler and Dejean, 2001). PML itself is highly sumoylated and its sumoylation is required for the formation of PML bodies (Ishov et al., 1999). It has been proposed that PML bodies may be cellular storage sites for sumoylated proteins due to the presence of a number of sumoylated and SUMO-binding proteins (Seeler and Dejean, 2001). We have now shown that multiple subunits of the shelterin telomere-binding complex are sumoylated, which is enhanced by MMS21. Furthermore, depletion of MMS21 in ALT cells inhibits shelterin sumoylation. Mutation of either TRF1 or TRF2 sumoylation sites substantially blocks their MMS21-mediated sumoylation and recruitment to PML bodies. This is consistent with the notion that sumoylation of at least the TRF1 and TRF2 components of shelterin by MMS21 is important for APB formation in ALT cells.

The detailed mechanism by which MMS21-dependent sumoylation of shelterin promotes APB formation is unknown. We envision two non-exclusive

models (Figure 7).  In the recruitment model, MMS21-induced sumoylation of shelterin in the nucleoplasm promotes the subsequent recruitment of shelterin and telomeres to PML bodies by the binding of SUMO to the SUMO-binding motifs of PML itself or other proteins in PML bodies.  In the maintenance model, MMS21 localizes to PML bodies independent of telomeres.  Upon the recruitment of shelterin to PML bodies, MMS21 sumoylates shelterin to facilitate the maintenance of telomeres at PML bodies.  Both mechanisms may occur in ALT cells and reinforce each other, thereby establishing a positive feedback loop.  In either model, sumoylation of shelterin facilitates localization of telomeres to PML bodies to promote telomere HR.  Unequal HR between the two sister telomeres generates one long and one short sister telomere (Figure 4-13).  Two cells with differing replicative potential are generated after sister chromatid separation and cell division.  The daughter cell with an elongated telomere will have an extended replicative potential.

We cannot rule out the possibility that the SMC5/6 complex has roles in telomere HR in addition to the recruitment of telomeres to PML bodies.  Recent evidence suggests a role of the SMC5/6 complex in the late steps of HR to prevent the accumulation of lethal intermediates (Ampatzidou et al., 2006; Branzei et al., 2006; Miyabe et al., 2006).  Furthermore, we observed a slightly higher rate of telomere shortening (~175bp/PD) than normally attributed to replicative attrition in telomerase-negative cells.  Although the underlying reasons

for this discrepancy are unknown at present, this observation is consistent with the

SMC5/6 complex having T-SCE-independent roles at telomeres in ALT cells.

For example, the SMC5/6 complex might protect telomeres against excessive

levels of inappropriate HR, such as T-loop HR that can result in telomere

shortening.  In addition to the SMC5/6 complex, the MRN complex protein,

NBS1, has also been shown to be required for APB formation (Jiang et al., 2005;

Wu et al., 2003), although the mechanism by which it promotes APB formation is

unknown.  Future studies are needed to examine the interplay between the

SMC5/6 complex and the MRN complex in promoting APB formation.

**Sumoylation of shelterin and telomere HR**

Interestingly, MMS21 stimulates the sumoylation of four of the six known

components of shelterin, including TRF1, TRF2, TIN2, and RAP1.  There are

numerous other examples in which multiple subunits of a given macromolecular

complex are sumoylated (Gocke et al., 2005).  Sumoylation of multiple

components within the same complex may alter its stability, potentially leading to

its disassembly.  It is conceivable that MMS21-dependent sumoylation of

shelterin may cause transient disassembly of the complex and the dissociation of

its components from telomeres in APBs.  This is an attractive model, since

previous studies have shown that the shelterin complex prevents HR through

binding to telomeric t-loops, therefore safeguarding telomerase-positive cells

from potentially dangerous telomeric HR (Wang et al., 2004). ALT cells need to overcome this inhibition to allow HR to lengthen telomeres. MMS21-induced sumoylation of shelterin may provide such a mechanism that deprotects telomeres to facilitate telomeric recombination in ALT cells. Consistent with this model, one putative sumoylation site of TRF2 is located in the TRFH domain that mediates the dimerization of TRF2 and its binding to TIN2. Therefore, sumoylation of TRF2 could potentially alter TRF2's interactions with itself or TIN2.

Whether sumoylation is a post-translational regulatory mechanism of shelterin in telomerase-positive cells remains to be determined. Recent reports have illustrated the involvement of sumoylation in the control of telomere length maintenance in telomerase-positive yeast (Xhemalce et al., 2007). Inactivation of Smt3 (yeast SUMO) or the Pli1 E3 SUMO ligase, but not MMS21, results in increased telomere length in yeast (Xhemalce et al., 2007). Therefore, it is likely that MMS21-independent sumoylation controls telomere length regulation in telomerase-positive cells.
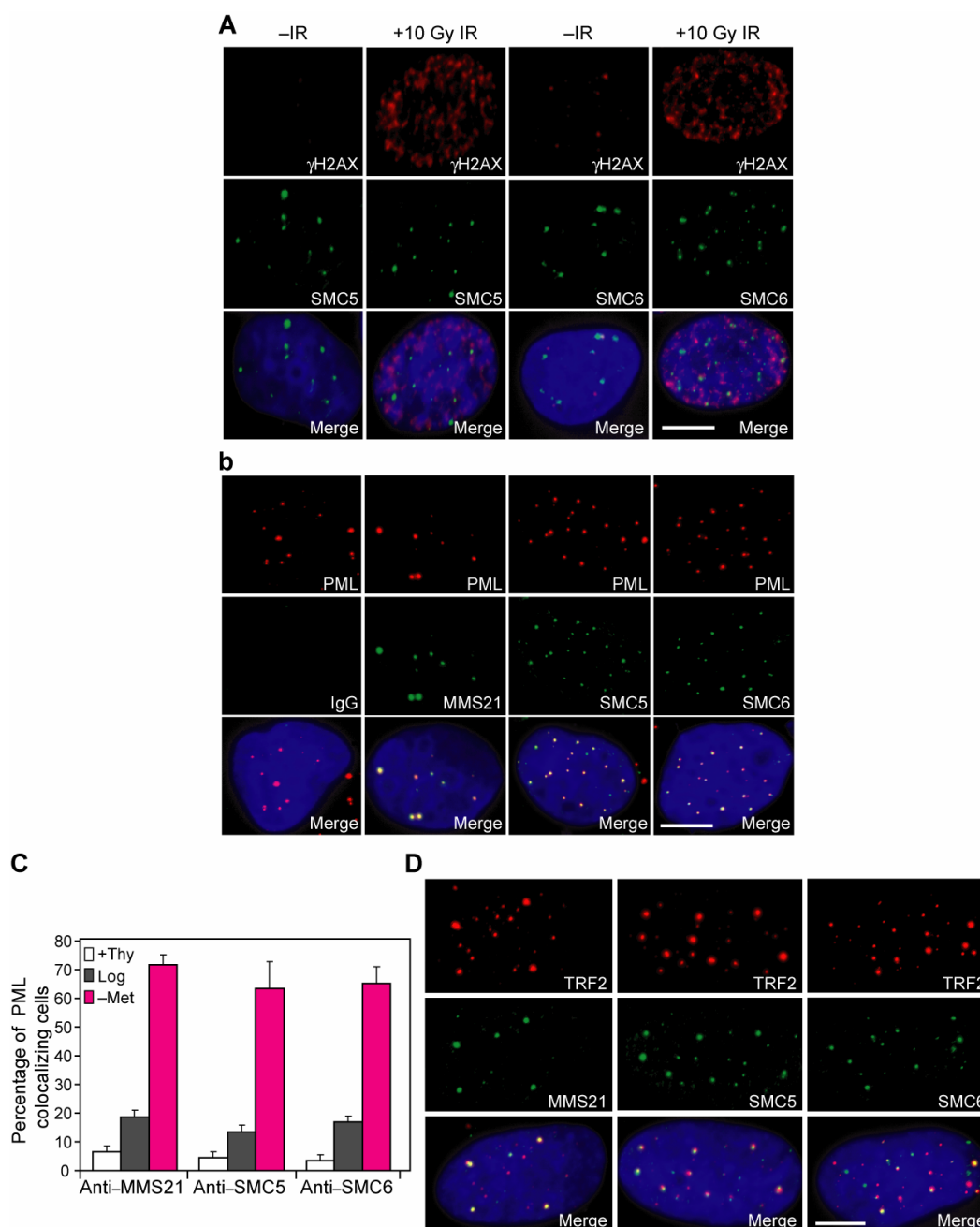
**Figure 4-1. The SMC5/6 complex localizes to PML nuclear bodies**
(A) SMC5/6 localizes to nuclear foci in U2OS cells that do not depend on or colocalize with DNA damage. Cells were untreated or treated with IR (10 grays) and stained one hour later with the indicated antibodies. (**B**) The SMC5/6 complex localizes to PML bodies in U2OS cells. U2OS cells were stained with

the indicated antibodies.  (**C**) Percentages of cells with colocalization of the SMC5/6 complex and PML bodies in log-phase, G1/S (+Thy), or G2/M (-Met) U2OS cells.  Results from three separate experiments were averaged with the standard deviations indicated.  (**D**) The SMC5/6 complex localizes to a subset of telomeres (TRF2) in U2OS cells.  Scale bars represent 5 μm.
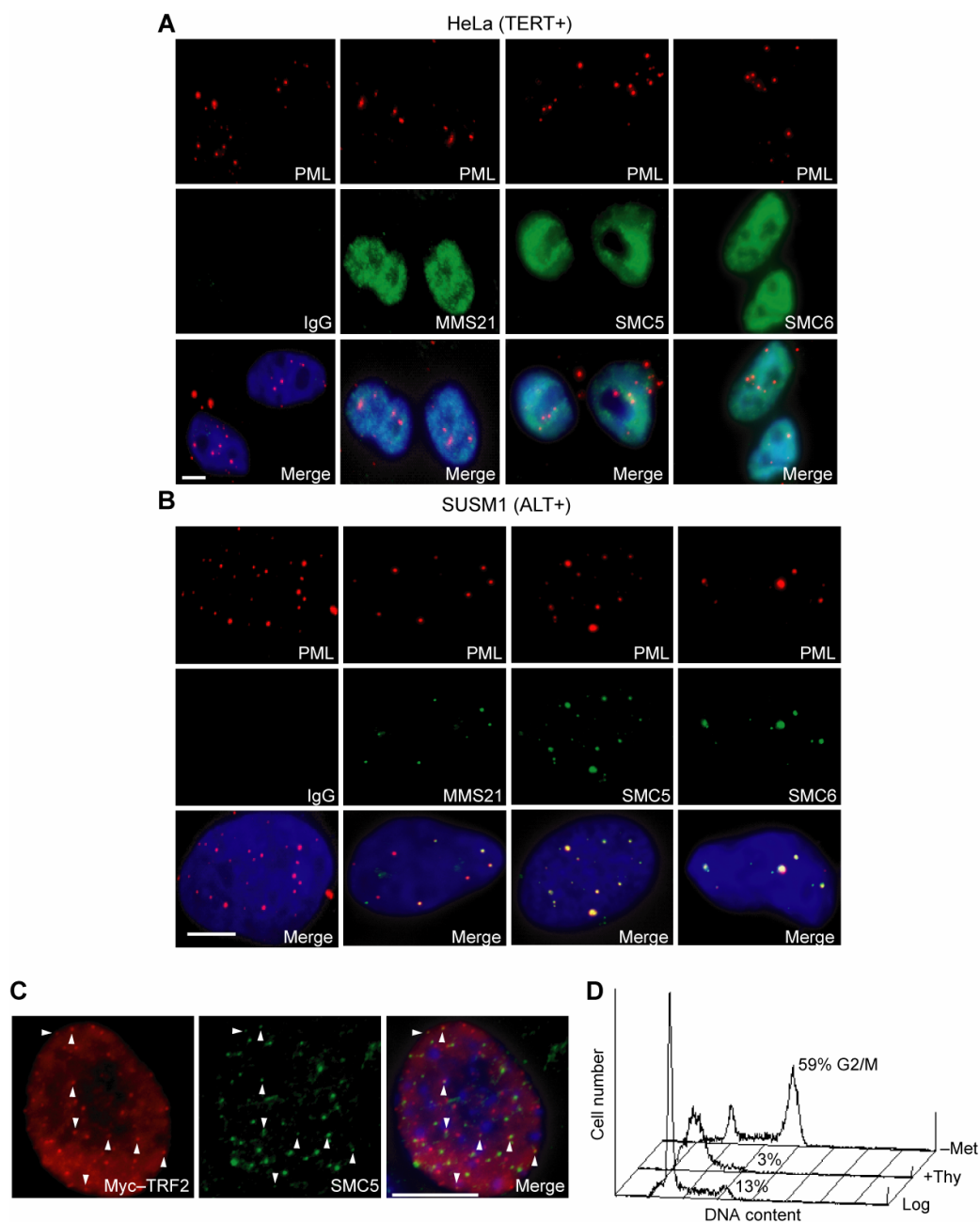
**Figure 4-2. The SMC5/6 complex localization in telomerase-positive and ALT cell lines**
(**A**) The SMC5/6 complex does not localize to PML bodies in telomerase-positive HeLa cells. (**B**) The SMC5/6 complex does localize to PML bodies in the ALT cell line, SUSM1. (**C**) SMC5 localizes with a subset of Myc-TRF2

telomere foci in the G5 mTerc$^{-/-}$ Wrn$^{-/-}$ Ras$^{v12}$ MEF ALT cell line. Arrowheads indicate colocalization events. (**D**) Cell cycle profile of U2OS cells either untreated (log), thymidine arrested (+thy), or methionine deprived (-met). The percentage of G2/M cells is shown for each condition. Scale bars represent 5 μm.
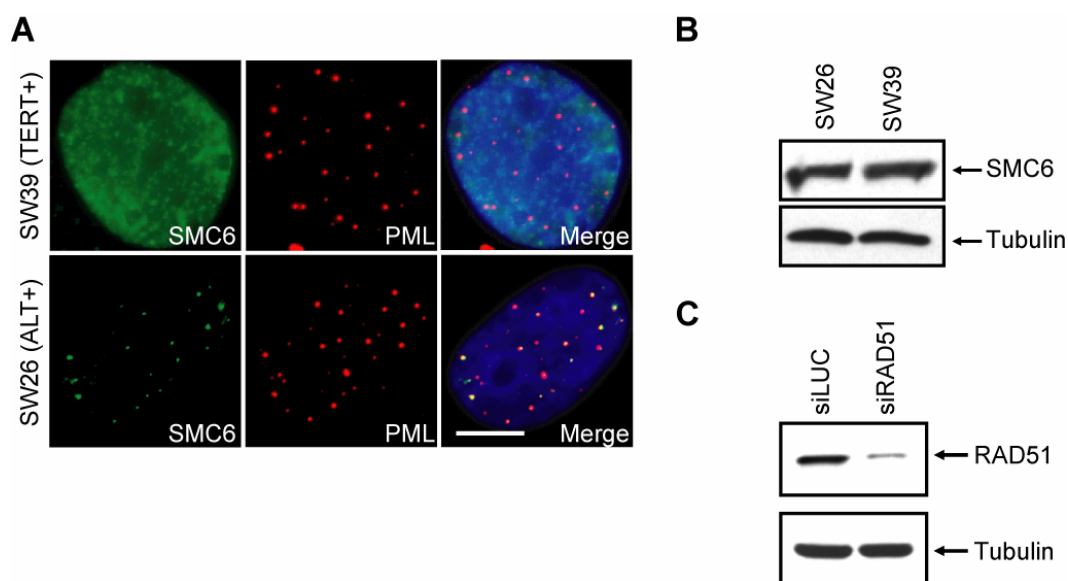
**Figure 4-3. The SMC5/6 complex localizes to PML bodies in ALT, but not telomerase-positive cells**
(**A**) SMC6 colocalizes with PML bodies in SW26 ALT cells, but not in SW39 telomerase-positive cells. The cells were stained with anti-SMC6 (green), anti-PML (red), and DAPI (blue). (**B**) Lysates of SW26 and SW39 cells were blotted with anti-SMC6 and anti-Tubulin. (**C**) U2OS cells described in (Figure 3A) were immunoblotted with anti-RAD51 to confirm RAD51 knockdown and anti-Tubulin (loading control). Scale bars represent 5 µm.
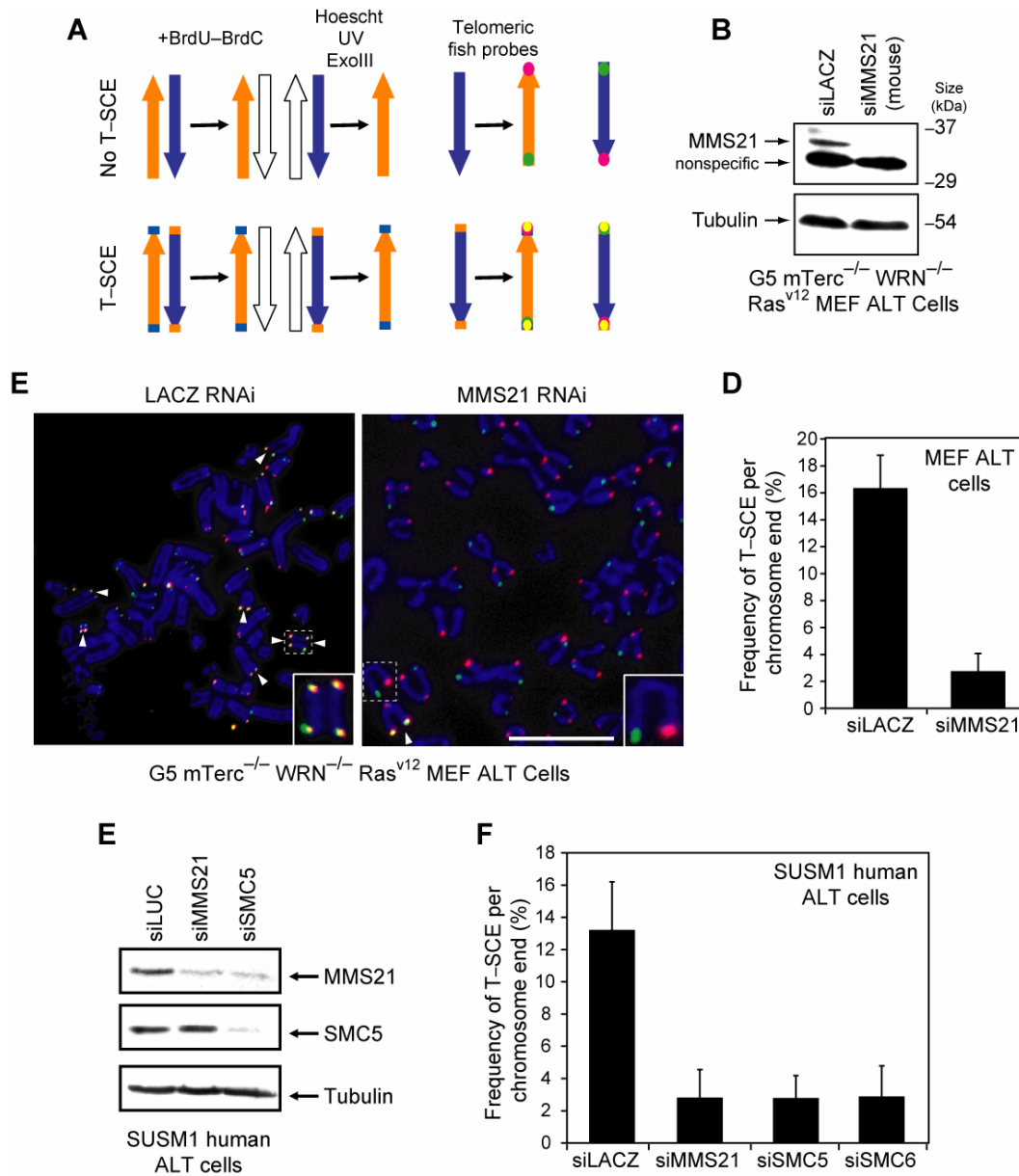
**Figure 4-4. Inhibition of the SMC5/6 complex decreases telomeric recombination (T-SCE)**

(**A**) Schematic illustration of the CO-FISH T-SCE assay. (**B**) Western blot analysis showing the efficiency of RNAi-mediated knockdown in G5 mTERC$^{-/-}$ WRN$^{-/-}$ RAS$^{v12}$ MEF ALT cells. (**C**) Chromosome spreads from LACZ- or MMS21-RNAi G5 mTERC$^{-/-}$ WRN$^{-/-}$ RAS$^{v12}$ MEF ALT cells were processed for CO-FISH as described in (A) with G-rich (red) and C-rich (green) telomeres

stained.  Arrowheads mark unequal T-SCE events (yellow).  (**D**) Quantitation of the frequency of unequal T-SCE events per chromosome end as depicted in (C). Results from three separate experiments were averaged with the standard deviations indicated.  (**E**) Western blot analysis showing the efficiency of RNAi-mediated knockdown in human SUSM1 ALT cells.  (**F**) Quantitation of the frequency of unequal T-SCE events per chromosome end in SUSM1 cells treated with SMC5/6-RNAi.  Results from three separate experiments were averaged with the standard deviations indicated.  Scale bar represents 5 μm.
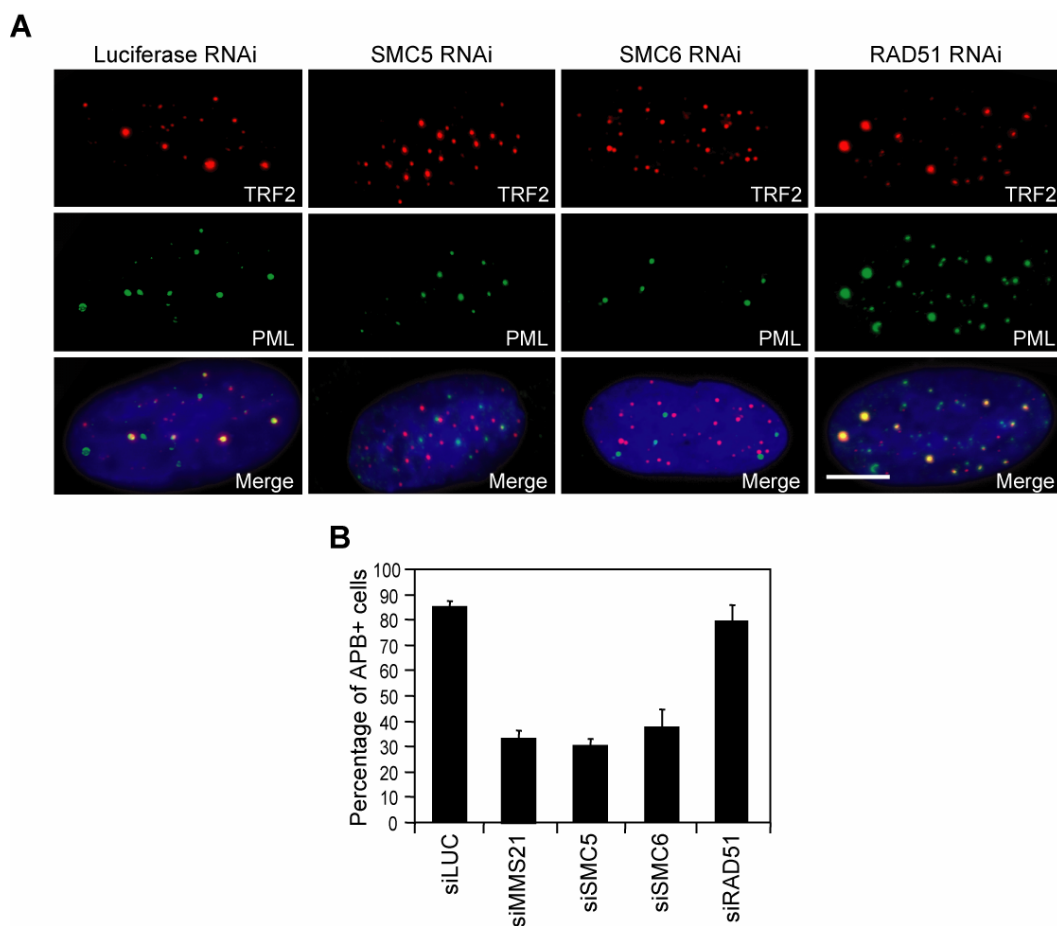
**Figure 4-5. The SMC5/6 complex is required for APB formation**
(**A**) U2OS cells were treated with the indicated siRNAs and APBs were analyzed by examining colocalization of TRF2 (red) and PML (green). (**B**) Quantitation of the cells shown in (A). Results from three separate experiments were averaged with the standard deviations indicated. Scale bars represent 5 μm.
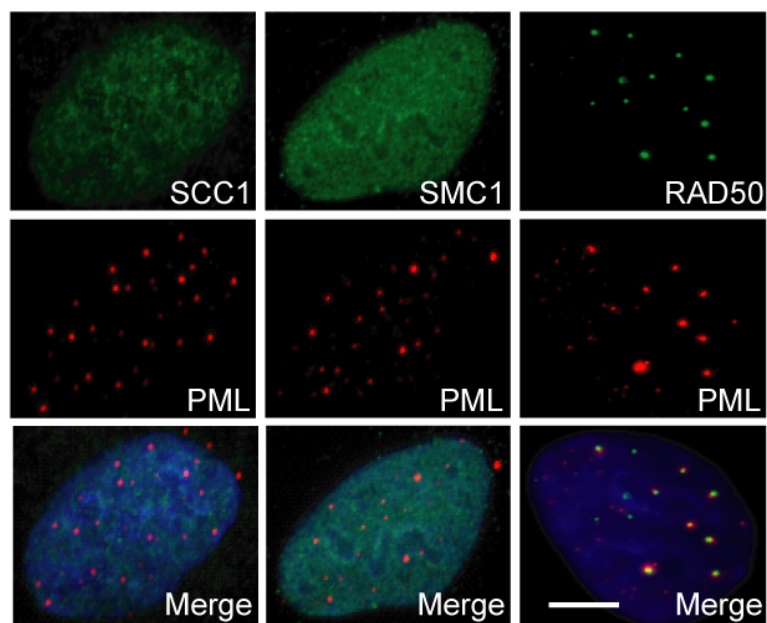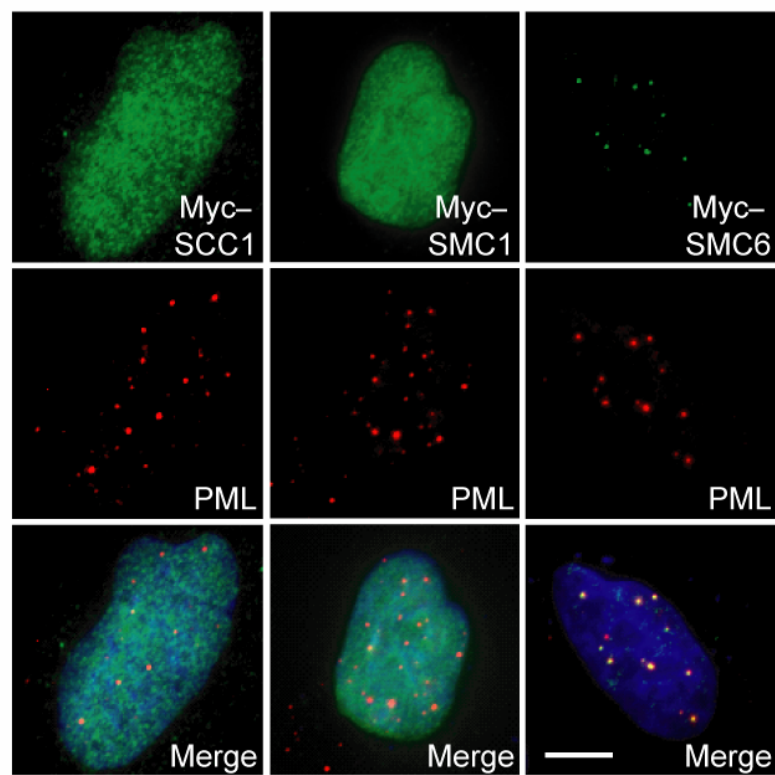
**Figure 4-6.  The cohesin complex does not localize to PML bodies**
(**A**) U2OS cells were stained with anti-SCC1 (green), anti-SMC1 (green), anti-RAD50 (green), anti-PML (red), and DAPI (blue).  (**B**) U2OS cells were transfected with Myc-tagged cohesin complex components (SCC1 or SMC1) or SMC6.  Cells were stained with anti-Myc (green), anti-PML (red), and DAPI (blue).  Scale bar represents 5 μm.
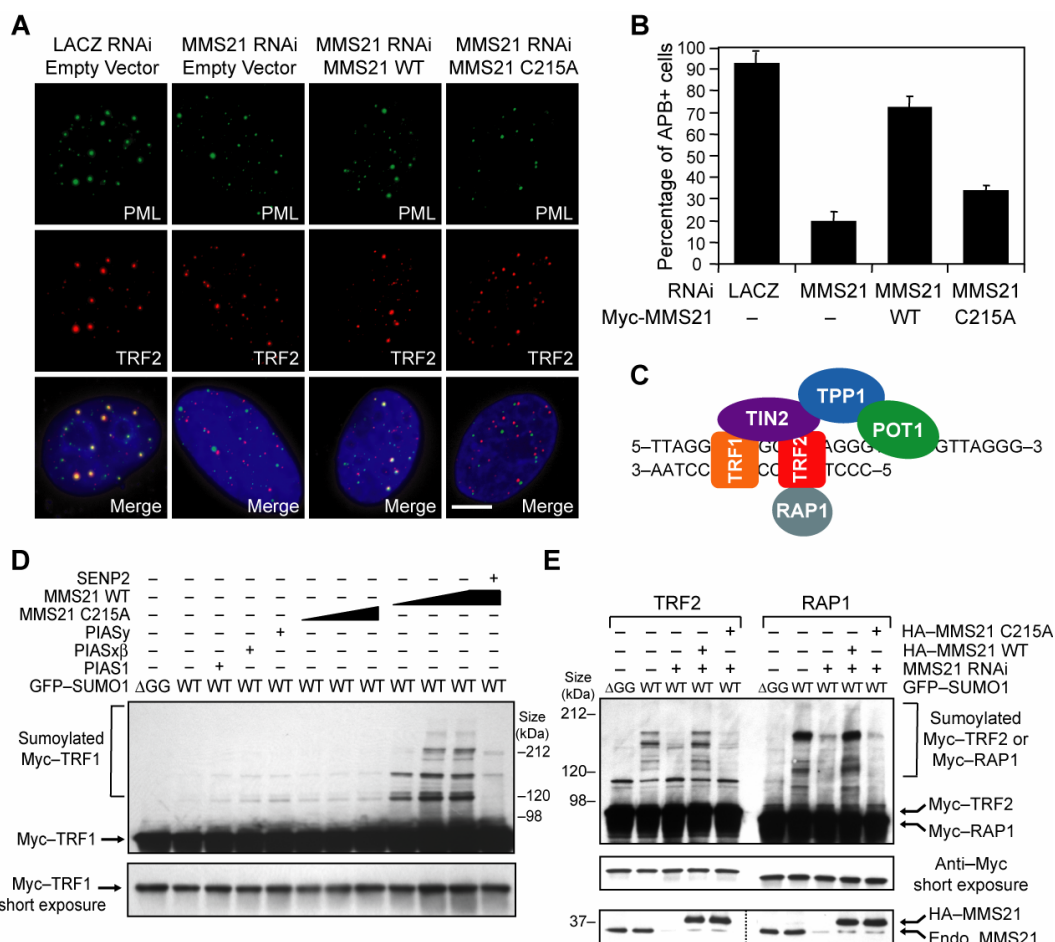
**Figure 4-7. MMS21 sumoylates the core telomere-binding proteins**
(**A**) The SUMO ligase activity of MMS21 is required for recruitment of telomeres to APBs. U2OS cells were transfected with the indicated siRNAs and subsequently with the indicated plasmids (empty, MMS21 wild-type, or C215A SUMO ligase dead). Cells were stained with the indicated antibodies and DAPI (blue). (**B**) Quantitation of the number of APB+ cells shown in (A). Results from three separate experiments are averaged with the standard deviations indicated. (**C**) Schematic illustration of the architecture of the shelterin telomere-binding complex (de Lange, 2005). (**D**) HeLa cells were transfected with the indicated constructs in addition to the Myc-TRF1 plasmid. Cells were immunoblotted with anti-Myc. GFP-SUMO1-ΔGG lacks the di-glycine carboxy-terminal motif required for its conjugation to substrates. PIAS1, PIASxβ, and PIASy plasmids were transfected at the highest concentrations indicated for the MMS21 plasmid. (**E**) U2OS cells were transfected with the indicated constructs in addition to either Myc-TRF2 or Myc-RAP1. HA-MMS21 wild-type (WT) or sumo-ligase dead

(C215A) contained silent point mutations in the siRNA binding region to prevent knockdown of the transgenes.  Cells were immunoblotted with anti-Myc or anti-MMS21.  Scale bar represents 5 μm.
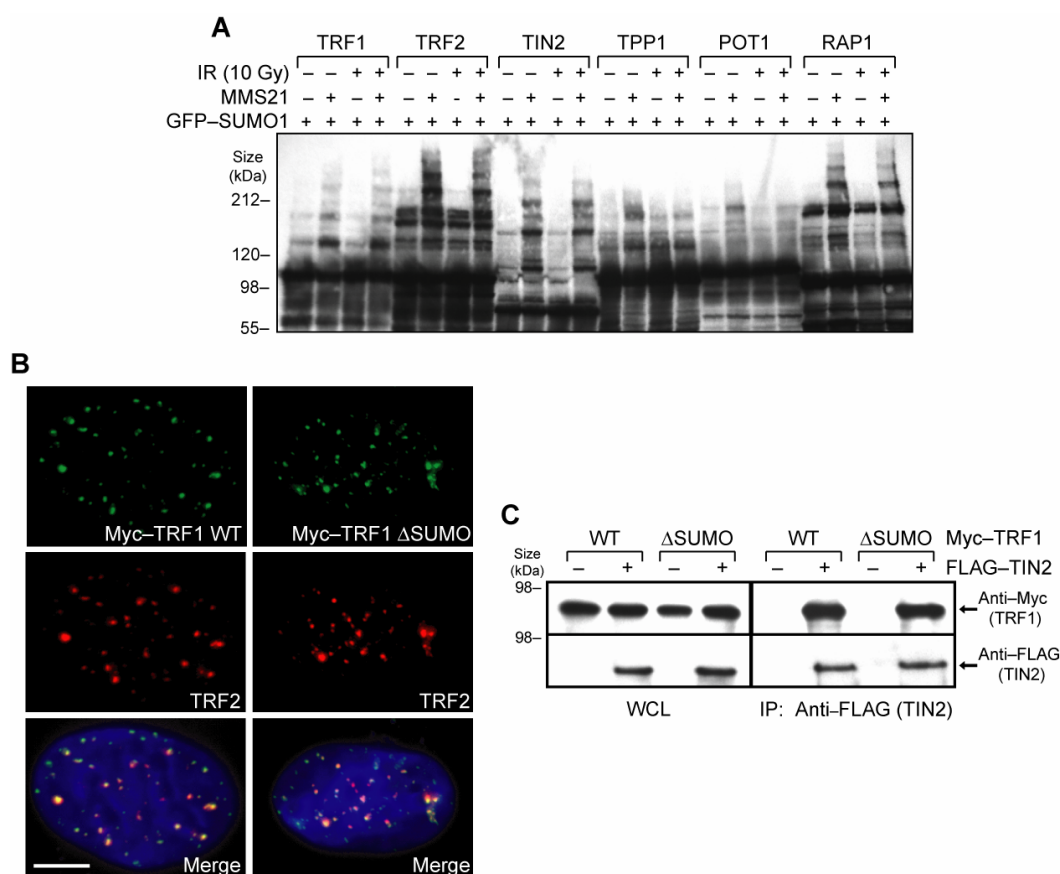
**Figure 4-8. The shelterin complex is sumoylated by MMS21 and does not effect its localization to telomeres**

(**A**) Components of the shelterin complex are sumoylated by MMS21. Plasmids encoding telomere-binding proteins (FLAG-YFP-tagged) were transfected into HeLa cells along with other indicated plasmids. Cells were either untreated or treated 24 hours after transfection with 10 grays of irradiation (IR). Cells were immunoblotted for telomere-binding proteins one hour after irradiation (anti-FLAG). (**B**) U2OS cells were transfected with Myc-tagged TRF1 wild-type (WT) or ΔSUMO. Cells were stained with anti-Myc (green), anti-TRF2 (red), and DAPI (blue). (**C**) TRF1 ΔSUMO mutant interacts with TIN2 similar to wild-type TRF1. Myc-TRF1 wild-type (WT) or ΔSUMO was expressed with or without FLAG-TIN2. Cell lysates were immunoprecipitated with anti-FLAG and blotted with the indicated antibodies. Scale bar represents 5 μm.
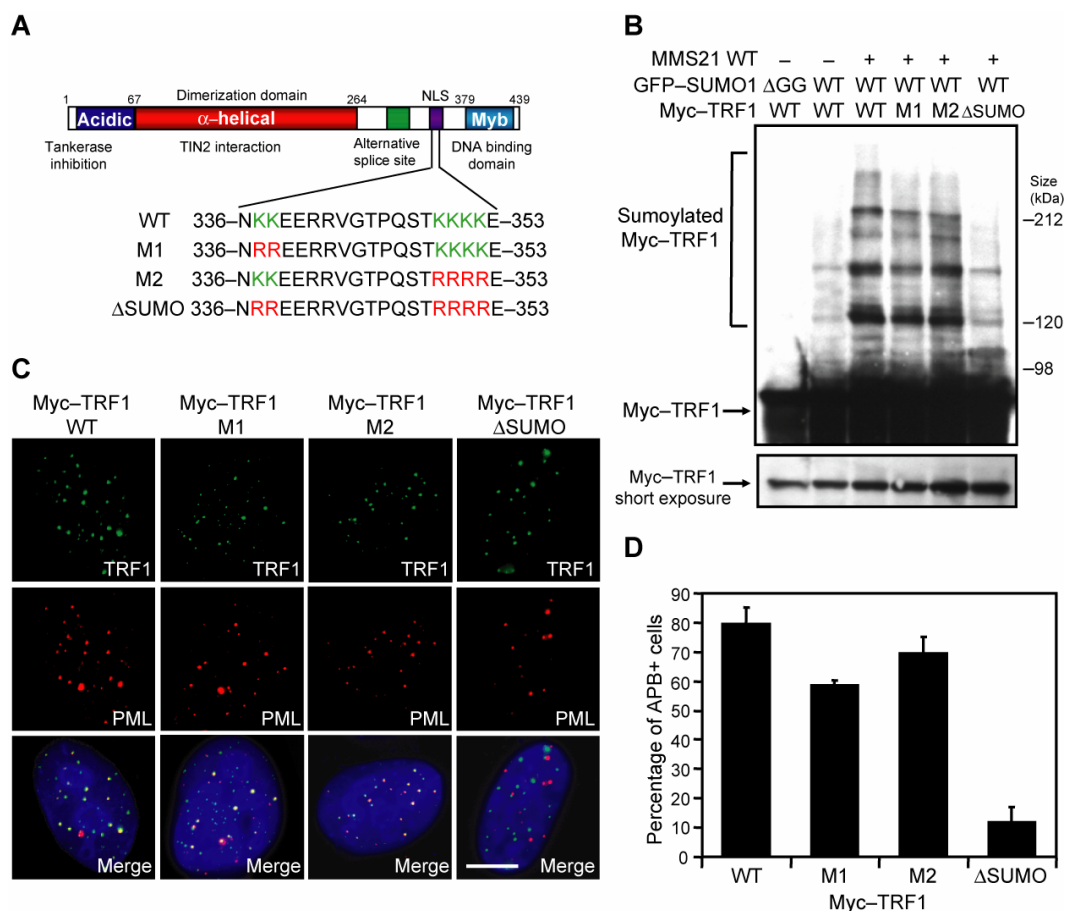
**Figure 4-9. MMS21-induced sumoylation of telomere-binding proteins is required for APB formation**
(**A**) Schematic illustration of putative TRF1 sumoylation sites and the mutations created. (**B**) Mutation of TRF1 sumoylation sites (ΔSUMO) decreases MMS21-induced sumoylation of TRF1. Myc-TRF1 WT, M1, M2, or ΔSUMO mutants were expressed in HeLa cells with the indicated plasmids. Cell lysates were immunoblotted with anti-Myc. (**C**) Myc-TRF1 ΔSUMO mutant does not localize to PML bodies in U2OS cells. U2OS cells were stained with anti-Myc (green), anti-PML (red), and DAPI (blue). (**D**) Quantitation of the percentage of APB+ cells shown in (C). Results from three separate experiments were averaged with the standard deviations indicated. Scale bar represents 5 µm.
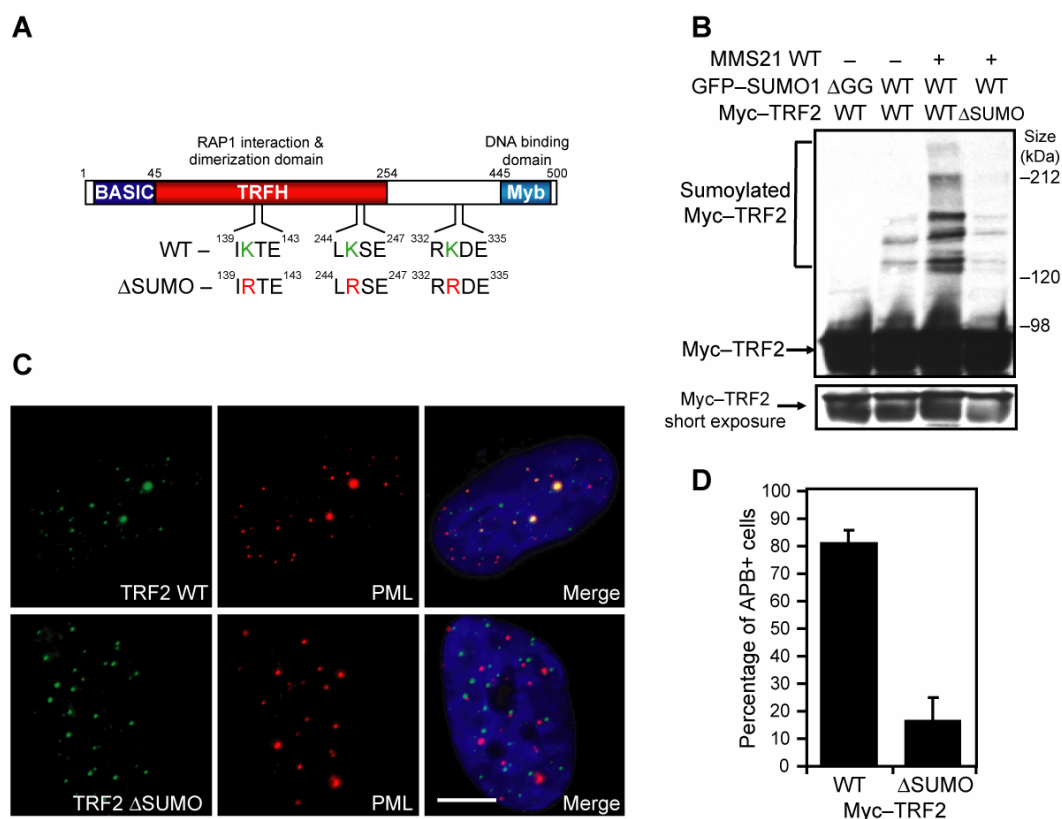
**Figure 4-10. MMS21-induced sumoylation of TRF2 is required for TRF2 recruitment to PML bodies**

(**A**) Schematic illustration of putative TRF2 sumoylation sites and the mutations created. (**B**) Mutation of TRF2 sumoylation sites (ΔSUMO) decreases MMS21-induced sumoylation of TRF2. Myc-TRF2 WT or ΔSUMO mutants were expressed in HeLa cells with the indicated plasmids. Cell lysates were immunoblotted with anti-Myc. (**C**) U2OS cells were transfected with Myc-tagged TRF2 wild-type (WT) or ΔSUMO and were stained with anti-Myc (green), anti-PML (red), and DAPI (blue). (**D**) Quantitation of the percentage of APB+ cells shown in (C). Results from three separate experiments were averaged with the standard deviations indicated. Scale bar represents 5 µm.
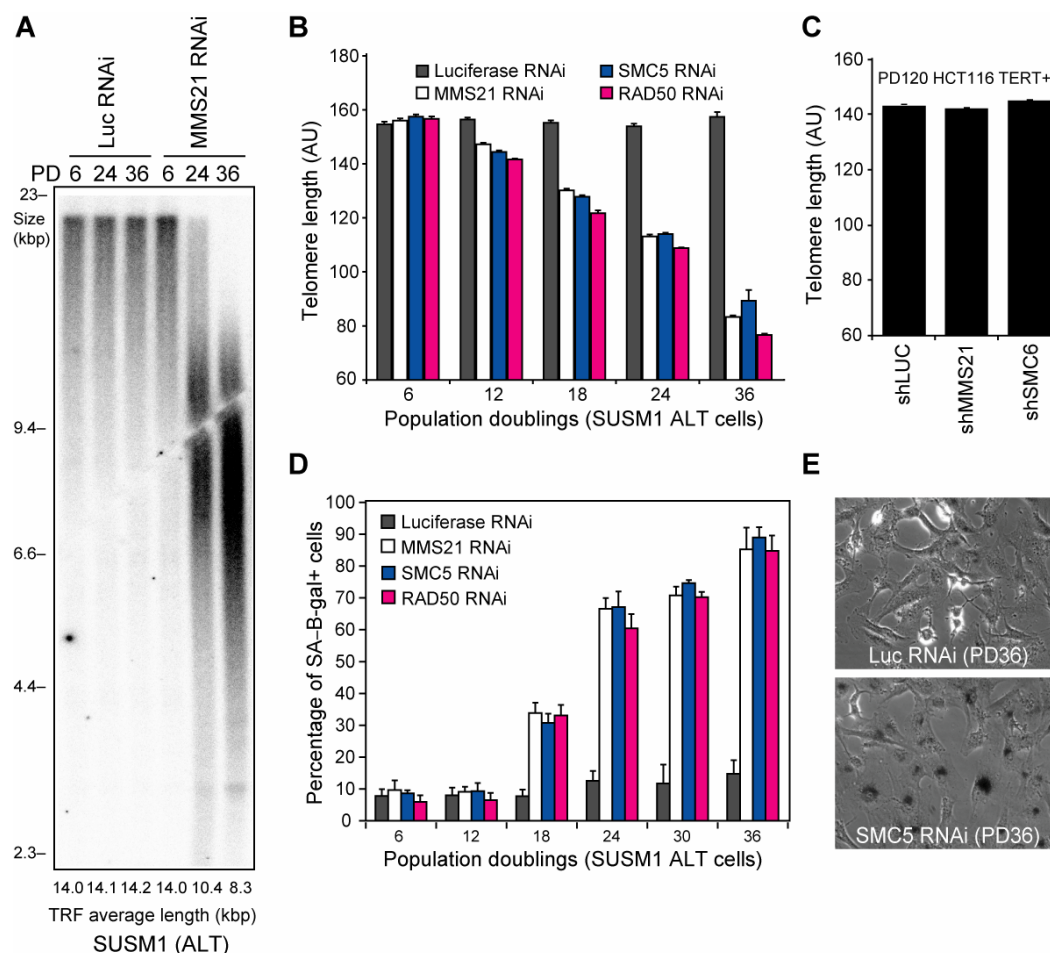
**Figure 4-11. Inhibition of the SMC5/6 complex results in telomeric shortening and cellular senescence**

(**A**) Telomere restriction fragment (TRF) analysis of SUSM1 cells treated with either siLuciferase or siMMS21 RNAi oligonucleotides for the indicated population doublings. Genomic DNA was probed with $^{32}$P-(TTAGGG)$_4$ oligonucleotide. Average telomere lengths are indicated below the gel. (**B**) SUSM1 cells were treated with the indicated siRNAs for the indicated number of population doublings. Relative telomere lengths were determined by Q-FISH and the average intensities shown for the indicated siRNAs and population doublings. Results from two separate experiments were averaged with the standard errors indicated. (**C**) Stable shRNA knockdown cell lines were made in telomerase-positive HCT116 cells with the indicated shRNAs and were maintained in culture for 120 population doublings. Relative telomere lengths were determined by Q-FISH and the average intensities shown for the indicated shRNAs. Results from two separate experiments were averaged with the standard errors indicated. (**D**)

SUSM1 cells were treated with the indicated siRNAs for the indicated number of population doublings. Senescent cells were observed by SA-β-galactosidase staining and the average number of SA-β-galactosidase-positive cells is shown. Results from two separate experiments were averaged with the standard deviations indicated. (**E**) Cells described in (D) showing SA-β-galactosidase-positive cells (dark cells).
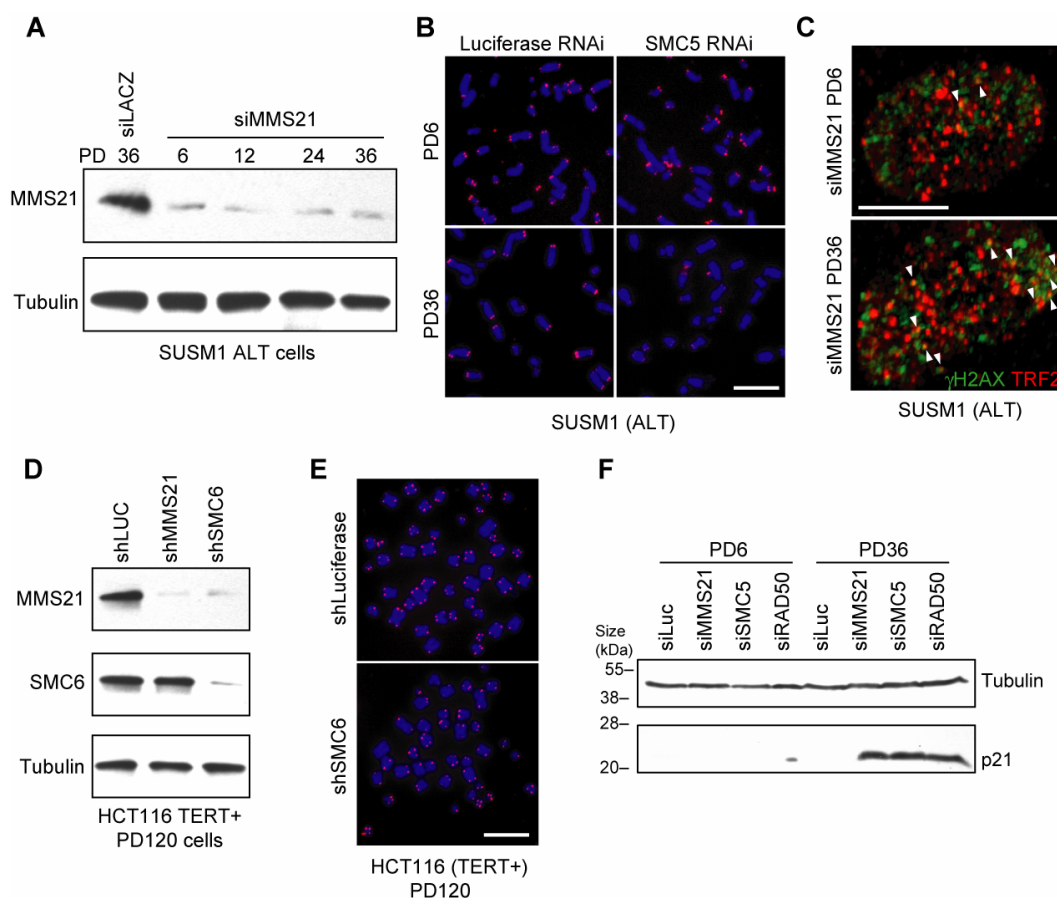
**Figure 4-12. Inhibition of the SMC5/6 complex results in telomeric shortening**

(**A**) SUSM1 cells were treated with the indicated siRNAs for the indicated number of population doublings. Cell lysates were immunoblotted with anti-MMS21 or anti-Tubulin. (**B**) Chromosome spreads from siRNA treated SUSM1 cells described in (A) were stained for G-rich telomeres (red). (**C**) SUSM1 cells described in (A) were immunostained with γH2AX (green) and anti-TRF2 (red) to detect uncapped or shortened telomeres. Arrows indicated colocalization event. (**D**) Stable shRNA knockdown cell lines were made in telomerase-positive HCT116 cells with the indicated shRNAs and were maintained in culture for 120 population doublings. Cell lysates were immunoblotted with anti-MMS21, anti-SMC6, or anti-Tubulin (loading control). (**E**) Chromosome spreads from cells described in (C) were stained for G-rich telomeres (red). (**F**) Cell lysates from SUSM1 cells described in (A) were immunoblotted with anti-p21 (a senescent marker) and anti-Tubulin (a loading control). Scale bars represent 5 μm.
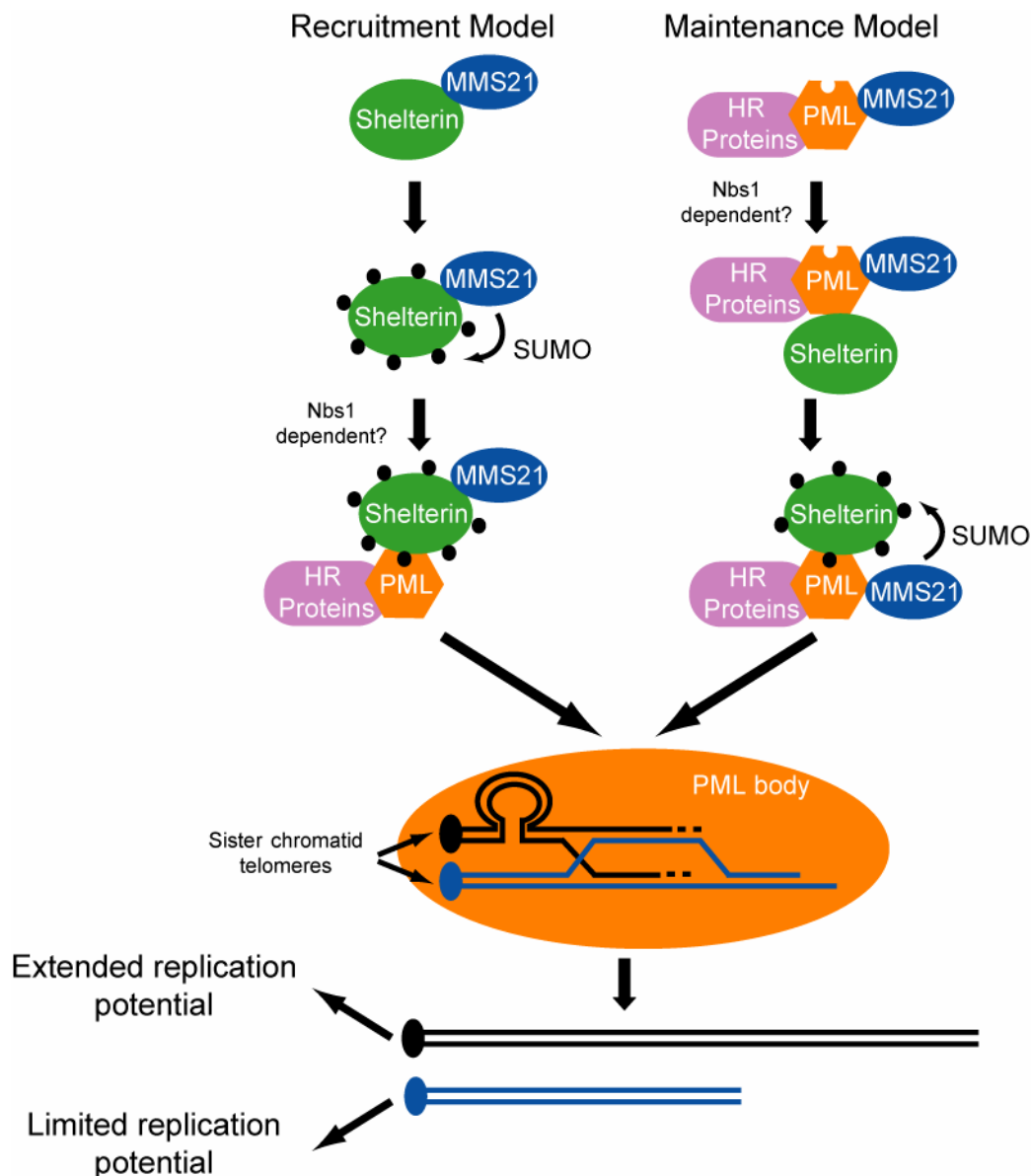
**Figure 4-13.  Two proposed models for how MMS21-induced shelterin sumoylation promotes telomere length maintenance in ALT cells**
In the recruitment model, MMS21 sumoylates the shelterin complex in the nucleoplasm, resulting in the subsequent recruitment of telomeres to PML bodies for telomere recombination and lengthening.  In the maintenance model, MMS21 localizes to PML bodies independently of telomeres.  Upon recruitment of telomeres to PML bodies, MMS21-induced sumoylation of shelterin maintains telomeres in PML bodies for telomere recombination.

**Table 4-1.  The SMC5/6 complex localizes to PML bodies and telomeres in ALT cells**

| SMC5/6 Subunit | PML foci with SMC5/6 (percent) | SMC5/6 foci with PML (percent) | TRF2 foci with SMC5/6 (percent) | SMC5/6 foci with TRF2 (percent) |
|---|---|---|---|---|
| MMS21 | 71.5 | 87.3 | 51.5 | 75.1 |
| SMC5 | 73.9 | 90.3 | 58.4 | 72.3 |
| SMC6 | 78.9 | 91.4 | 55.1 | 76.0 |

**Table 4-2.  The SMC5/6 complex localizes to PML nuclear bodies in ALT cells**

| Cell Line | Cell Type | Immortalization | SMC5/6 Foci | Telomere Maintenance |
|-----------|-----------|-----------------|-------------|----------------------|
| U2OS | Epithelial; Bone osteosarcoma | Tumor | + | ALT |
| SUSM1 | Fibroblast; Liver | Chemical | + | ALT |
| Saos-2 | Epithelial; Bone osteosarcoma | Tumor | + | ALT |
| SW-26 | Fibrobast; Lung | SV40 | + | ALT |
| SW-39 | Fibroblast; Lung | SV40 | — | Telomerase |
| 293 | Epithelial; Kidney | Adenovirus | — | Telomerase |
| HeLa | Epithelial; Cervical carcinoma | Tumor | — | Telomerase |
| H1299 | Epithelial; Non-small cell lung carcinoma | Tumor | — | Telomerase |
| MCF7 | Epithelial; Breast adenocarcinoma | Tumor | — | Telomerase |

**Table 4-3.  Knockdown of the SMC5/6 complex in ALT cells results in telomere abnormalities**

| Cell line | Telomere maintenance | RNAi treatment | Population doublings | Chromosome ends analyzed | Signal free ends (%) | End-to-end fusions per cell |
|---|---|---|---|---|---|---|
| SUSM1 | ALT | siLACZ | 6 | 4550 | 4.37 | 0.20 |
| SUSM1 | ALT | siMMS21 | 6 | 3938 | 4.62 | 0.26 |
| SUSM1 | ALT | siSMC5 | 6 | 4511 | 4.74 | 0.24 |
| SUSM1 | ALT | siLACZ | 36 | 4074 | 5.38 | 0.24 |
| SUSM1 | ALT | siMMS21 | 36 | 4282 | 27.02 | 1.27 |
| SUSM1 | ALT | siSMC5 | 36 | 4104 | 26.66 | 1.14 |
| HCT116 | Telomerase | shLUC | 120 | 3940 | 1.17 | 0.00 |
| HCT116 | Telomerase | sMMS21 | 120 | 4288 | 1.24 | 0.05 |
| HCT116 | Telomerase | shSMC6 | 120 | 3973 | 1.21 | 0.05 |

# CHAPTER V:  CONCLUSIONS AND FUTURE DIRECTIONS

## HUMAN MMS21 AS A SUMO LIGASE

We have identified the human homolog of MMS21 and showed that it is

an E3 SUMO ligase (Figure 2-1).  After screening numerous proteins known to be

sumoylated and potential sumoylation targets of MMS21, we identified SMC6

and TRAX as targets for MMS21 sumoylation (Figure 2-5).  The function of these

sumoylation events is currently unknown.  MMS21-induced sumoylation of

SMC6 could be a basal or regulatory event.  Sumoylation of SMC6 may be

necessary for the formation and/or stability of the SMC5/6 complex.  In addition,

it may also regulate the localization of the SMC5/6 complex to distinct chromatin

domains, such as DSBs.  Little is known about how MMS21-induced sumoylation

of TRAX could alter its function.  Future studies will be necessary to determine if

TRAX functions in DNA repair and if MMS21-induced sumoylation affects its

activity.  Identification of the MMS21-induced sumoylation sites on TRAX and

SMC6 will be essential for determining the effects of their sumoylation.

We have also shown that the SUMO ligase activity of MMS21 is required

to prevent DNA damage-induced apoptosis (Figure 2-6).  This requirement is due

to the role of MMS21 in DNA repair, not in DNA damage-induced cell cycle

checkpoint (Figures 2-7 and 2-8).  Knockdown of MMS21 does not disrupt

initiation of the cell cycle checkpoint by ATM/ATR-mediated CHK2

phosphorylation (Figure 2-7).  However, in yeast it has been shown that the

SMC5/6 complex is required for maintenance of a prolonged DNA damage-

induced cell cycle checkpoint (Harvey et al., 2004).  Future studies are necessary

to determine what activity of the SMC5/6 complex promotes DNA damage-

induced cell cycle checkpoint maintenance.


## THE SMC5/6 AND COHESIN COMPLEXES AT DSBS


To determine the role of the SMC5/6 complex in DNA repair, we

examined the contribution of the SMC5/6 complex to repair of DSBs by intra-,

extra-, or sister chromatid HR and NHEJ.  We showed that the SMC5/6 complex

is only required for sister chromatid HR (Figures 3-1, 3-2, 3-5, and 3-6).  In fact,

inhibition of the SMC5/6 complex increased the frequency of intra- and extra-

chromatid HR and NHEJ (Figures 3-1, 3-2, and 3-5).  These results highlight the

competition between HR and NHEJ for repair of DSBs.  We observed that by

specifically inhibiting sister chromatid HR, we could increase the frequency of

gene targeting (episomal HR; Figure 3-2).  This has potentially important clinical

implications because the use of gene targeting to correct endogenous, deleterious

mutations is hampered by the low efficiency of gene targeting.

We next examined the function of the SMC5/6 complex in sister chromatid HR. We showed that the SMC5/6 complex localizes to I-SceI endonuclease-induced DSBs (Figure 3-10). The precise mechanisms controlling the localization of the SMC5/6 complex to DSBs is unknown. However, we observed that the recruitment of the SMC5/6 complex is inhibitable by caffeine, suggesting that ATM, ATR, and/or DNA-PK play a role in the recruitment of the SMC5/6 complex to DSBs. (data not shown) Interestingly, SMC6 has been shown to be phosphorylated in human cells, but the function of this phosphorylation is unknown (Taylor et al., 2001). Future studies are needed to determine if ATM, ATR, and/or DNA-PK control localization of the SMC5/6 complex at DSBs by directly phosphorylating the SMC5/6 complex or if the phosphorylation of other substrates at DSBs, such as γH2AX, are important. We and others have also observed that the localization of the SMC5/6 complex to DSBs is not dependent on the cohesin SCC2 chromatin loader (data not shown and (Lindroos et al., 2006)). It will be interesting in the future to determine if other proteins that associate with the SMC5/6 complex, such as NSE5 and NSE6, play a role in the localization of the SMC5/6 complex to DSBs.

Similar to the SMC5/6 complex, the SMC1/3 cohesin complex also localizes to DSBs and is specifically required for sister chromatid HR. Based on these observations, we examined whether the cohesin and SMC5/6 complexes crosstalk at DSBs. We showed that the recruitment of the cohesin complex to I-

SceI endonuclease-induced DSBs is dependent on the SMC5/6 complex (Figure

3-12). The exact mechanism by which the SMC5/6 complex facilitates

recruitment of the SMC1/3 cohesin complex to DSBs is unknown. However, we

found that one potential mechanism by which the SMC5/6 complex could

facilitate the recruitment of the SMC1/3 cohesin complex to DSBs is by

sumoylation of two SMC1/3 cohesin complex components, SCC1 and SA2

(Figure 3-14). Future studies are needed to identify the MMS21-induced

sumoylation sites on SCC1 and/or SA2 and to determine whether these

sumoylation events are required for localization of the SMC1/3 cohesin complex

to DSBs and for sister chromatid HR.


## THE SMC5/6 COMPLEX AND TELOMERE RECOMBINATION


In addition to sister chromatid HR, we examined whether the SMC5/6

complex is required for telomere HR. Certain types of cancer cells utilize a

mechanism known as alternative lengthening of telomeres (ALT) to elongate their

telomeres and achieve unlimited replicative potential (Henson et al., 2002). ALT

cells mediate telomere elongation by telomere sister chromatid HR (Dunham et

al., 2000). We have determined that the SMC5/6 complex is required for

telomere HR and lengthening and extended replicative potential in ALT cells

(Figures 4-4, 4-11, and 4-12). One defining characteristic of ALT cells is the

localization of telomeres to PML nuclear bodies (Muntoni and Reddel, 2005).

We showed that the SMC5/6 complex also localizes to PML bodies in ALT, but

not telomerase-positive, cells (Figures 4-1 and 4-2). The mechanism by which the

SMC5/6 complex only localizes to PML bodies in ALT, but not telomerase-

positive, cells is unknown. It will be interesting to determine if the sumoylation

of SMC6 is differentially controlled in ALT and telomerase-positive cells and if

this sumoylation is important for localization of the SMC5/6 complex to PML

bodies in ALT cells.

We next examined the mechanism by which the SMC5/6 complex

promotes telomere HR in ALT cells. We showed that the SMC5/6 complex is

required for the localization of telomeres to PML bodies in ALT cells (Figure 4-

5). This localization was dependent on MMS21-induced sumoylation of the

telomere-binding shelterin complex (Figures 4-7 and 4-9). We proposed that the

MMS21-induced sumoylation of the shelterin complex promotes high affinity

interaction between the PML protein's SUMO-binding domain and the SUMO-

conjugated shelterin protein components, such as TRF1 and TRF2. This type of

SUMO-conjugation induced localization of proteins to PML bodies has previous

been noted for several proteins, such as DAXX (Lin et al., 2006). Future work is

necessary to determine whether the shelterin complex sumoylation occurs in the

nucleoplasm to drive telomeres to PML bodies or if shelterin sumoylation occurs

at PML bodies to maintain telomeres in PML bodies for HR. It will also be

interesting to determine the contribution of the SMC5/6 complex-associated, SUMO-like protein NIP45/RAD60 in telomere recombination and recruitment of the SMC5/6 complex and telomeres to PML bodies in ALT cells.

## OVERALL CONCLUSIONS

In conclusion, this work has revealed a number of interesting discoveries on the function of the human SMC5/6 complex. In general, it highlights the role of the SMC5/6 complex in orchestrating several cellular processes, such as sister chromatid cohesion, homologous recombination, DNA repair, and replicative potential. The SMC5/6 complex coordinates these processes through spatiotemporal regulation of proteins by posttranslational modifications, such as sumoylation. This idea that large complexes of proteins coordinate various cellular processes through posttranslational modification of effector proteins is likely to be a conserved mechanism throughout biology.

# BIBLIOGRAPHY

Abraham, R.T. (2004). PI 3-kinase related kinases: 'big' players in stress-induced signaling pathways. DNA Repair (Amst) *3*, 883-887.

Achatz, M.I., Olivier, M., Le Calvez, F., Martel-Planche, G., Lopes, A., Rossi, B.M., Ashton-Prolla, P., Giugliani, R., Palmero, E.I., Vargas, F.R.*, et al.* (2007). The TP53 mutation, R337H, is associated with Li-Fraumeni and Li-Fraumeni-like syndromes in Brazilian families. Cancer Lett *245*, 96-102.

Ampatzidou, E., Irmisch, A., O'Connell, M.J., and Murray, J.M. (2006). Smc5/6 is required for repair at collapsed replication forks. Mol Cell Biol *26*, 9387-9401.

Andrews, E.A., Palecek, J., Sergeant, J., Taylor, E., Lehmann, A.R., and Watts, F.Z. (2005). Nse2, a component of the Smc5-6 complex, is a SUMO ligase required for the response to DNA damage. Mol Cell Biol *25*, 185-196.

Aparicio, O., Geisbert, J.V., Sekinger, E., Yang, A., Moqtaderi, Z., and Struhl, K. (2005). Chromatin Immunoprecipitations for Determining the Association of Proteins with Specific Genomic Sequences In Vivo. Current Protocols in Molecular Biology, 21.23.21-21.23.33.

Arnaudeau, C., Lundin, C., and Helleday, T. (2001). DNA double-strand breaks associated with replication forks are predominantly repaired by homologous recombination involving an exchange mechanism in mammalian cells. J Mol Biol *307*, 1235-1245.

Arumugam, P., Gruber, S., Tanaka, K., Haering, C.H., Mechtler, K., and Nasmyth, K. (2003). ATP hydrolysis is required for cohesin's association with chromosomes. Curr Biol *13*, 1941-1953.

Baetz, K.K., Krogan, N.J., Emili, A., Greenblatt, J., and Hieter, P. (2004). The ctf13-30/CTF13 genomic haploinsufficiency modifier screen identifies the yeast chromatin remodeling complex RSC, which is required for the establishment of sister chromatid cohesion. Molecular and cellular biology *24*, 1232-1244.

Bartek, J., Lukas, C., and Lukas, J. (2004). Checking on DNA damage in S phase. Nat Rev Mol Cell Biol *5*, 792-804.

Bartek, J., and Lukas, J. (2003). Chk1 and Chk2 kinases in checkpoint control and cancer. Cancer Cell *3*, 421-429.

Bekker-Jensen, S., Lukas, C., Kitagawa, R., Melander, F., Kastan, M.B., Bartek, J., and Lukas, J. (2006). Spatial organization of the mammalian genome surveillance machinery in response to DNA strand breaks. J Cell Biol *173*, 195-206.

Bharadwaj, R., and Yu, H. (2004). The spindle checkpoint, aneuploidy, and cancer. Oncogene *23*, 2016-2027.

Birkenbihl, R.P., and Subramani, S. (1992). Cloning and characterization of rad21 an essential gene of Schizosaccharomyces pombe involved in DNA double-strand-break repair. Nucleic Acids Res *20*, 6605-6611.

Blackburn, E.H. (2001). Switching and signaling at the telomere. Cell *106*, 661-673.

Blow, J.J., and Tanaka, T.U. (2005). The chromosome cycle: coordinating replication and segregation. Second in the cycles review series. EMBO Rep *6*, 1028-1034.

Bodnar, A.G., Ouellette, M., Frolkis, M., Holt, S.E., Chiu, C.P., Morin, G.B., Harley, C.B., Shay, J.W., Lichtsteiner, S., and Wright, W.E. (1998). Extension of life-span by introduction of telomerase into normal human cells. Science *279*, 349-352.

Borden, K.L. (2002). Pondering the promyelocytic leukemia protein (PML) puzzle: possible functions for PML nuclear bodies. Mol Cell Biol *22*, 5259-5269.

Branzei, D., and Foiani, M. (2005). The DNA damage response during DNA replication. Curr Opin Cell Biol *17*, 568-575.

Branzei, D., Sollier, J., Liberi, G., Zhao, X., Maeda, D., Seki, M., Enomoto, T., Ohta, K., and Foiani, M. (2006). Ubc9- and mms21-mediated sumoylation counteracts recombinogenic events at damaged replication forks. Cell *127*, 509-522.

Brewer, B.J., and Fangman, W.L. (1988). A replication fork barrier at the 3' end of yeast ribosomal RNA genes. Cell *55*, 637-643.

Bryan, T.M., Englezou, A., Dalla-Pozza, L., Dunham, M.A., and Reddel, R.R. (1997). Evidence for an alternative mechanism for maintaining telomere length in human tumors and tumor-derived cell lines. Nat Med *3*, 1271-1274.

Bryan, T.M., Englezou, A., Gupta, J., Bacchetti, S., and Reddel, R.R. (1995). Telomere elongation in immortal human cells without detectable telomerase activity. EMBO J *14*, 4240-4248.

Burma, S., Chen, B.P., and Chen, D.J. (2006). Role of non-homologous end joining (NHEJ) in maintaining genomic integrity. DNA Repair (Amst) *5*, 1042-1048.

Burma, S., Chen, B.P., Murphy, M., Kurimasa, A., and Chen, D.J. (2001). ATM phosphorylates histone H2AX in response to DNA double-strand breaks. J Biol Chem *276*, 42462-42467.

Calsou, P., Delteil, C., Frit, P., Drouet, J., and Salles, B. (2003). Coordinated assembly of Ku and p460 subunits of the DNA-dependent protein kinase on DNA ends is necessary for XRCC4-ligase IV recruitment. J Mol Biol *326*, 93-103.

Chan, D.W., Chen, B.P., Prithivirajsingh, S., Kurimasa, A., Story, M.D., Qin, J., and Chen, D.J. (2002). Autophosphorylation of the DNA-dependent protein kinase catalytic subunit is required for rejoining of DNA double-strand breaks. Genes Dev *16*, 2333-2338.

Ciosk, R., Shirayama, M., Shevchenko, A., Tanaka, T., Toth, A., Shevchenko, A., and Nasmyth, K. (2000). Cohesin's binding to chromosomes depends on a separate complex consisting of Scc2 and Scc4 proteins. Molecular cell *5*, 243-254.

Collins, A.R. (2004). The comet assay for DNA damage and repair: principles, applications, and limitations. Mol Biotechnol *26*, 249-261.

Cong, Y.S., Wright, W.E., and Shay, J.W. (2002). Human telomerase and its regulation. Microbiol Mol Biol Rev *66*, 407-425, table of contents.

Curry, J.D., Li, L., and Schlissel, M.S. (2005). Quantification of Jkappa signal end breaks in developing B cells by blunt-end linker ligation and qPCR. J Immunol Methods *296*, 19-30.

de Jager, M., van Noort, J., van Gent, D.C., Dekker, C., Kanaar, R., and Wyman, C. (2001). Human Rad50/Mre11 is a flexible complex that can tether DNA ends. Mol Cell *8*, 1129-1135.

de Lange, T. (2005). Shelterin: the protein complex that shapes and safeguards human telomeres. Genes Dev *19*, 2100-2110.

De Piccoli, G., Cortes-Ledesma, F., Ira, G., Torres-Rosell, J., Uhle, S., Farmer, S., Hwang, J.Y., Machin, F., Ceschia, A., McAleenan, A*., et al.* (2006). Smc5-Smc6 mediate DNA double-strand-break repair by promoting sister-chromatid recombination. Nat Cell Biol *8*, 1032-1034.

Degrassi, F., De Salvia, R., Tanzarella, C., and Palitti, F. (1989). Induction of chromosomal aberrations and SCE by camptothecin, an inhibitor of mammalian topoisomerase I. Mutat Res *211*, 125-130.

Digweed, M., and Sperling, K. (2004). Nijmegen breakage syndrome: clinical manifestation of defective response to DNA double-strand breaks. DNA Repair (Amst) *3*, 1207-1217.

DiTullio, R.A., Jr., Mochan, T.A., Venere, M., Bartkova, J., Sehested, M., Bartek, J., and Halazonetis, T.D. (2002). 53BP1 functions in an ATM-dependent checkpoint pathway that is constitutively activated in human cancer. Nat Cell Biol *4*, 998-1002.

Dunham, M.A., Neumann, A.A., Fasching, C.L., and Reddel, R.R. (2000). Telomere maintenance by recombination in human cells. Nat Genet *26*, 447-450.

Elbashir, S.M., Harborth, J., Lendeckel, W., Yalcin, A., Weber, K., and Tuschl, T. (2001). Duplexes of 21-nucleotide RNAs mediate RNA interference in cultured mammalian cells. Nature *411*, 494-498.

Ford, D., Easton, D.F., Bishop, D.T., Narod, S.A., and Goldgar, D.E. (1994). Risks of cancer in BRCA1-mutation carriers. Breast Cancer Linkage Consortium. Lancet *343*, 692-695.

Fousteri, M.I., and Lehmann, A.R. (2000). A novel SMC protein complex in Schizosaccharomyces pombe contains the Rad18 DNA repair protein. EMBO J *19*, 1691-1702.

Fujioka, Y., Kimata, Y., Nomaguchi, K., Watanabe, K., and Kohno, K. (2002). Identification of a novel non-structural maintenance of chromosomes (SMC) component of the SMC5-SMC6 complex involved in DNA repair. J Biol Chem *277*, 21585-21591.

Gasior, S.L., Wong, A.K., Kora, Y., Shinohara, A., and Bishop, D.K. (1998). Rad52 associates with RPA and functions with rad55 and rad57 to assemble meiotic recombination complexes. Genes Dev *12*, 2208-2221.

Gassmann, R., Vagnarelli, P., Hudson, D., and Earnshaw, W.C. (2004). Mitotic chromosome formation and the condensin paradox. Experimental cell research *296*, 35-42.

Gill, G. (2004). SUMO and ubiquitin in the nucleus: different functions, similar mechanisms? Genes Dev *18*, 2046-2059.

Gocke, C.B., Yu, H., and Kang, J. (2005). Systematic Identification and Analysis of Mammalian Small Ubiquitin-like Modifier Substrates. J Biol Chem *280*, 5004-5012.

Grobelny, J.V., Godwin, A.K., and Broccoli, D. (2000). ALT-associated PML bodies are present in viable cells and are enriched in cells in the G(2)/M phase of the cell cycle. J Cell Sci *113*, 4577-4585.

Gruber, S., Haering, C.H., and Nasmyth, K. (2003). Chromosomal cohesin forms a ring. Cell *112*, 765-777.

Haering, C.H., Lowe, J., Hochwagen, A., and Nasmyth, K. (2002a). Molecular architecture of SMC proteins and the yeast cohesin complex. Mol Cell *9*, 773-788.

Haering, C.H., Lowe, J., Hochwagen, A., and Nasmyth, K. (2002b). Molecular architecture of SMC proteins and the yeast cohesin complex. Molecular cell *9*, 773-788.

Haering, C.H., Schoffnegger, D., Nishino, T., Helmhart, W., Nasmyth, K., and Lowe, J. (2004). Structure and stability of cohesin's Smc1-kleisin interaction. Mol Cell *15*, 951-964.

Hagstrom, K.A., and Meyer, B.J. (2003). Condensin and cohesin: more than chromosome compactor and glue. Nat Rev Genet *4*, 520-534.

Hakimi, M.A., Bochar, D.A., Schmiesing, J.A., Dong, Y., Barak, O.G., Speicher, D.W., Yokomori, K., and Shiekhattar, R. (2002). A chromatin remodelling complex that loads cohesin onto human chromosomes. Nature *418*, 994-998.

Hanna, J.S., Kroll, E.S., Lundblad, V., and Spencer, F.A. (2001). Saccharomyces cerevisiae CTF18 and CTF4 are required for sister chromatid cohesion. Molecular and cellular biology *21*, 3144-3158.

Hardeland, U., Steinacher, R., Jiricny, J., and Schar, P. (2002). Modification of the human thymine-DNA glycosylase by ubiquitin-like proteins facilitates enzymatic turnover. EMBO J *21*, 1456-1464.

Harley, C.B., Futcher, A.B., and Greider, C.W. (1990). Telomeres shorten during ageing of human fibroblasts. Nature *345*, 458-460.

Harvey, S.H., Sheedy, D.M., Cuddihy, A.R., and O'Connell, M.J. (2004). Coordination of DNA damage responses via the Smc5/Smc6 complex. Mol Cell Biol *24*, 662-674.

Hawley, R.S., and Marcus, C.H. (1989). Recombinational controls of rDNA redundancy in Drosophila. Annu Rev Genet *23*, 87-120.

Henson, J.D., Hannay, J.A., McCarthy, S.W., Royds, J.A., Yeager, T.R., Robinson, R.A., Wharton, S.B., Jellinek, D.A., Arbuckle, S.M., Yoo, J.*, et al.* (2005). A robust assay for alternative lengthening of telomeres in tumors shows the significance of alternative lengthening of telomeres in sarcomas and astrocytomas. Clin Cancer Res *11*, 217-225.

Henson, J.D., Neumann, A.A., Yeager, T.R., and Reddel, R.R. (2002). Alternative lengthening of telomeres in mammalian cells. Oncogene *21*, 598-610.

Heyer, W.D., Ehmsen, K.T., and Solinger, J.A. (2003). Holliday junctions in the eukaryotic nucleus: resolution in sight? Trends Biochem Sci *28*, 548-557.

Hirano, T. (2002). The ABCs of SMC proteins: two-armed ATPases for chromosome condensation, cohesion, and repair. Genes Dev *16*, 399-414.

Hirano, T. (2005a). Condensins: organizing and segregating the genome. Curr Biol *15*, R265-275.

Hirano, T. (2005b). SMC proteins and chromosome mechanics: from bacteria to humans. Philos Trans R Soc Lond B Biol Sci *360*, 507-514.

Hirano, T. (2006a). At the heart of the chromosome: SMC proteins in action. Nature reviews *7*, 311-322.

Hirano, T. (2006b). At the heart of the chromosome: SMC proteins in action. Nat Rev Mol Cell Biol *7*, 311-322.

Ho, J.C., Warr, N.J., Shimizu, H., and Watts, F.Z. (2001). SUMO modification of Rad22, the Schizosaccharomyces pombe homologue of the recombination protein Rad52. Nucleic Acids Res *29*, 4179-4186.

Hoege, C., Pfander, B., Moldovan, G.L., Pyrowolakis, G., and Jentsch, S. (2002). RAD6-dependent DNA repair is linked to modification of PCNA by ubiquitin and SUMO. Nature *419*, 135-141.

Hopfner, K.P., Craig, L., Moncalian, G., Zinkel, R.A., Usui, T., Owen, B.A., Karcher, A., Henderson, B., Bodmer, J.L., McMurray, C.T., *et al.* (2002). The Rad50 zinc-hook is a structure joining Mre11 complexes in DNA recombination and repair. Nature *418*, 562-566.

Hu, B., Liao, C., Millson, S.H., Mollapour, M., Prodromou, C., Pearl, L.H., Piper, P.W., and Panaretou, B. (2005). Qri2/Nse4, a component of the essential Smc5/6 DNA repair complex. Mol Microbiol *55*, 1735-1750.

Hudson, D.F., Vagnarelli, P., Gassmann, R., and Earnshaw, W.C. (2003). Condensin is required for nonhistone protein assembly and structural integrity of vertebrate mitotic chromosomes. Developmental cell *5*, 323-336.

Ishov, A.M., Sotnikov, A.G., Negorev, D., Vladimirova, O.V., Neff, N., Kamitani, T., Yeh, E.T., Strauss, J.F., 3rd, and Maul, G.G. (1999). PML is critical for ND10 formation and recruits the PML-interacting protein daxx to this nuclear structure when modified by SUMO-1. J Cell Biol *147*, 221-234.

Ivanov, D., and Nasmyth, K. (2005). A topological interaction between cohesin rings and a circular minichromosome. Cell *122*, 849-860.

Jasin, M. (1996). Genetic manipulation of genomes with rare-cutting endonucleases. Trends Genet *12*, 224-228.

Jessberger, R. (2002). The many functions of SMC proteins in chromosome dynamics. Nat Rev Mol Cell Biol *3*, 767-778.

Jiang, W.Q., Zhong, Z.H., Henson, J.D., Neumann, A.A., Chang, A.C., and Reddel, R.R. (2005). Suppression of alternative lengthening of telomeres by Sp100-mediated sequestration of the MRE11/RAD50/NBS1 complex. Mol Cell Biol *25*, 2708-2721.

Johnson, E.S. (2004). Protein modification by SUMO. Annu Rev Biochem *73*, 355-382.

Johnson, E.S., and Gupta, A.A. (2001). An E3-like factor that promotes SUMO conjugation to the yeast septins. Cell *106*, 735-744.

Johnson, F.B., Marciniak, R.A., McVey, M., Stewart, S.A., Hahn, W.C., and Guarente, L. (2001). The Saccharomyces cerevisiae WRN homolog Sgs1p participates in telomere maintenance in cells lacking telomerase. EMBO J *20*, 905-913.

Johnson, R.D., and Jasin, M. (2000). Sister chromatid gene conversion is a prominent double-strand break repair pathway in mammalian cells. EMBO J *19*, 3398-3407.

Kastan, M.B., and Bartek, J. (2004). Cell-cycle checkpoints and cancer. Nature *432*, 316-323.

Kenna, M.A., and Skibbens, R.V. (2003). Mechanical link between cohesion establishment and DNA replication: Ctf7p/Eco1p, a cohesion establishment factor, associates with three different replication factor C complexes. Molecular and cellular biology *23*, 2999-3007.

Khanna, K.K., and Jackson, S.P. (2001). DNA double-strand breaks: signaling, repair and the cancer connection. Nat Genet *27*, 247-254.

Kim, J.S., Krasieva, T.B., LaMorte, V., Taylor, A.M., and Yokomori, K. (2002a). Specific recruitment of human cohesin to laser-induced DNA damage. J Biol Chem *277*, 45149-45153.

Kim, S.T., Lim, D.S., Canman, C.E., and Kastan, M.B. (1999). Substrate specificities and identification of putative substrates of ATM kinase family members. J Biol Chem *274*, 37538-37543.

Kim, S.T., Xu, B., and Kastan, M.B. (2002b). Involvement of the cohesin protein, Smc1, in Atm-dependent and independent responses to DNA damage. Genes Dev *16*, 560-570.

Kimura, K., and Hirano, T. (1997). ATP-dependent positive supercoiling of DNA by 13S condensin: a biochemical implication for chromosome condensation. Cell *90*, 625-634.

Kimura, K., Rybenkov, V.V., Crisona, N.J., Hirano, T., and Cozzarelli, N.R. (1999). 13S condensin actively reconfigures DNA by introducing global positive writhe: implications for chromosome condensation. Cell *98*, 239-248.

Kitagawa, R., Bakkenist, C.J., McKinnon, P.J., and Kastan, M.B. (2004). Phosphorylation of SMC1 is a critical downstream event in the ATM-NBS1-BRCA1 pathway. Genes Dev *18*, 1423-1438.

Kogoma, T. (1996). Recombination by replication. Cell *85*, 625-627.

Koshland, D.E., and Guacci, V. (2000). Sister chromatid cohesion: the beginning of a long and beautiful relationship. Curr Opin Cell Biol *12*, 297-301.

Laud, P.R., Multani, A.S., Bailey, S.M., Wu, L., Ma, J., Kingsley, C., Lebel, M., Pathak, S., DePinho, R.A., and Chang, S. (2005). Elevated telomere-telomere recombination in WRN-deficient, telomere dysfunctional cells promotes escape from senescence and engagement of the ALT pathway. Genes Dev *19*, 2560-2570.

Lee, K.M., and O'Connell, M.J. (2006). A new SUMO ligase in the DNA damage response. DNA Repair (Amst) *5*, 138-141.

Lehmann, A.R. (2005). The role of SMC proteins in the responses to DNA damage. DNA Repair (Amst) *4*, 309-314.

Lehmann, A.R., Walicka, M., Griffiths, D.J., Murray, J.M., Watts, F.Z., McCready, S., and Carr, A.M. (1995). The rad18 gene of Schizosaccharomyces pombe defines a new subgroup of the SMC superfamily involved in DNA repair. Mol Cell Biol *15*, 7067-7080.

Lengronne, A., Katou, Y., Mori, S., Yokobayashi, S., Kelly, G.P., Itoh, T., Watanabe, Y., Shirahige, K., and Uhlmann, F. (2004). Cohesin relocation from sites of chromosomal loading to places of convergent transcription. Nature *430*, 573-578.

Lieber, M.R., Ma, Y., Pannicke, U., and Schwarz, K. (2004). The mechanism of vertebrate nonhomologous DNA end joining and its role in V(D)J recombination. DNA Repair (Amst) *3*, 817-826.

Lin, D.Y., Huang, Y.S., Jeng, J.C., Kuo, H.Y., Chang, C.C., Chao, T.T., Ho, C.C., Chen, Y.C., Lin, T.P., Fang, H.I.*, et al.* (2006). Role of SUMO-interacting motif in Daxx SUMO modification, subnuclear localization, and repression of sumoylated transcription factors. Mol Cell *24*, 341-354.

Lindroos, H.B., Strom, L., Itoh, T., Katou, Y., Shirahige, K., and Sjogren, C. (2006). Chromosomal association of the Smc5/6 complex reveals that it functions in differently regulated pathways. Mol Cell *22*, 755-767.

Lisby, M., Barlow, J.H., Burgess, R.C., and Rothstein, R. (2004). Choreography of the DNA damage response: spatiotemporal relationships among checkpoint and repair proteins. Cell *118*, 699-713.

Lisby, M., and Rothstein, R. (2004). DNA damage checkpoint and repair centers. Curr Opin Cell Biol *16*, 328-334.

Lisby, M., and Rothstein, R. (2005). Localization of checkpoint and repair proteins in eukaryotes. Biochimie *87*, 579-589.

Liu, B., and Alberts, B.M. (1995). Head-on collision between a DNA replication apparatus and RNA polymerase transcription complex. Science *267*, 1131-1137.

Liu, Q., Guntuku, S., Cui, X.S., Matsuoka, S., Cortez, D., Tamai, K., Luo, G., Carattini-Rivera, S., DeMayo, F., Bradley, A*., et al.* (2000). Chk1 is an essential kinase that is regulated by Atr and required for the G(2)/M DNA damage checkpoint. Genes Dev *14*, 1448-1459.

Liu, Y., Tarsounas, M., O'Regan, P., and West, S.C. (2007). Role of RAD51C and XRCC3 in genetic recombination and DNA repair. J Biol Chem *282*, 1973-1979.

Londono-Vallejo, J.A., Der-Sarkissian, H., Cazes, L., Bacchetti, S., and Reddel, R.R. (2004). Alternative lengthening of telomeres is characterized by high rates of telomeric exchange. Cancer Res *64*, 2324-2327.

Lundblad, V., and Blackburn, E.H. (1993). An alternative pathway for yeast telomere maintenance rescues est1- senescence. Cell *73*, 347-360.

Maeda, D., Seki, M., Onoda, F., Branzei, D., Kawabe, Y., and Enomoto, T. (2004). Ubc9 is required for damage-tolerance and damage-induced interchromosomal homologous recombination in S. cerevisiae. DNA Repair (Amst) *3*, 335-341.

Mao, Y., Sun, M., Desai, S.D., and Liu, L.F. (2000). SUMO-1 conjugation to topoisomerase I: A possible repair response to topoisomerase-mediated DNA damage. Proc Natl Acad Sci U S A *97*, 4046-4051.

Matsuoka, S., Huang, M., and Elledge, S.J. (1998). Linkage of ATM to cell cycle regulation by the Chk2 protein kinase. Science *282*, 1893-1897.

Maul, G.G., Negorev, D., Bell, P., and Ishov, A.M. (2000). Review: properties and assembly mechanisms of ND10, PML bodies, or PODs. J Struct Biol *129*, 278-287.

McDonald, W.H., Pavlova, Y., Yates, J.R., 3rd, and Boddy, M.N. (2003). Novel essential DNA repair proteins Nse1 and Nse2 are subunits of the fission yeast Smc5-Smc6 complex. J Biol Chem *278*, 45460-45467.

Melby, T.E., Ciampaglio, C.N., Briscoe, G., and Erickson, H.P. (1998). The symmetrical structure of structural maintenance of chromosomes (SMC) and MukB proteins: long, antiparallel coiled coils, folded at a flexible hinge. J Cell Biol *142*, 1595-1604.

Melchionna, R., Chen, X.B., Blasina, A., and McGowan, C.H. (2000). Threonine 68 is required for radiation-induced phosphorylation and activation of Cds1. Nat Cell Biol *2*, 762-765.

Mengiste, T., Revenkova, E., Bechtold, N., and Paszkowski, J. (1999). An SMC-like protein is required for efficient homologous recombination in Arabidopsis. EMBO J *18*, 4505-4512.

Michaelis, C., Ciosk, R., and Nasmyth, K. (1997). Cohesins: chromosomal proteins that prevent premature separation of sister chromatids. Cell *91*, 35-45.

Mirzoeva, O.K., and Petrini, J.H. (2001). DNA damage-dependent nuclear dynamics of the Mre11 complex. Mol Cell Biol *21*, 281-288.

Miyabe, I., Morishita, T., Hishida, T., Yonei, S., and Shinagawa, H. (2006). Rhp51-dependent recombination intermediates that do not generate checkpoint signal are accumulated in Schizosaccharomyces pombe rad60 and smc5/6 mutants after release from replication arrest. Mol Cell Biol *26*, 343-353.

Montelone, B.A., and Koelliker, K.J. (1995). Interactions among mutations affecting spontaneous mutation, mitotic recombination, and DNA repair in yeast. Curr Genet *27*, 102-109.

Moreno-Herrero, F., de Jager, M., Dekker, N.H., Kanaar, R., Wyman, C., and Dekker, C. (2005). Mesoscale conformational changes in the DNA-repair complex Rad50/Mre11/Nbs1 upon binding DNA. Nature *437*, 440-443.

Morikawa, H., Morishita, T., Kawane, S., Iwasaki, H., Carr, A.M., and Shinagawa, H. (2004). Rad62 protein functionally and physically associates with the smc5/smc6 protein complex and is required for chromosome integrity and recombination repair in fission yeast. Mol Cell Biol *24*, 9401-9413.

Morishita, T., Tsutsui, Y., Iwasaki, H., and Shinagawa, H. (2002). The Schizosaccharomyces pombe rad60 gene is essential for repairing double-strand

DNA breaks spontaneously occurring during replication and induced by DNA-damaging agents. Mol Cell Biol *22*, 3537-3548.

Moynahan, M.E., Chiu, J.W., Koller, B.H., and Jasin, M. (1999). Brca1 controls homology-directed DNA repair. Mol Cell *4*, 511-518.

Moynahan, M.E., Pierce, A.J., and Jasin, M. (2001). BRCA2 is required for homology-directed repair of chromosomal breaks. Mol Cell *7*, 263-272.

Muller, S., Hoege, C., Pyrowolakis, G., and Jentsch, S. (2001). SUMO, ubiquitin's mysterious cousin. Nat Rev Mol Cell Biol *2*, 202-210.

Muntoni, A., and Reddel, R.R. (2005). The first molecular details of ALT in human tumor cells. Hum Mol Genet *14 Spec No. 2*, R191-196.

Nabetani, A., Yokoyama, O., and Ishikawa, F. (2004). Localization of hRad9, hHus1, hRad1, and hRad17 and caffeine-sensitive DNA replication at the alternative lengthening of telomeres-associated promyelocytic leukemia body. J Biol Chem *279*, 25849-25857.

Nasim, A., and Smith, B.P. (1975). Genetic control of radiation sensitivity in Schizosaccharomyces pombe. Genetics *79*, 573-582.

Nasmyth, K. (2002). Segregating sister genomes: the molecular biology of chromosome separation. Science *297*, 559-565.

Nasmyth, K., and Haering, C.H. (2005a). The structure and function of SMC and kleisin complexes. Annual review of biochemistry *74*, 595-648.

Nasmyth, K., and Haering, C.H. (2005b). The structure and function of SMC and kleisin complexes. Annu Rev Biochem *74*, 595-648.

Novatchkova, M., Bachmair, A., Eisenhaber, B., and Eisenhaber, F. (2005). Proteins with two SUMO-like domains in chromatin-associated complexes: the RENi (Rad60-Esc2-NIP45) family. BMC Bioinformatics *6*, 22.

Ono, T., Fang, Y., Spector, D.L., and Hirano, T. (2004). Spatial and temporal regulation of Condensins I and II in mitotic chromosome assembly in human cells. Molecular biology of the cell *15*, 3296-3308.

Ono, T., Losada, A., Hirano, M., Myers, M.P., Neuwald, A.F., and Hirano, T. (2003). Differential contributions of condensin I and condensin II to mitotic chromosome architecture in vertebrate cells. Cell *115*, 109-121.

Onoda, F., Takeda, M., Seki, M., Maeda, D., Tajima, J., Ui, A., Yagi, H., and Enomoto, T. (2004). SMC6 is required for MMS-induced interchromosomal and sister chromatid recombinations in Saccharomyces cerevisiae. DNA Repair (Amst) *3*, 429-439.

Palecek, J., Vidot, S., Feng, M., Doherty, A.J., and Lehmann, A.R. (2006). The Smc5-Smc6 DNA repair complex. bridging of the Smc5-Smc6 heads by the KLEISIN, Nse4, and non-Kleisin subunits. J Biol Chem *281*, 36952-36959.

Paull, T.T., and Gellert, M. (1998). The 3' to 5' exonuclease activity of Mre 11 facilitates repair of DNA double-strand breaks. Mol Cell *1*, 969-979.

Pebernard, S., McDonald, W.H., Pavlova, Y., Yates, J.R., 3rd, and Boddy, M.N. (2004). Nse1, Nse2, and a novel subunit of the Smc5-Smc6 complex, Nse3, play a crucial role in meiosis. Mol Biol Cell *15*, 4866-4876.

Pebernard, S., Wohlschlegel, J., McDonald, W.H., Yates, J.R., 3rd, and Boddy, M.N. (2006). The Nse5-Nse6 dimer mediates DNA repair roles of the Smc5-Smc6 complex. Mol Cell Biol *26*, 1617-1630.

Peng, C.Y., Graves, P.R., Thoma, R.S., Wu, Z., Shaw, A.S., and Piwnica-Worms, H. (1997). Mitotic and G2 checkpoint control: regulation of 14-3-3 protein binding by phosphorylation of Cdc25C on serine-216. Science *277*, 1501-1505.

Perrem, K., Colgin, L.M., Neumann, A.A., Yeager, T.R., and Reddel, R.R. (2001). Coexistence of alternative lengthening of telomeres and telomerase in hTERT-transfected GM847 cells. Mol Cell Biol *21*, 3862-3875.

Petronczki, M., Siomos, M.F., and Nasmyth, K. (2003). Un menage a quatre: the molecular biology of chromosome segregation in meiosis. Cell *112*, 423-440.

Phipps, J., Nasim, A., and Miller, D.R. (1985). Recovery, repair, and mutagenesis in Schizosaccharomyces pombe. Adv Genet *23*, 1-72.

Pichler, A., Gast, A., Seeler, J.S., Dejean, A., and Melchior, F. (2002). The nucleoporin RanBP2 has SUMO1 E3 ligase activity. Cell *108*, 109-120.

Pierce, A.J., Johnson, R.D., Thompson, L.H., and Jasin, M. (1999). XRCC3 promotes homology-directed repair of DNA damage in mammalian cells. Genes Dev *13*, 2633-2638.

Porteus, M.H., and Baltimore, D. (2003). Chimeric nucleases stimulate gene targeting in human cells. Science *300*, 763.

Porteus, M.H., and Carroll, D. (2005). Gene targeting using zinc finger nucleases. Nat Biotechnol *23*, 967-973.

Potts, P.R., Porteus, M.H., and Yu, H. (2006). Human SMC5/6 complex promotes sister chromatid homologous recombination by recruiting the SMC1/3 cohesin complex to double-strand breaks. EMBO J *25*, 3377-3388.

Potts, P.R., and Yu, H. (2005). Human MMS21/NSE2 is a SUMO ligase required for DNA repair. Mol Cell Biol *25*, 7021-7032.

Prakash, L., and Prakash, S. (1977a). Isolation and characterization of MMS-sensitive mutants of Saccharomyces cerevisiae. Genetics *86*, 33-55.

Prakash, S., and Prakash, L. (1977b). Increased spontaneous mitotic segregation in MMS-sensitive mutants of Saccharomyces cerevisiae. Genetics *87*, 229-236.

Puget, N., Knowlton, M., and Scully, R. (2005). Molecular analysis of sister chromatid recombination in mammalian cells. DNA Repair (Amst) *4*, 149-161.

Raffa, G.D., Wohlschlegel, J., Yates, J.R., 3rd, and Boddy, M.N. (2006). SUMO-binding motifs mediate the Rad60-dependent response to replicative stress and self-association. J Biol Chem *281*, 27973-27981.

Rajagopalan, H., and Lengauer, C. (2004). Aneuploidy and cancer. Nature *432*, 338-341.

Rodrigue, A., Lafrance, M., Gauthier, M.C., McDonald, D., Hendzel, M., West, S.C., Jasin, M., and Masson, J.Y. (2006). Interplay between human DNA repair proteins at a unique double-strand break in vivo. EMBO J *25*, 222-231.

Rodriguez, M.S., Dargemont, C., and Hay, R.T. (2001). SUMO-1 conjugation in vivo requires both a consensus modification motif and nuclear targeting. J Biol Chem *276*, 12654-12659.

Rogan, E.M., Bryan, T.M., Hukku, B., Maclean, K., Chang, A.C., Moy, E.L., Englezou, A., Warneford, S.G., Dalla-Pozza, L., and Reddel, R.R. (1995). Alterations in p53 and p16INK4 expression and telomere length during spontaneous immortalization of Li-Fraumeni syndrome fibroblasts. Mol Cell Biol *15*, 4745-4753.

Rothkamm, K., Kruger, I., Thompson, L.H., and Lobrich, M. (2003). Pathways of DNA double-strand break repair during the mammalian cell cycle. Mol Cell Biol *23*, 5706-5715.

Sancar, A., Lindsey-Boltz, L.A., Unsal-Kacmaz, K., and Linn, S. (2004). Molecular mechanisms of mammalian DNA repair and the DNA damage checkpoints. Annu Rev Biochem *73*, 39-85.

Sanchez, Y., Wong, C., Thoma, R.S., Richman, R., Wu, Z., Piwnica-Worms, H., and Elledge, S.J. (1997). Conservation of the Chk1 checkpoint pathway in mammals: linkage of DNA damage to Cdk regulation through Cdc25. Science *277*, 1497-1501.

Schar, P., Fasi, M., and Jessberger, R. (2004). SMC1 coordinates DNA double-strand break repair pathways. Nucleic Acids Res *32*, 3921-3929.

Seeler, J.S., and Dejean, A. (2001). SUMO: of branched proteins and nuclear bodies. Oncogene *20*, 7243-7249.

Sergeant, J., Taylor, E., Palecek, J., Fousteri, M., Andrews, E.A., Sweeney, S., Shinagawa, H., Watts, F.Z., and Lehmann, A.R. (2005). Composition and architecture of the Schizosaccharomyces pombe Rad18 (Smc5-6) complex. Mol Cell Biol *25*, 172-184.

Shay, J.W., and Bacchetti, S. (1997). A survey of telomerase activity in human cancer. Eur J Cancer *33*, 787-791.

Sjogren, C., and Nasmyth, K. (2001). Sister chromatid cohesion is required for postreplicative double-strand break repair in Saccharomyces cerevisiae. Curr Biol *11*, 991-995.

Skibbens, R.V., Corson, L.B., Koshland, D., and Hieter, P. (1999). Ctf7p is essential for sister chromatid cohesion and links mitotic chromosome structure to the DNA replication machinery. Genes Dev/ *13*, 307-319.

Smogorzewska, A., and de Lange, T. (2004). Regulation of telomerase by telomeric proteins. Annu Rev Biochem *73*, 177-208.

Sonoda, E., Hochegger, H., Saberi, A., Taniguchi, Y., and Takeda, S. (2006). Differential usage of non-homologous end-joining and homologous recombination in double strand break repair. DNA Repair (Amst) *5*, 1021-1029.

Sonoda, E., Matsusaka, T., Morrison, C., Vagnarelli, P., Hoshi, O., Ushiki, T., Nojima, K., Fukagawa, T., Waizenegger, I.C., Peters, J.M*., et al.* (2001). Scc1/Rad21/Mcd1 is required for sister chromatid cohesion and kinetochore function in vertebrate cells. Dev Cell *1*, 759-770.

Stelter, P., and Ulrich, H.D. (2003). Control of spontaneous and damage-induced mutagenesis by SUMO and ubiquitin conjugation. Nature *425*, 188-191.

Stewart, G.S., Wang, B., Bignell, C.R., Taylor, A.M., and Elledge, S.J. (2003). MDC1 is a mediator of the mammalian DNA damage checkpoint. Nature *421*, 961-966.

Stray, J.E., Crisona, N.J., Belotserkovskii, B.P., Lindsley, J.E., and Cozzarelli, N.R. (2005). The Saccharomyces cerevisiae Smc2/4 condensin compacts DNA into (+) chiral structures without net supercoiling. The Journal of biological chemistry *280*, 34723-34734.

Strom, L., Karlsson, C., Lindroos, H.B., Wedahl, S., Katou, Y., Shirahige, K., and Sjogren, C. (2007). Postreplicative formation of cohesion is required for repair and induced by a single DNA break. Science *317*, 242-245.

Strom, L., Lindroos, H.B., Shirahige, K., and Sjogren, C. (2004). Postreplicative recruitment of cohesin to double-strand breaks is required for DNA repair. Mol Cell *16*, 1003-1015.

Strom, L., and Sjogren, C. (2007). Chromosome segregation and double-strand break repair - a complex connection. Curr Opin Cell Biol *19*, 344-349.

Sugawara, N., Ivanov, E.L., Fishman-Lobell, J., Ray, B.L., Wu, X., and Haber, J.E. (1995). DNA structure-dependent requirements for yeast RAD genes in gene conversion. Nature *373*, 84-86.

Sugiyama, T., and Kowalczykowski, S.C. (2002). Rad52 protein associates with replication protein A (RPA)-single-stranded DNA to accelerate Rad51-mediated displacement of RPA and presynaptic complex formation. J Biol Chem *277*, 31663-31672.

Sung, P., Krejci, L., Van Komen, S., and Sehorn, M.G. (2003). Rad51 recombinase and recombination mediators. J Biol Chem *278*, 42729-42732.

Swedlow, J.R., and Hirano, T. (2003). The making of the mitotic chromosome: modern insights into classical questions. Mol Cell *11*, 557-569.

Tanaka, T., Cosma, M.P., Wirth, K., and Nasmyth, K. (1999). Identification of cohesin association sites at centromeres and along chromosome arms. Cell *98*, 847-858.

Tatebayashi, K., Kato, J., and Ikeda, H. (1998). Isolation of a Schizosaccharomyces pombe rad21ts mutant that is aberrant in chromosome segregation, microtubule function, DNA repair and sensitive to hydroxyurea: possible involvement of Rad21 in ubiquitin-mediated proteolysis. Genetics *148*, 49-57.

Taylor, D.L., Ho, J.C., Oliver, A., and Watts, F.Z. (2002). Cell-cycle-dependent localisation of Ulp1, a Schizosaccharomyces pombe Pmt3 (SUMO)-specific protease. J Cell Sci *115*, 1113-1122.

Taylor, E.M., Moghraby, J.S., Lees, J.H., Smit, B., Moens, P.B., and Lehmann, A.R. (2001). Characterization of a novel human SMC heterodimer homologous to the Schizosaccharomyces pombe Rad18/Spr18 complex. Mol Biol Cell *12*, 1583-1594.

Torres-Rosell, J., Machin, F., and Aragon, L. (2005a). Smc5-Smc6 complex preserves nucleolar integrity in S. cerevisiae. Cell Cycle *4*, 868-872.

Torres-Rosell, J., Machin, F., Farmer, S., Jarmuz, A., Eydmann, T., Dalgaard, J.Z., and Aragon, L. (2005b). SMC5 and SMC6 genes are required for the segregation of repetitive chromosome regions. Nat Cell Biol *7*, 412-419.

Torres-Rosell, J., Sunjevaric, I., De Piccoli, G., Sacher, M., Eckert-Boulet, N., Reid, R., Jentsch, S., Rothstein, R., Aragon, L., and Lisby, M. (2007). The Smc5-Smc6 complex and SUMO modification of Rad52 regulates recombinational repair at the ribosomal gene locus. Nat Cell Biol *9*, 923-931.

Toth, A., Ciosk, R., Uhlmann, F., Galova, M., Schleiffer, A., and Nasmyth, K. (1999). Yeast cohesin complex requires a conserved protein, Eco1p(Ctf7), to establish cohesion between sister chromatids during DNA replication. Genes Dev *13*, 320-333.

Unal, E., Arbel-Eden, A., Sattler, U., Shroff, R., Lichten, M., Haber, J.E., and Koshland, D. (2004). DNA damage response pathway uses histone modification to assemble a double-strand break-specific cohesin domain. Mol Cell *16*, 991-1002.

Unal, E., Heidinger-Pauli, J.M., and Koshland, D. (2007). DNA double-strand breaks trigger genome-wide sister-chromatid cohesion through Eco1 (Ctf7). Science *317*, 245-248.

Verkade, H.M., Bugg, S.J., Lindsay, H.D., Carr, A.M., and O'Connell, M.J. (1999). Rad18 is required for DNA repair and checkpoint responses in fission yeast. Mol Biol Cell *10*, 2905-2918.

Walker, J.R., Corpina, R.A., and Goldberg, J. (2001). Structure of the Ku heterodimer bound to DNA and its implications for double-strand break repair. Nature *412*, 607-614.

Wang, R.C., Smogorzewska, A., and de Lange, T. (2004). Homologous recombination generates T-loop-sized deletions at human telomeres. Cell *119*, 355-368.

Ward, I.M., Wu, X., and Chen, J. (2001). Threonine 68 of Chk2 is phosphorylated at sites of DNA strand breaks. J Biol Chem *276*, 47755-47758.

West, S.C. (2003a). Molecular views of recombination proteins and their control. Nat Rev Mol Cell Biol *4*, 435-445.

West, S.C. (2003b). Molecular views of recombination proteins and their control. Nat Rev Mol Cell Biol *4*, 435-445.

Wolff, S. (1977). Sister chromatid exchange. Annu Rev Genet *11*, 183-201.

Wright, W.E., Pereira-Smith, O.M., and Shay, J.W. (1989). Reversible cellular senescence: implications for immortalization of normal human diploid fibroblasts. Mol Cell Biol *9*, 3088-3092.

Wu, G., Jiang, X., Lee, W.H., and Chen, P.L. (2003). Assembly of functional ALT-associated promyelocytic leukemia bodies requires Nijmegen Breakage Syndrome 1. Cancer Res *63*, 2589-2595.

Wu, G., Lee, W.H., and Chen, P.L. (2000). NBS1 and TRF1 colocalize at promyelocytic leukemia bodies during late S/G2 phases in immortalized telomerase-negative cells. Implication of NBS1 in alternative lengthening of telomeres. J Biol Chem *275*, 30618-30622.

Wyman, C., and Kanaar, R. (2006). DNA double-strand break repair: all's well that ends well. Annu Rev Genet *40*, 363-383.

Wyman, C., Ristic, D., and Kanaar, R. (2004). Homologous recombination-mediated double-strand break repair. DNA Repair (Amst) *3*, 827-833.

Xhemalce, B., Riising, E.M., Baumann, P., Dejean, A., Arcangioli, B., and Seeler, J.S. (2007). Role of SUMO in the dynamics of telomere maintenance in fission yeast. Proc Natl Acad Sci U S A *104*, 893-898.

Xie, A., Puget, N., Shim, I., Odate, S., Jarzyna, I., Bassing, C.H., Alt, F.W., and Scully, R. (2004). Control of sister chromatid recombination by histone H2AX. Mol Cell *16*, 1017-1025.

Yaneva, M., Kowalewski, T., and Lieber, M.R. (1997). Interaction of DNA-dependent protein kinase with DNA and with Ku: biochemical and atomic-force microscopy studies. EMBO J *16*, 5098-5112.

Yankiwski, V., Marciniak, R.A., Guarente, L., and Neff, N.F. (2000). Nuclear structure in normal and Bloom syndrome cells. Proc Natl Acad Sci USA *97*, 5214-5219.

Yazdi, P.T., Wang, Y., Zhao, S., Patel, N., Lee, E.Y., and Qin, J. (2002). SMC1 is a downstream effector in the ATM/NBS1 branch of the human S-phase checkpoint. Genes Dev *16*, 571-582.

Yeager, T.R., Neumann, A.A., Englezou, A., Huschtscha, L.I., Noble, J.R., and Reddel, R.R. (1999). Telomerase-negative immortalized human cells contain a novel type of promyelocytic leukemia (PML) body. Cancer Res *59*, 4175-4179.

Zhao, X., and Blobel, G. (2005). A SUMO ligase is part of a nuclear multiprotein complex that affects DNA repair and chromosomal organization. Proc Natl Acad Sci U S A *102*, 4777-4782.

Zhou, B.B., and Elledge, S.J. (2000). The DNA damage response: putting checkpoints in perspective. Nature *408*, 433-439.

Zhu, X.D., Kuster, B., Mann, M., Petrini, J.H., and de Lange, T. (2000). Cell-cycle-regulated association of RAD50/MRE11/NBS1 with TRF2 and human telomeres. Nat Genet *25*, 347-352.

# VITAE

Patrick Ryan Potts was born in Rutherfordton, North Carolina, on July 11, 1979, to Robert James Potts and Brenda Whiteside Potts. After completing his work at Rutherfordton-Spindale High School, Rutherfordton, North Carolina in 1997, he entered the University of North Carolina at Chapel Hill. He received the degree of Bachelor of Science with a major in biology and minor in chemistry from the University of North Carolina at Chapel Hill in December, 2000. During his time as an undergraduate, he spent three years as a part-time lab assistant in the Department of Pediatrics – Endocrinology. He also performed undergraduate research studying *Manduca sexta*. After receiving his bachelor degree, he spent the following two and a half years as a research technician in the Neuroscience center at the University of North Carolina at Chapel Hill studying the regulation of cell death in neurons. In August, 2003 he entered the Graduate School of Basic Sciences at the University of Texas Southwestern Medical Center at Dallas. He is expected to graduate in December, 2007 with the degree of Doctor of Philosophy in Cell Regulation.


Permanent Address:   730 Rock Springs Church Rd
                     Rutherfordton, NC  28139